Max-Planck-Institute für Molekulare Pflanzenphysiologie

Redox signalling in plants

Dissertation
zur Erlangung des akademischen Grades
"doctor rerum naturalium"
(Dr. rer. nat.)
in der Wissenschaftsdisziplin " Molekulare Pflanzenphysiologie "

eingereicht an der
Mathematisch-Naturwissenschaftlichen Fakultät
der Universität Potsdam

von
Beata Siemiątkowska
Potsdam, im November 2019

Supervisor: Prof. Dr. Mark Stitt

Reviewers: Prof. Dr. Lee Sweetlove
Prof. Dr. Iris Finkemeier

Published online on the
Publication Server of the University of Potsdam:
https://doi.org/10.25932/publishup-48911
https://nbn-resolving.org/urn:nbn:de:kobv:517-opus4-489119

Eidestattliche Erklärung

Hiermit versichere ich, die vorliegende Arbeit selbstständig angefertigt und keine anderen als die angegebenen Quellen und Hilfsmittel verwendet zu haben. Ich versichere ebenfalls, dass die Arbeit an keiner anderen Hochschule als der Universität Potsdam eingereicht wurde.

_____

Potsdam, den Beata Siemiątkowska

Summary

Once proteins are synthesized, they can additionally be modified by post-translational modifications (PTMs). Proteins containing reactive cysteine thiols, stabilized in their deprotonated form due to their local environment as thiolates (RS-), serve as redox sensors by undergoing a multitude of oxidative PTMs (Ox-PTMs). Ox-PTMs such as S-nitrosylation or formation of inter- or intra-disulfide bridges induce functional changes in these proteins. Proteins containing cysteines, whose thiol oxidation state regulates their functions, belong to the so-called redoxome. Such Ox-PTMs are controlled by site-specific cellular events that play a crucial role in protein regulation, affecting enzyme catalytic sites, ligand binding affinity, protein-protein interactions or protein stability. Reversible protein thiol oxidation is an essential regulatory mechanism of photosynthesis, metabolism, and gene expression in all photosynthetic organisms. Therefore, studying PTMs will remain crucial for understanding plant adaptation to external stimuli like fluctuating light conditions. Optimizing methods suitable for studying plants Ox-PTMs is of high importance for elucidation of the redoxome in plants. This study focusses on thiol modifications occurring in plant and provides novel insight into *in vivo* redoxome of *Arabidopsis thaliana* in response to light *vs.* dark. This was achieved by utilizing a resin-assisted thiol enrichment approach. Furthermore, confirmation of candidates on the single protein level was carried out by a differential labelling approach. The thiols and disulfides were differentially labelled, and the protein levels were detected using immunoblot analysis. Further analysis was focused on light-reduced proteins. By the enrichment approach many well studied redox-regulated proteins were identified. Amongst those were fructose 1,6-bisphosphatase (FBPase) and sedoheptulose-1,7-bisphosphatase (SBPase) which have previously been described as thioredoxin system targeted enzymes. The redox regulated proteins identified in the current study were compared to several published, independent results showing redox regulated proteins in Arabidopsis leaves, root, mitochondria and specifically S-nitrosylated proteins. These proteins were excluded as potential new candidates but remain as a proof-of-concept to the enrichment experiments to be effective. Additionally, CSP41A and CSP41B proteins, which emerged from this study as potential targets of redox-regulation, were analyzed by Ribo-Seq. The active translatome study of *csp41a* mutant *vs.* wild-type showed most of the significant changes at end of the night, similarly as *csp41b*. Yet, in both mutants only several chloroplast-encoded genes were altered. Further studies of CSP41A and CSP41B proteins are needed to reveal their functions and elucidate the role of redox regulation of these proteins.

Zusammenfassung

Wenn Proteine synthetisiert sind, können sie zusätzlich noch post-translationelle Modifikationen (PTM) aufweisen. Proteine, die wegen ihres lokalen Umfeldes reaktive Cysteinthiole in ihrer stabilen deprotonierten Thiolat-Form aufweisen, dienen als Redoxsensoren indem sie eine Vielzahl von oxidativen PTMs (Ox-PTMs) enthalten können. Ox-PTMs wie die S-Nitrosylierung oder die Bildung von Inter- oder Intradisulfidbrücken induzieren funktionelle Veränderungen in diesen Proteinen. Cystein-haltige Proteine, deren Funktion durch diese Thioloxidierung gesteuert werden, gehören zu dem so genannten Redoxom. Die Ox-PTMs werden durch ortsspezifische zelluläre Prozesse gesteuert, die eine essentielle Rolle bei der Proteinregulation spielen und welche das katalytische Zentrum, die Ligandenbindungsaffinität, Protein-Protein-Interaktionen oder die Proteinstabilität beeinflussen können. Die umkehrbare Proteinthioloxidierung ist ein essentieller regulatorischer Mechanismus in der Photosynthese, dem Metabolismus und der Genexpression photosynthetischer Organismen. Es ist demnach wichtig PTMs zu untersuchen, um zu verstehen wie sich Pflanzen an externe Stimuli wie das Licht anpassen können. Es ist von großer Bedeutung für das Redoxom-Forschungsgebiet Methoden zur Untersuchung von pflanzlichen Ox-PTMs zu verbessern. Die vorliegende Arbeit konzentriert sich auf Thiolveränderungen, die in Pflanzen auftreten, und gibt einen Einblick in das *in vivo* Redoxom von *Arabidopsis thaliana* als Reaktion auf Licht oder Dunkelheit. Dieses wurde ermöglicht durch eine auf Harz-basierende Thiol-Anreicherung. Darüber hinaus konnten Kandidaten auf dem Einzelproteinlevel durch eine Differentialmarkierungsmethode bestätigt werden. Thiole und Disulfide wurden unterschiedlich markiert und die Proteine durch spezifische Antikörper mittels Proteinblotanalyse erkannt. Weitere Analysen fokussierten sich auf im Licht reduzierte Proteine. Durch die Anreicherungsmethode konnten viele bereits untersuchte redox-regulierte Proteine identifiziert werden. Unter diesen waren unter anderem die Fruktose-1,6-Bisphosphatase (FBPase) sowie die Seduheptulose-1,7-Bisphosphatase (SBPase), welche als Thioredoxin-gesteuerte Enzyme beschrieben sind. Die redox-regulierten Proteine, die in dieser Studie identifiziert werden konnten, wurden mit veröffentlichten unabhängigen Ergebnissen verglichen und dieses führte zu einer Vielzahl an redox-regulierten Proteinen in Arabidopsisblättern, -Wurzeln und -Mitochondrien sowie S-nitrosylierten Proteinen. Diese Proteine wurden zwar als neue potentielle Kandidaten ausgeschlossen, zeigten allerdings die Effektivität der Anreicherungsmethode. Darüber hinaus wurden die Proteine CSP41 A and CSP41 B, welche in dieser Studie als potentielle Ziele der Redox-Regulation identifiziert wurden, durch Ribo-seq analysiert.

Acknowledgments

I would like to thank my PhD Advisory Committee members: Dr. Ute Armbruster, Professor Dr. Alisdair Fernie and Dr. Mark Aurel Schöttler for their advice and support. I am grateful especially to Dr. Armbruster for her scientific input, her kindness and understanding. I would like to also especially thank to Prof. Dr. Fernie for his scientific advice and expertise.

I would like to thank Dr. Alexander Graf for his supervision at the beginning of my PhD and to my principal supervisor Professor Dr. Mark Stitt.

I would like to acknowledge all the members of AG Armbruster, AG Fernie and AG Graf for good working atmosphere and help.

I would like to thank my friend Dr. Michal Gorka for sharing his knowledge and experience with mass spectrometry. Also to all my collaborators and especially to: Dr. Haim Trebes, Dr. Ewelina Sokolowska, Dr. Arkadiusz Zupok and Dr. Aleksandra Skirycz.

Finally, I would like to thank my family, especially my sister for her support and my nephew for cheering me up, my friends, especially to Dr. Dema Alhajturki, Liliana Calzadiaz Ramirez, Dr. Venkatesh Periyakavanam Thirumalai Kumar, Michal Uflewski, Dr. Tanja Seibert and Dr. Franziska Fichtner. List of all the great people that I have met during my PhD would be longer than the thesis itself, thank you all!

Contents

List of tables

List of figures

List of supplemental tables

List of abbreviations

ADP - Adenosine diphosphate

AGC - ascorbate-glutathione cycle;

AGPase - ADPGlc pyrophosphorylase

AMP - adenylyl 5′-monophosphate

ATP - Adenosine triphosphate

BN - Blue Native

CBB - Calvin–Benson–Bassham cycle

CSP41A- Chloroplast stem-loop binding protein of 41 kDa A

CSP41B - Chloroplast stem-loop binding protein of 41 kDa B

Cytb6f - cytochrome b6f comlex

DNA - Deoxyribonucleic acid

EOD - end of the day

EON - end of the night

FBPase - fructose 1,6-bisphosphatase

FDR - false discovery rate

FTR - Ferredoxin-Thioredoxin Reductase

GO - glycolate oxidase

IAM - iodoacetamide

LC-MS/MS - liquid chromatography – Tandem mass spectrometry

LHCII - light harvesting complex II

mRNA- Messenger RNA

MPI - Max Planck Institute

NADP - Nicotinamide adenine dinucleotide phosphate

NADPH - reduced form of NADP+

NEM - N-ethylmalemide

NPQ - non-photochemical queanching

OPPP - oxidative pentose phosphate pathway

Ox-PTM - Oxidative post-translational modification

PC - plastocyanin

PGR5 - proton gradient regulation 5

PGRL1 - proton gradient regulation 5 like 1

PQ - plastoquinone

PSI - photosystem I

PSII - photosystem II

PTM - Post-translational modification

RNA - Ribonucleic acid

RNS - reactive nitrogen species

ROS - reactive oxygen species

RSS - reactive sufur species

SOD - superoxide dismutase

CAT - catalase

SOQ1 - Supressor of Quenching 1

TCA - tricarboxylic acid cycle

TCAH - trichloroacetic acid

TRX - thioredoxin

WWC - water-water cycle

1. Introduction

1.1. Protein post-translational modifications (PTM)

A central dogma of biology formulates that the coding information within the cell is stored as deoxyribonucleic acid (DNA), is transcribed into ribonucleic acid (RNA), to be then translated into protein. The basic DNA chain of a cell provides few possibilities to encode for proteins. The possibilities for the final protein structure are further expanded at the level of the messenger RNA (mRNA) by, among others, the presence of alternative promoters, variations in mRNA transcription initiation, and termination, alternative splicing of transcripts (Chorev et al., 2015). Protein levels can further be determined by transcript levels and transcript stability, as well as processes on the translational and post-translational level. Once proteins are synthesized they can additionally be modified by post-translational modifications (PTMs). PTMs occur in various forms including (i) a covalently bound chemical group (i.e., phosphorylation, acetylation, methylation, and redox-based modifications), (ii) a covalently bound polypeptide (i.e., ubiquitination, ubiquitin-like protein conjugation and SUMOylation) and (iii) a covalently bound complex molecule (i.e. acylation, prenylation, glycosylation, ADP-ribosylation, AMPylation). Additionally, amino acids may be directly modified (e.g., deamidation, eliminyolation) or proteins may be cleaved at target sequences (Figure 1) (Spoel, 2018). This thesis mainly focusses on thiol modifications. In plants these PTMs serve an important function to regulate protein and enzyme activities in response to light and oxidative stress.

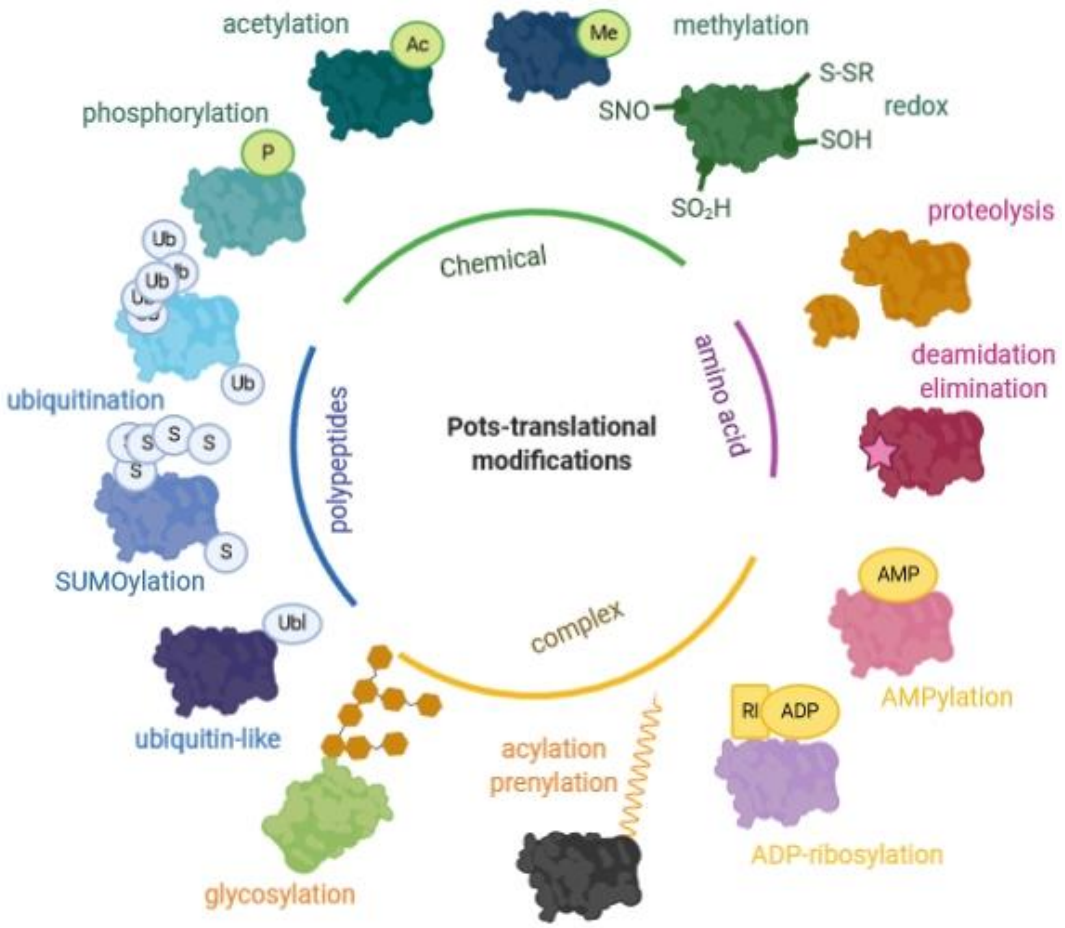

Figure 1 Variation of PTMs
This diagram illustrates the variety of PTMs with regard to their type. Notably, chemical modification such as phosphorylation (P), acetylation (Ac), methylation (Me) and redox based modifications like S-nitrosylation (SNO), thiolation (S-S), S- sulfenylation (SOH) and sulfination (SO_2H) are reversible. Polypeptide modifications like ubiquitination (Ub) and ubiquitin-like (Ubl) or SUMOylation are enzymatically reversible. Modifications by complex molecules are also reversible and include glycosylation and lipidation, ADP-ribosylation (Ri-ADP) and other. Other modifications of amino acids or polypeptide backbone, such as deamidation, eliminylation and cleavage by proteolysis, are irreversible (figure after (Spoel, 2018 . Figure prepared using BioRender.

1.2. Protein thiol modifications

Often thiols are oxidized to form disulfide bridges. In the endoplasmic reticulum (ER), where conditions are oxidizing, disulfide formation contributes to protein folding and structure (Onda, 2013). Proteins are then exported outside of the cell, where conditions are also oxidizing. Disulfide bridge formation also occurs when the redox potential of the cell or compartment decreases, with the resulting disulfide bridges subsequently leading to a functional change in the protein (e.g. changing enzymatic activity). While the other oxidative thiol modification (besides disulfide bridges), occur when thiols react with oxidant molecules

such as reactive oxygen species, reactive nitrogen species and reactive sulfur species (ROS, RNS, RSS, respectively). Previously these molecules had been considered as toxic byproducts of metabolism only (Mittler, 2017). However, they are now emerging as important signalling molecules, which perform part of their regulatory function by generating Ox-PTMs (Foyer and Noctor, 2005). Although proteins make up to 68% of the oxidation targets in the cell, carbohydrates, unsaturated lipids and nucleic acids are also subjected to oxidative modifications (Rinalducci et al., 2008).

Proteins with cysteines, whose thiol oxidation state controls their functions, belong to the so-called redoxome. These proteins contain reactive cysteine thiols, which are stabilized in their deprotonated form due to their local environment as thiolates (RS^-). Thiolates serve as redox sensors by undergoing a multitude of modifications (Figure 2, Burgoyne and Eaton, 2010). Most redox modifications occur non-enzymatically, and are mediated by a spontaneous reaction with ROS, RNS or RSS. A general notion is that all the types of modifications are randomly spread across the proteome. However, emerging evidence indicates that thiol redox modifications are tightly controlled by site-specific cellular events, that play an important role in protein regulation by either affecting enzyme catalytic sites, ligand binding affinity, protein-protein interactions or protein stability (Yang and Lee, 2015).

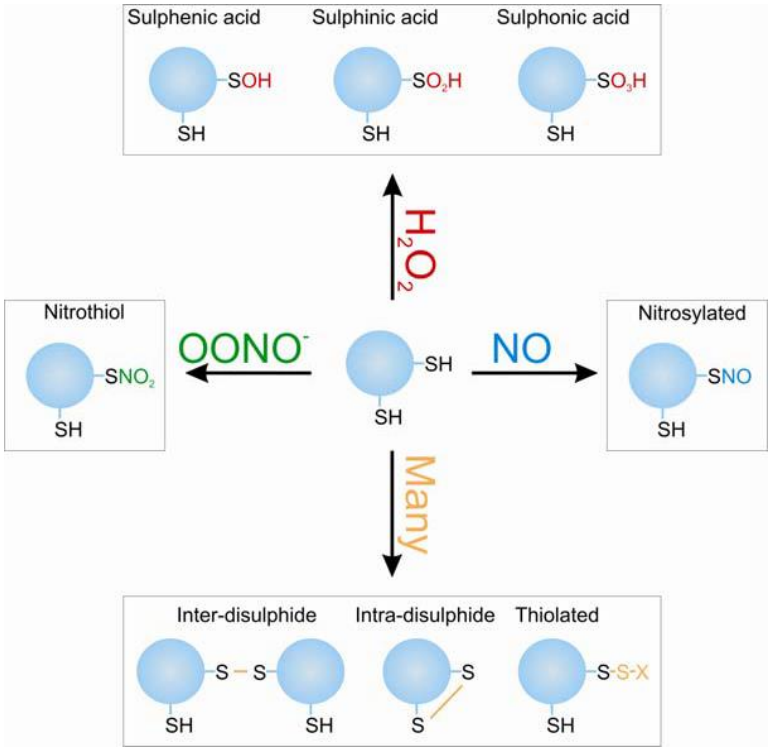

Figure 2 Redox modification of proteins
An overview of Ox-PTMs formed with cysteine residues. The figure shows a target with two thiols reacting with various oxidants. Reaction with peroxynitrate ($ONOO^-$) leads to formation of nitrosothiol (SNO_2); hydrogen peroxide (H_2O_2) leads to sulphenic acid (SOH), sulphinic acid (SO_2H) or sulphonic acid (SO_3H); with nitric oxide (NO•) leads to nitrosylation (SNO); many other oxidants lead to formation or inter- or intra-disulphide or other modifications (reviewed by Burgoyne and Eaton, 2010).

1.3. Ox-PTMs as switch between light and dark metabolism

During the day, light energy is the natural and plentiful energy source for plant metabolism. The biological process photosynthesis converts light energy into chemical potential initially in the form of the reducing equivalent dihydronicotinamide-adenine dinucleotide phosphate (NADPH) and the energy equivalent adenosine triphosphate (ATP). These are then used to drive plant metabolism including the fixation of carbon via the Calvin-Benson-Basham cycle. In the day, transitory storage carbohydrates (mainly starch) are build that can then be used as the energy source in the night to drive plant metabolism (Scialdone et al., 2013). Clearly, this bipartite metabolism of plants has to be reflected on the level of the activity of enzymes involved in either day or night metabolism. Here, Ox-PTMs play an important role. During the day, light energy is used to oxidize water and transfer the electrons via multiple electron transfer reactions to NADPH (reduced form NADP) forming NADP+ (oxidized from NADP). $NADP^+$ is reduced by ferredoxin (Fd), which in turn receives the electrons from photosystem I (PSI). When reduced Fd and NADPH accumulate in response to

light, they act as signalling molecules to feed forward on multiple enzymatic reactions located in the chloroplast, which are necessary for metabolism during the day (Kaiser et al., 2018). This feed-forward activation of enzymes by reducing Ox-PTMs is mediated via the thioredoxin system (Figure 3). When light is turned off, another thioredoxin system coupled with peroxiredoxins catalyzed the reoxidation of thiols and thus a change in the activity of the target enzyme (Martins et al., 2018; Sugiura et al., 2019).

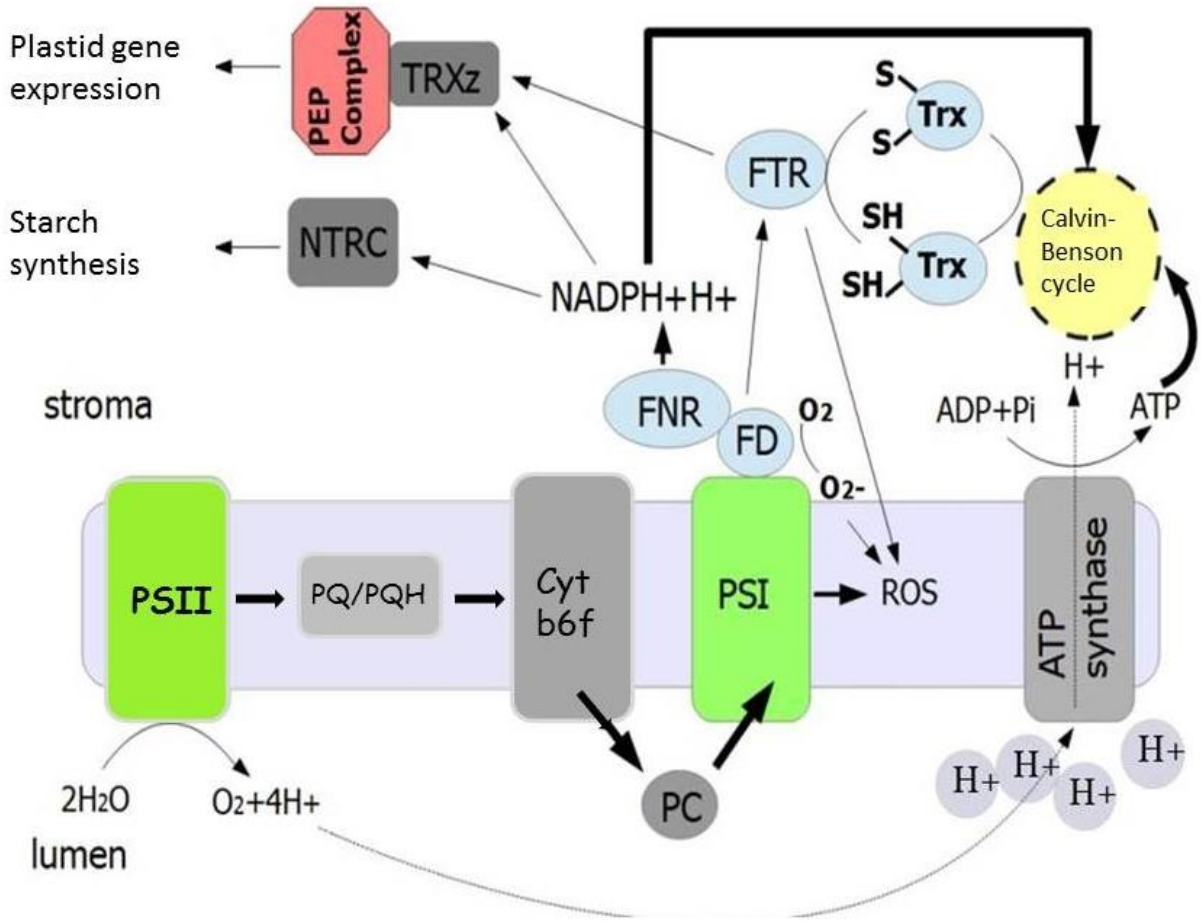

Figure 3 Photosynthetic electron transfer chain pathways
The thylakoid membrane with PSII, Cyt b6f, PSI and the ATP synthase. The thin black lines represent electrons transport directions. ROS are mainly generated by PSI. Additionally, the cartoon also depicts the interplay of Trxs with the Calvin-Benson Cycle and PEP complex. Ndh - NADH dehydrogenase-like, PQ/PQH – plastoquinone (oxidized/reduced), PC-plastocyanin, FD – ferredoxin, FNR - ferredoxin-NADP+ reductase, FTR - Ferredoxin-Thioredoxin reductase, TRX – thioredoxin, PEP complex - plastid-encoded RNA polymerase complex, Cytb6f – cytochrome b6f, PSI – photosystem I, PSII – photosystem II (modified after Shaikhali and Wingsle, 2017 .

The chloroplast thioredoxin system regulates metabolism in response to dark and light. Thioredoxins (TRXs) are ubiquitous small oxidoreductases (approximately 12 kDa) (Schurmann and Jacquot, 2000). At least seven types of TRXs (f, m, x, y, z, h, and o), comprising more than 20 isoforms have been identified in *Arabidopsis thaliana.* They are located in all cellular compartments, i.e. the plastids, mitochondria, and cytosol (Meyer et al., 2005). Most TRXs can be reduced by donation of an electron from reduced Ferredoxin via the reactions catalyzed by ferredoxin-thioredoxin reductase (FTR). TRX z has different properties as it can be reduced by TRX f, m, x, and y but not by FTR (Bohrer et al., 2012). In Arabidopsis, three NADPH-dependent thioredoxin reductases (NTR) isoforms have been identified in mitochondria (NTRA), cytosol (NTRB) and chloroplast (NTRC). NTRC has an additional Trx domain in contrast with NTRA and NTRB (Moon et al., 2006). Five types of TRXs are localized to the chloroplast (f, m, y, and z). The chloroplastic drought-induced stress protein of 32 kDa (CDSP32), six ACHT-type and two WCRKC-type proteins belong to the chloroplast TRX-like proteins having an atypical redox-active motif in the active site of the regulatory protein (Meyer et al., 2008). The mechanism of transmitting the light signal from ferredoxin to FTR and thioredoxin to target enzyme are well described for regulated enzymes such as fructose 1,6-bisphosphatase (FBPase), sedoheptulose bisphosphatase (SBPase) or ADPGlc pyrophosphorylase (AGPase) (Geigenberger and Fernie, 2014). However the mechanism of deactivation has only recently become understood (Buchanan and Balmer, 2005). The oxidation cascade *in vivo* has been elucidated in several landmark publications (Ojeda et al., 2018; Vaseghi et al., 2018). In the dark, reducing equivalents are transferred from the target enzymes to Trx, then to 2-cys peroxiredoxin (2CP), and finally to H_2O_2. Furthermore, a previously unknown Trx-like 2 protein (TrxL2) was identified as a main oxidant of enzymes upon darkening (Yoshida et al., 2018). Light activation of glucose-6-phosphate dehydrogenase is also linked to this cascade according to new studies (Yoshida et al., 2019). A substantial body of evidence suggests that PSII is also linked to a network where light regulation plays a role, and as well redox regulation. The Light Harvesting Complex II (LHCII) functions as a mediator for efficient light energy distribution between PSI and PSII. It is known that a small part of total LHC-II undergoes reversible phosphorylation in response to low or medium light. The model most widely accepted for sensing the imbalance in excitation is based on phosphorylation of LHC-II by a redox regulated kinase. The kinase is activated depending on plastoquinone (PQ) reduction (Gal et al., 1997). Apart from the PQ mechanism, LHC-II is also regulated by a PSI thiol-based system. The evidence comes from studies undertaken in *Chlamydomonas* where a LHC-II protein kinase was identified (Nield et

al., 2004). In the light, thioredoxins and other thiols in the stroma become reduced. The inhibition occurs only in case the kinase is in a fully oxidized state, as determined by its association with the oxidized cytochrome *b*6*/f* complex. When thioredoxin becomes more oxidized, LHC-II kinase returns to the deactivated state (Depege et al., 2003).

1.4. Light dependent thiol modifications of proteins in plants

Light induces thiol-disulfide exchange, modulating plant metabolism and switching it between dark respiration and photosynthesis. Light exposure leads to production of NADPH as a reducing equivalent which drives the ferredoxin/thioredoxin system. The chloroplast enzymes of CBB were the first to be linked to redox regulation. CBB is strictly controlled by light, with its enzymes, with the exception of glucose-6-phosphate dehydrogenase, activated in light and deactivated in dark (Jacquot, 2018). The biochemical investigation of the light activation and dark deactivation led to the discovery of the ferredoxin/thioredoxin system. The reduced Trx is the main activator of redox regulated enzymes. The deactivation in the dark is also linked to a chain of actions involving Trx (Figure 4). The chain is composed of Trx, 2 Cys peroxiredoxin, and H_2O_2 as recently shown by Yoshida *et al.* (Yoshida et al., 2018).

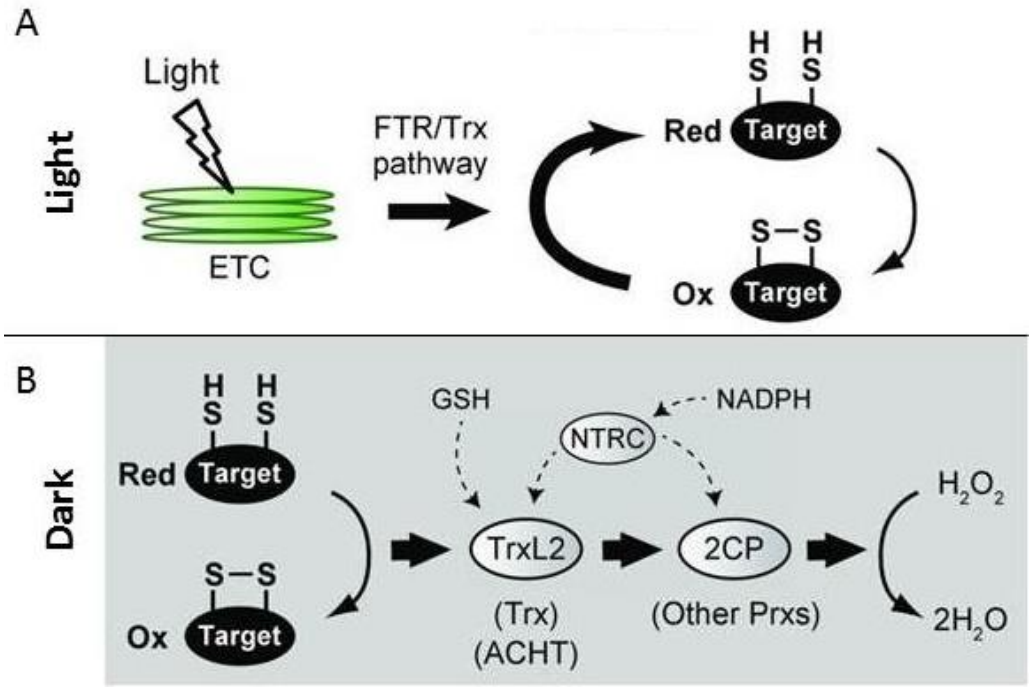

Figure 4 Simplified working model of chloroplast Trx regulation
(A) The widely studied and generally accepted model of light activation of target enzymes by TFR-Trx system. (B) The new model of dark deactivation of target enzymes by oxidation via the TrxL2/2CP.
(After Yoshida et al., 2018)

1.4.1. The Ox-PTMs in homeostasis

The accumulation of ROS has been shown to occur during developmental processes such as extracellular ATP signalling (Song et al., 2006), root growth (Foreman et al., 2003), gravitropism (Joo et al., 2001), , and pollen-tube growth (Potocký et al., 2007). Nevertheless, the best studied examples of proteins under ox-PTM regulation to date are those of enzymes involved in the Calvin-Benson-Bassam cycle (Schurmann and Buchanan, 2008), sulfur metabolism (Kopriva et al., 2012), and starch metabolism (Glaring et al., 2012). There is also substantial knowledge about transcription factors regulation by redox signaling system (Dietz, 2014).

1.4.1.1. Photosynthesis, metabolism and gene expression

1.4.1.1.1. Redox dependent gene expression

In plants many transcription factors (TF) are linked with redox homeostasis. Examples of early response to stimuli like increasing temperature and other factors are heat shock factors (HsF). HSFA1D was shown to translocate to the nucleus under an excess of high light (Jung et al., 2013). Another member of this family, HSFA8 was shown to be responsive to increasing H_2O_2 (Dietz, 2014). Several transcription factors involved in plant development were also shown to be redox regulated. A transcription factor ATHB9 that controls shoot patterning by affecting meristem development, organ polarity and vascular differentiation has three conserved cysteines, two of them in its DNA binding domain. DNA binding is only possible when the two cysteines are in the reduced state; activation of this TF is dependent on Trx (Comelli and Gonzalez, 2007).

1.4.1.1.2. Redox dependent key metabolic pathways

Miotchondra house the tricarboxylic acid (TCA) cycle, which plays a central role in adenosine triphosphate (ATP) generation and providing carbon skeletons for a range of biosynthetic processes. Mitochondria harbor a Trx system similar to that of the chloroplast. Double mutant of cytosolic and mitochondrial NADP-TRX reductase a and b (*ntra/ntrb*) and mitochondrial TrxO1 mutant (*trxo1*) were shown to have an impact on TCA cycle enzymes, independent from chloroplast activity. A decrease of ATP-citrate lyase (ACL), succinyl-CoA ligase (SCoAL), and mitochondrial/cytosolic NAD^+-dependent MDH was observed in both mutants, while an increase was observed in fumarase (FUM), citrate synthase (CS), succinate dehydrogenase (SDH) and aconitase (ACO). Furthermore, CS, SDH, FUM and ACL were confirmed as Trx targets *in vitro.* Trxs were identified as master regulators in TCA cycle itself and associated citrate shunt pathway (Daloso et al., 2015). Another study elucidated in detail

the regulation of CS by disulfide bridge formation. In its inactive form, CS is a dimer formed by intramolecular disulfide bridge by Cys_{325}, with activation dependent on reduction by Trx followed by folding into an active dimer independent on disulfides (Schmidtmann et al., 2014). An *in vivo* decrease of cytosolic MDH (cytMDH1) activity was also observed in the H_2O_2 scavenging enzyme catalase mutant (*cat2*), and once more in *ntra/ntrb* mutants, that were shown to have lower Trx-h activity. An intramolecular disulfide bond by Cys_{330} introduced by cytosolic Trx was shown to play a role in the enzymes's self-protection against over oxidation. Importantly it was shown that the cytosolic and chloroplastic isoforms of MDH are sensitive to H_2O_2 stress, but not the mitochondrial form (Huang et al., 2017).

1.4.1.1.3. Redox regulation of photosynthesis in chloroplast

In plastids, two forms of Trx system are present, and over 20 Trx isoforms (Meyer 2012). The ferredoxin-dependet Trx (Fd-Trx) system mainly operates in light, as it receives the reducing equivalent from PSI via reduced ferredoxin and ferredoxin-thioredoxin reductase (FTR). The involved Trxs are Trxf1 and Trxf2; four isoforms of Trxm, Trxx, Trxy1 and Trxy2 (Schurmann and Buchanan, 2008). This system is involved in CBB enzyme light activation (Geigenberger and Fernie, 2014), starch synthesis (Thormahlen et al., 2013), ATP synthesis (Hisabori et al., 2013) and malate-oxaloacetate shuttle (Miginiac-Maslow et al., 2000). Moreover Trxy1 and Trxy2 are involved in oxidative stress and Trxz in regulation of transcription in plastids (Collin et al., 2004; Arsova et al., 2010). The second Trx system operating in the chloroplast is dependent on NADPH. A single enzyme is mainly involved in this system, namely NADPH-dependent thioredoxin reductase (NTRC). NTRC has the ability to function in the dark due to NADPH production by oxidative pentose phosphate pathway (Cejudo et al., 2014).

Beside the specialized functions of FTR and NTRC dependent thioredoxin systems a cross talk between the two and redundancy was investigated. It was shown that NTRC interacts with CF1γ subunit of the ATP synthase; this was suggested to be important for *in vivo* activation of ATP synthase in low light conditions (Nikkanen et al., 2016). A crosstalk of Trxs' was also shown due to ability of not only Trxf but also Trxm1, 2 regulating CBB (Okegawa and Motohashi, 2015). Again NTRC was identified to be a player in CBB regulation under low light (Nikkanen et al., 2016).

1.4.2. The Ox-PTMs in stress

Oxidative stress occurs in plants as a result of various abiotic stressors such as high temperature (heat), drought stress/dehydration, heavy metal toxicity, salinity, and biotic stressors such as herbivory and plant-pathogen attack. Under these conditions ROS levels increase, resulting in oxidation of DNA, lipids and proteins. However, during plant adaptation, ROS is scavenged and repair mechanisms reduce at least some of the oxidized molecules. At the same time ROSs function as signaling molecule in plant adaptation to stress encounters (Krishnamurthy and Rathinasabapathi, 2014). The balance between production and metabolism of ROS is crucial to determine the cell fate. Among ROS H_2O_2 (hydrogen peroxide) seems to best studied model for a signalling molecule due to its higher stability and longer half-life. ROS such as O_2^- (superoxide), $^1O_2$ (singlet oxygen), HO (hydroxyl radical). or H_2O_2 (hydrogen peroxide) have different half-lives and affinity to other molecules, among those $^1O_2$, HO are very short lived and highly reactive, while H_2O_2 has lower reactivity and a longer half-live (Neil et al., 2002). Excess H_2O_2 generation occurs after plant exposure to excess of excitation energy, extreme temperatures, ozone exposure, imbalance in phytohormone levels, dehydration, UV irradiation, wounding and pathogen attack (Karpinski et al., 1999). H_2O_2 is also generated enzymatically in response to specific environmental stimuli; primarily it comes from the activity of Respiratory burst oxidase homolog protein D oxidase (RBOHD oxidase), NADPH oxidase, cell wall peroxidases, amine oxidase, oxalate oxidase and flavin-containing oxidases (Bolwell et al., 2002). Independently of its source, H_2O_2 acts by inducing molecular and physiological responses within a cell. Additionally, H_2O_2 functions as an integrator of signalling pathways (Bowler and Fluhr, 2000). For example pre-exposure to heat stress induces tolerance towards subsequent pathogen attack and the response is linked to oxidative burst co-occurring with heat treatment (Vallelian-Bindschedler et al., 1998). One emerging model in stress adaptation is the change in ratio between reduced and oxidized glutathione (GSH/GSSG) levels (Figure 5) following production of H_2O_2 that constitute the early changes leading to physiological response or modification of gene expression (Trewavas and Malho, 1997). According to this process, increases in H_2O_2 and subsequent changes in the ratio between GSH and GSSG, redox signaling seems to be involved in acclimation to chilling by specific transcription factors activation and antioxidative enzymes. It was shown that priming the seedlings with H_2O_2 induces stress tolerance mechanisms leading to increase tolerance to chilling, drought, pathogen etc., (Yu et al., 2003) (Hilker et al., 2016).

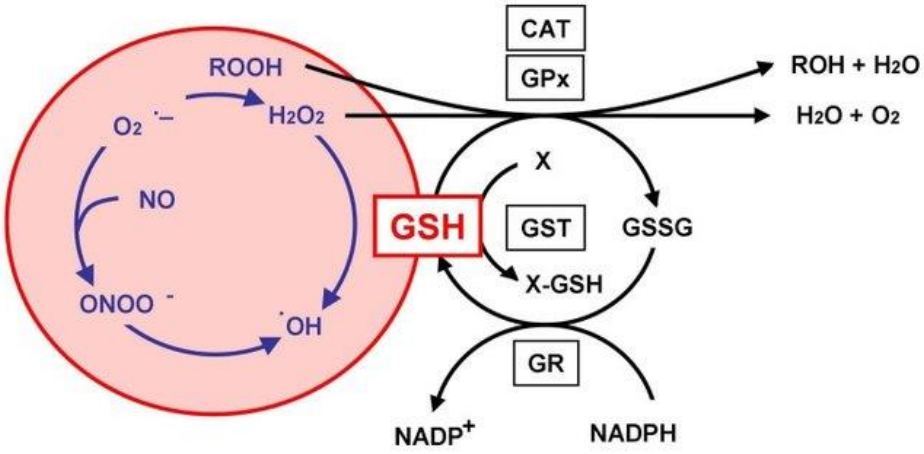

Figure 5 Simplified overview of the glutathione system
In the center of the cycle is glutathione (GSH) as an antioxidant. The enzyme specifically degrading hydrogen peroxide (H_2O_2) water and hydroperoxides (ROOH) to alcohols is GSH peroxidase (GPx). The oxidized form of GSH is GSH disulfide (GSSG), which can be reduced back to GSH in a reaction of GSH reductase (GR) with NADPH. H_2O_2 but not ROOH can be removed under physiological conditions by catalase. GSH is able to form conjugates with plethora of andogenous and xenobiotic compounds (X). Removal of those is mediated by GSH-S transferase (GST). GSH also takes part in non-enzymatic reactions with superoxide (O_2•−), nitric oxide (NO), hydroxyl radical (•OH), and peroxynitrite (ONOO−)(Aoyama and Nakaki, 2012).

1.5. Examples of known redox regulated enzymes

Pioneers of redox studies identified redox state change of cysteine residue as a switch of function in enzymes involved in photosynthesis. Over the years more processes have been identified as redox regulated. Enzymes of processes such as carbon assimilation, seed germination, transcription, translation, cell-division, redox-signaling, radical scavenging and detoxification have been linked to regulation by Ox-PTMs (Montrichard et al., 2009). Besides these, the fluctuation in light intensity and their balance in plant photosynthetic and metabolic pathways have not been yet studied in detail and the aid of new methods could potentially be used to investigate the relationship between light intensities and cellular fitness (Figure 6).

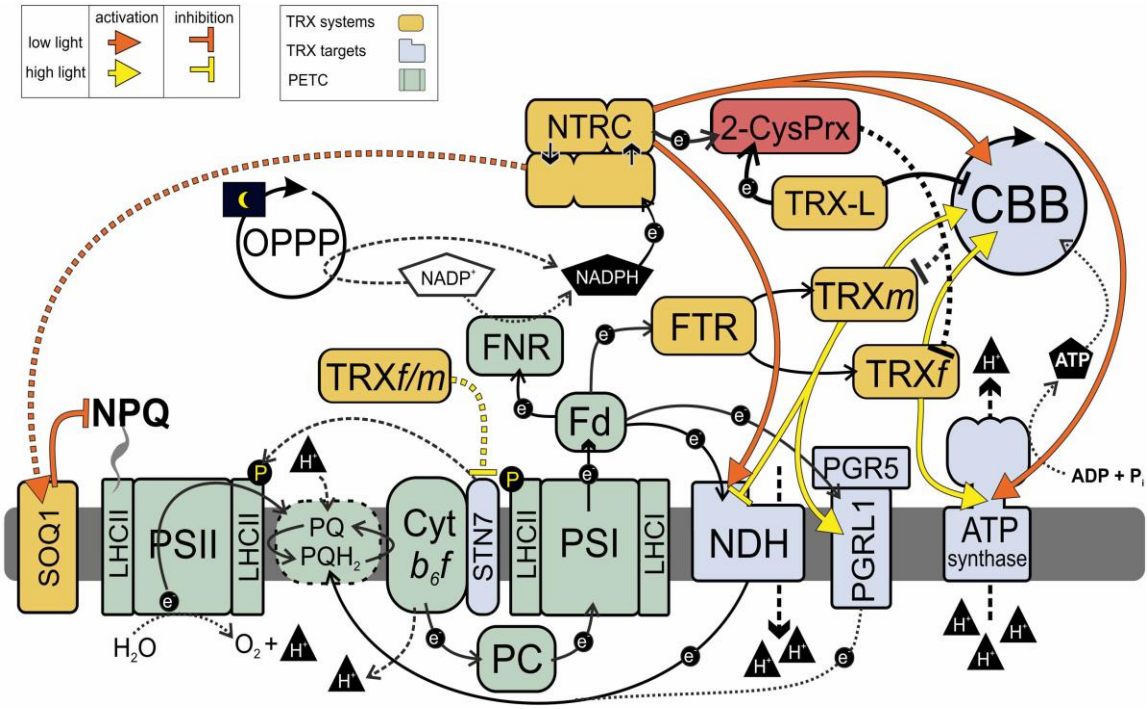

Figure 6 Photosynthesis balancing by FTR-Trx system
FTR-Trx system and NTRC in light transition from dark to light and from low to high light. Dotted arrows represent hypothetical effects. The redox regulation concept in plants grew fastly from simple idea of Trx system to this complex and multi-player research field.

SOQ1 - Supressor of Quenching 1; NPQ – non-photochemical quenching; OPPP - oxidative pentose phosphate pathway; TRXf/m – thioredoxin family f or m; TRXf – thioredoxin f; TRXm – thioredoxin m; TRX-L – thioredoxin L; LHCII – light harvesting complex II; PSII – photosystem II; PQ – plastoquinone; PQH_2 - reduced plastoquinone; $Cytb_6f$ – cytochrome b_6f comlex; STN7- protein kinase; required for state transitions, phosphorylation of the major antenna complex (LHCII) between PSII and PSI, and light adaptation; PC – plastocyanin; PSI – photosystem I; NDH - NADH dehydrogenase-like (NDH) complex; PGRL1 – proton gradient regulation 5 like 1; PGR5 – proton gradient regulation 5; FTR - ferredoxin-thioredoxin Reductase; CBB – Calvin–Benson–Bassham cycle; 2-CysPrx - 2-cysteine peroxiredoxin (After Nikkanen and Rintamaki, 2019).

1.5.1.1. Fructose 1,6-bisphosphatase (FBPase) light induced redox modifications

Chloroplast fructose 1,6-bisphosphatase (ctFBPase) catalyses the hydrolysis of fructose 1,6-bisphosphate to fructose 6-phosphate and P_i in the Calvin-Benson-Bassham cycle (CBB). Since the reaction is irreversible it is an important point of CBB regulation. FBPase functions as a homotetramer. FBPase is a well-known target of Trx f. Chloroplastic FBPase as opposed to the cytosolic one contains 3 cysteines placed in the regulatory loop and allowing for the redox regulation of the enzyme, by formation of disulfide bridge. The cysteines were numbered based on *Pisum sativum* (C_{173}, C_{178}, and C_{153}). C_{153} was shown as an important residue in formation of the regulatory intermolecular bridge with C_{173}, a cysteine to serine mutation at 178th residue was shown to be involved in the bridge formation (Balmer et al.,

2001). In the oxidized form the ctFBase has a loop with 3 cystienes being stabilized with the disulfide bridge. While in reduced form, the loop is loosened, enabling an efficient binding of Mg^{2+} and the substrate (fructose biphosphate), leading to increased FBPase activity. Oxidized FBPase has a basal activity (20-30%) and becomes fully active after reduction of disulfide by Trx-f (Figure 7). For the enzyme to stay active components of the Fdx/Trx system need to be maintained in a highly reduced state, FBPase is highly susceptible to oxidation by various oxidants (Schurmann and Buchanan, 2008).

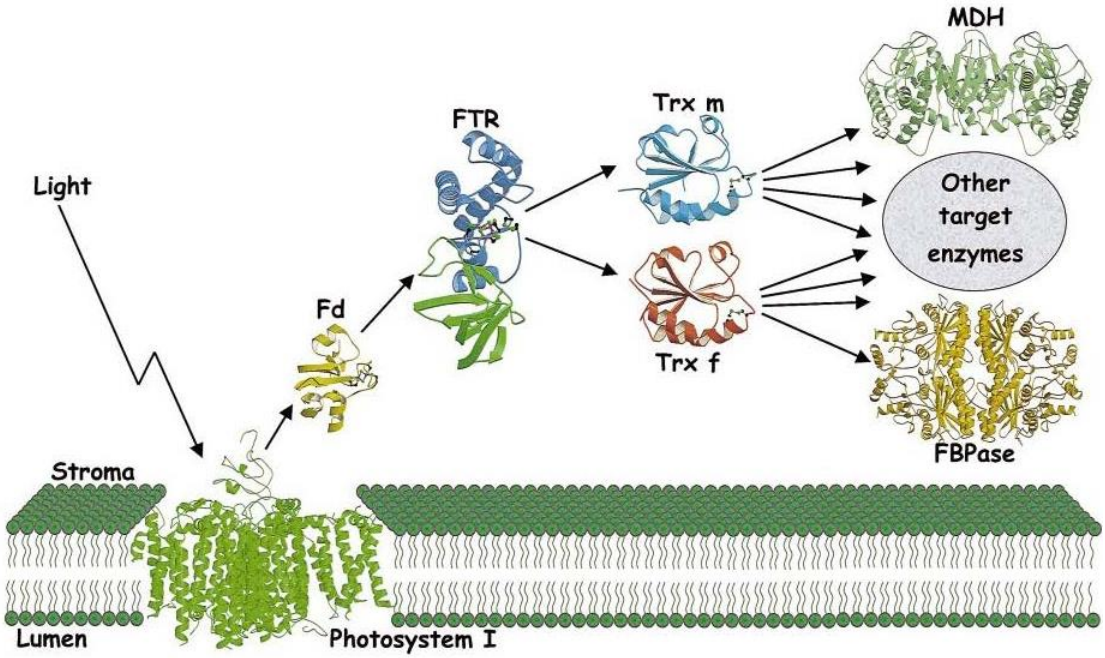

Figure 7 FBPase activation by the ferredoxin-thioredoxin system
The FTR-Trx system provides reducing equivalents for FBPase reduction. Upon illumination electron transfer chain reduces Fd by PSI, Fd reduces FTR, FTR reduces Trxs e.g. Trxm and Trxf. Trxf is the main regulator of FBPase, the enzyme is activated upon reduction.

Recently a cross-talk between Ox-PTMs of FBPase was revealed by a series of studies *in vitro* and *in vivo* on *Pisum sativum* FBPase. The *in vitro* assays revealed C_{153} to be nitrosylated. Light dependent S-nitrosylation was detected *in vivo* on reduced FBPase after GSNO infiltration. ctFBPase was nitsoylated in *P. sativum* leaves under light, but an opposite was detected under dark cycle. The *P. sativum* Trx-f was shown to have denitrosylated the protein. An interesting model was proposed for nitrosylation as a control module for FPBase in pea (Figure 8) and conserved in other species such as *Arabidopsis thaliana* (Serrato et al., 2018). It is tempting to conclude C_{49} and C_{190} of ctFBPase are involved in bridge formation, after the *in vitro* assays in *Spinacia oleracea*, the functional role behind this modification remain to be investigated (after .

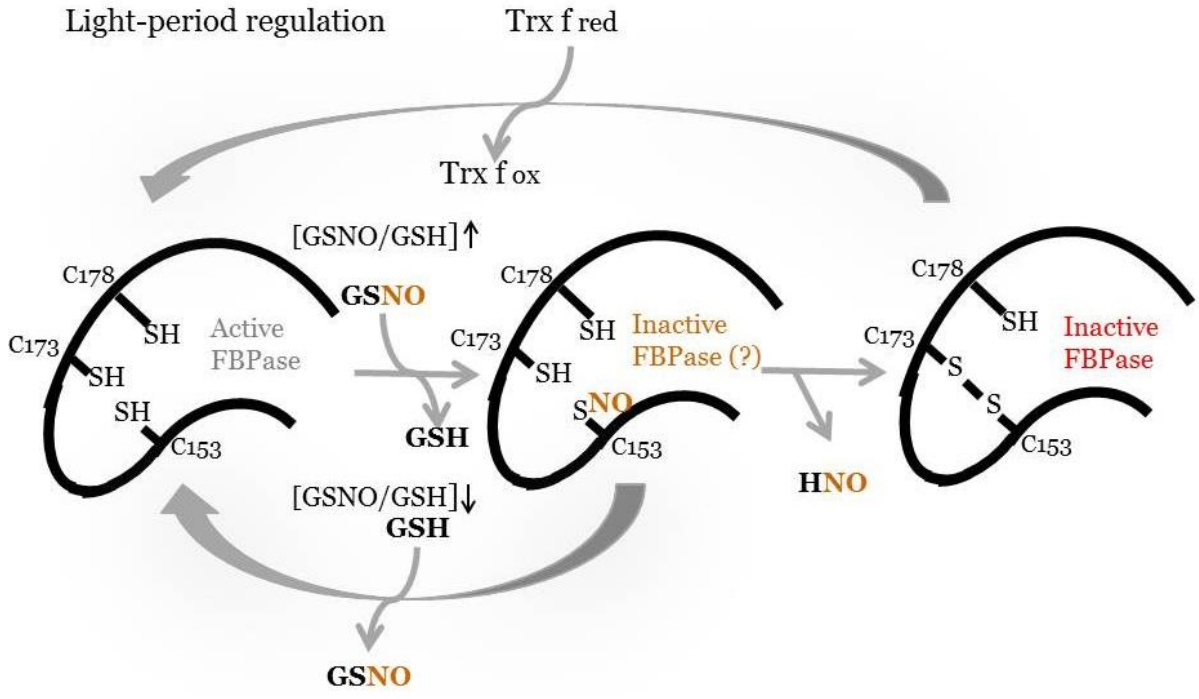

Figure 8 A model of FBPase regulation, as proposed by Serrato et al.
Regulation of the disulfide bridge of FBPase is provided by Trxf, yet the S-nitrosylation of C_{153} is mediated by GSNO triggers formation of the regulatory disulfide bridge between C_{153} and C_{173} even in the light period when FBPase is kept reduced by Trxf (after Serrato et al., 2018).

1.5.1.2. Dusk to Dawn regulation of ADP-glucose pyrophosphorylase (AGPase)

ADP-glucose pyrophosphorylase (AGPase) catalyzes the first step in starch synthesis reaction. In higher plants the enzyme is a hetero tetramer that contains two regulatory and two catalytic subunits (AGPS, 51kDa and AGPB, 50kDa, respectively). The enzyme activity is known to be under allosteric regulation with glycerate-3-phosphate (3PGA) as an activator and inorganic orthophosphate (Pi) as an inhibitor(Sowokinos, 1981). 3PGA is phosphorylated and reduced by the products of photosynthetic electron transport (ATP and NADPH) to produce triose phosphates (triose-P). The triose-P is exported from the chloroplast to the cytosol. In the cytosol, triose-P is used for sucrose synthesis. The Pi is released during this reaction and transported back to chloroplast (Edwards and Walker, 1983). Carbon assimilated during photosynthesis is partially exported into the cytosol for sucrose synthesis and partially retains in the chloroplast to be used for starch synthesis. As described earlier, leaf starch synthesis takes place in chloroplast, and is regulated under diurnal cycles (Stitt and Grosse, 1988). Other than allosteric control, AGPase activity is also dependent on Ox-PTM. *In vitro* reactions undertaken in a hetrologous system in *E. coli* showed the possibility to form disulfide bridge between C_{82} of the two AGPB subunits (Fu et al., 1998). The cross talk of

allosteric regulation and Ox-PTM regulation was untangled by studies in the starch deficient mutant (*pgm*), supplemented with or without sugars. It was shown that AGPB dimerization *in planta* decreased the AGPase activity, on the other hand, monomerization of AGPB increased it. Initially, the AGPB monomerization decreases rapidly after subjecting plants to darkness and increases quickly after illumination. Next, AGPase monomerization can be increased by external sugar supply under darkness. Colletively, light and sugar act in an additive manner in AGPse activity modulation. The AGPase allosteric regulation and redox regulation together control the flux of carbon into starch (Hendriks et al., 2003).

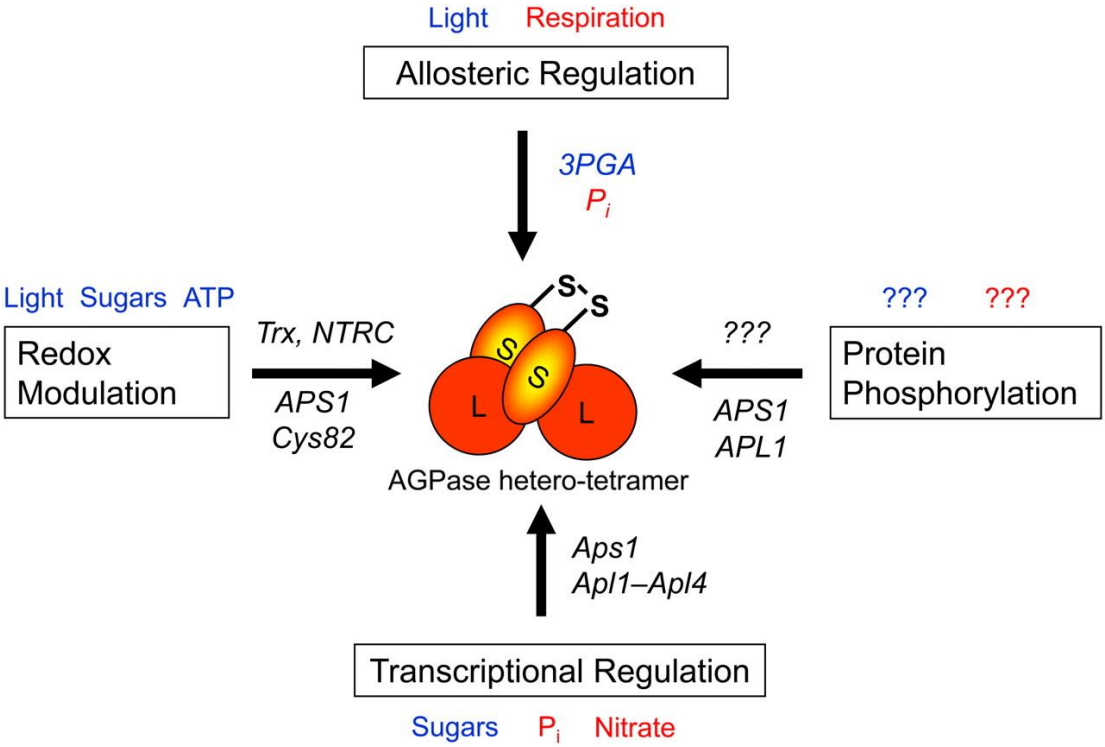

Figure 9 AGPase multilevel regulation
Top, allosteric regulation by 3PGAand Pi, balances the AGPase activity in a manner depending on photosynthesis and sucrose synthesis, operates within seconds. Left, ox-PTM regulation by disulfide bridge formation depending on light and sugar signals, operates in a time frame of minutes to hours. This process is dependent on the FTR-Trx system and NTRC system. Right, possible regulation by phosphorylation. Bottom, transcriptional regulation in response to carbon and nutrients availability, requires days to develop.
Red color – inhibition, blue color – activation. L – regulatory subunit of AGPase that is larger (51 kDa); S – catalytic subunit of AGPase that is smaller (50 kDa) (After Geigenberger, 2011).

1.6. Sources of reactive oxygen species

Plants generate high amounts of ROS from photosynthetic metabolism as well as respiration and even increase the production during stress. Plants have to continuously cope with ROS. Unlike other organisms e.g. human or yeast, plants possess more antioxidant proteins coding genes and protein responsible for dithiol/disulfide exchange reactions (Cejudo et al., 2014). ROS in plants play a dual role, on one hand they signal, and they also act to damage the cell (Mittler, 2017).

1.6.1. ROS sources in plant cell

The ROS species present in plant are: superoxide radical ($O^{\bullet -}_2$), hydrogen peroxide (H_2O_2), hydroxyl radical ($OH^{\bullet}$) and singlet oxygen ($^1O_2$). ROS production in plant cells occurs *via* different mechanisms during biotic or abiotic stress or physiological activity. ROS are continuously produced under physiological conditions as an outcome of reactions in cellular compartments (Rinalducci et al., 2008). To avoid harmful effects, ROS are readily scavenged by ROS-scavenging enzymes, production of antioxidant compounds and increase in metal-chelating proteins that are involved in scavenging of ROS and peptides with antioxidant properties. In plants, ROS are mainly generated in chloroplasts, peroxisomes, mitochondria as well as in the apoplast, microbodies like peroxisomes or glyoxysomes, cytosol and endoplasmic reticulum (Figure 10; Apel and Hirt, 2004).

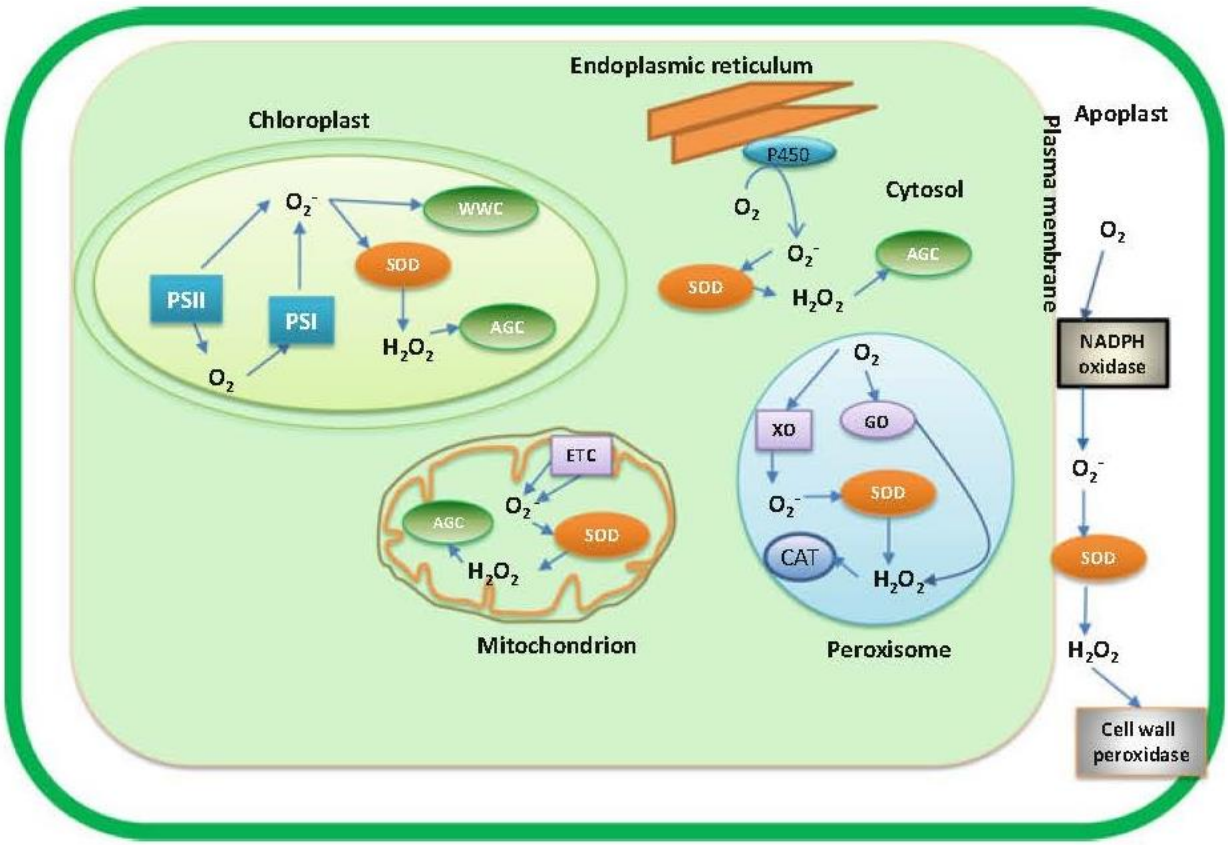

Figure 10 ROS generation pathways in various compartments
In the chloroplast, superoxide is produced at PSII and PSI, it is converted to hydrogen peroxide by SOD, hydrogen peroxide can be scavenged by ascorbate-glutathione cycle (AGC) and by water-water cycle (WWC). In plasma-membrane superoxide is generated by NADPH oxidase and is converted by SOD to hydrogen peroxide that in the end is used by cell wall peroxidase. In mitochondria complex I and III generate ROS, there SOD and AGC are scavengers. In peroxisomes mainly GO and XO produce ROS, CAT and SOD are scavengers. In endoplasmic reticulum cytochrome P-450 generates superoxide, SOD and AGC are scavengers (after Apel and Hirt, 2004).

WWC – water-water cycle; AGC – ascorbate-glutathione cycle; GO – glycolate oxidase; XO – acyl-CoA oxidase and xanthine oxidase; SOD – superoxide dismutase; CAT - catalase (after book(Reactive Oxygen And Nitrogen Species Signaling and Communication in Plants 2015).

1.6.2. Chloroplasts are the main source of ROS production in a plant cell

In leaves, the main source of ROS is the chloroplast, due to light-driven photosynthesis. The major generation site of ROS in the thylakoid is photosystem I (PSI). At PSI, ROS is produced by photo-reduction of O_2 by the water-water cycle (Mehler reaction). At first superoxide free radical ($O^{\bullet -}_2$) is produced and can then be dismutated to H_2O_2.

Enzymes catalysing this reaction are thylakoid bound and stromal superoxide dismutases (SODs) (Smirnoff and Arnaud, 2019). Plastid terminal oxidase (PTOX) can also contribute to ROS production, it accepts electrons from plastoquinol and reduces oxygen to water. When the plastoquinone is highly reduced, PTOX is able to generate superoxide, likely as a signalling molecule to change expression of genes needed for acclimation (Krieger-Liszkay and Feilke, 2015). ROS production was also demonstrated in photosystem II (PSII). In physiological conditions, NADPH is produced by the photosynthetic electron transport reactions in the thylakoid membrane, which are driven in the presence of light. NADPH is used in the Calvin-Benson cycle to reduce CO_2 (Edreva, 2005). Chlorophyll molecules also contribute to ROS production. A part of electron flow is diverted from ferredoxin to O_2, reducing it to superoxide free radical ($O^{\bullet -}_2$) (Rinalducci et al., 2008). Once produced the $O^{\bullet -}_2$ may generate more reactive ROS. It can be protonated to HO_2 in the lumen side of membrane. On the stromal side of the membrane $O^{\bullet -}_2$, is enzymatically (by Superoxide Dismutase (SOD)) or spontaneously dismutated to H_2O_2 and O_2. Subsequently, the H_2O_2 can be scavenged by catalyses or enzymes and metabolites of the ascorbate-glutathione cycle or transformed to the more toxic HO• (Noctor and Foyer, 1998). Oxygen can be activated also in light dependent reactions mediated by chlorophyll excitation (Rinalducci et al., 2008).

1.6.3. Mitochondrion as a source of ROS

The second biggest source of ROS in the photosynthesizing plant cell is the mitochondrion with its respiratory Electron Tranport Chain (ETC). Here, the ETC consists of complex I (NADH: ubiquinone oxidoreductase,), complex II (succinate dehydrogenase), complex III (coenzyme Q: cytochrome c – oxidoreductase) and IV (cytochrome c oxidase) and five additional oxidoreductases. Four of these oxidoreductases catalyze electron transfer from NADH or NADPH to ubiquinone and the fifth is the alternative oxidase (AOX), which catalyzes the direct electron transfer from ubiquinol to molecular oxygen (Moller et al., 2007). AOX does not couple electron transport to proton translocation across the inner mitochondrial membrane thus they are recognized as dissipating reactions. The main sites of ROS production are complexes I and III where the superoxide ion is formed, which is further reduced by superoxide dismutases to H_2O_2. H_2O_2 can react with Fe^{2+} and Cu^{+} to produce highly toxic hydroxyl radicals and can also penetrate membranes and leave the mitochondrion (Sweetlove and Foyer, 2004).

1.6.4. RNS sources in plant cell

Reactive nitrogen species (RNS) include molecules like nitric oxide (•NO) and its derived molecules: nitrogen dioxide (NO_2), dinitrogen trioxide (N_2O_3) and peroxynitrate ($ONOOO^-$) (Couturier et al., 2013). RNS originate from NO• that is formed in the plant cell. During metabolism it is produced non-enzymatically in the presence of ascorbate and as a by-product of nitrate reductase (NR), particularly under hypoxic conditions (Gupta and Igamberdiev, 2016). Enzymatically, it is formed from nitrate by the activity of the nitrite:nitric oxide reductase (Ni-NOR), and from L-arginine and oxygen by a putative nitric oxide synthase (NOS). However there might be more production sites of NO•, as it is known that under biotic and abiotic stress plants produce early and transient bursts of nitric oxide. When the concentration of NO• is high, and in presence of ROS, RNS are produced. NO• reacts with superoxide forming peroxynitrite and peroxynitrous acid. Peroxynitrite degrades rapidly producing hydroxyl (HO•) and nitrogen dioxide (NO_2). Nitrogen dioxide can directly initiate lipid peroxidation, sulphydryls oxidation and nitrification of aromatic residues of proteins (Rinalducci et al., 2008). In soybean, two independent pathways were identified for NO• production in chloroplast. One is activity of NOS-like enzyme employing Arg/NADPH and another dependent on nitrite. The reaction of NO• with $O^{\bullet -}_2$ can lead to damages even in physiological conditions by producing $ONOO^-$ on the other hand NO• and other species can regulate a plethora of downstream effects in chloroplast (Jasid et al., 2006).

1.7. Methods for oxidative PTMs study

Protein thiols are crucial component of redox signalling and homeostasis, regulation of enzymatic activity and protein function. Because of the unique properties of cysteine they are especially susceptible to reactions with ROS and RNS, which results in a variety of reversible and non-reversible modifications. A number of approaches are currently applied in order to elucidate redox modified proteins in proteomes of different organisms. Most research is focused on oxidative stress but there is also a growing interest in redox homeostasis (Dumont and Rivoal, 2019). One general consideration in redoxome studies is sample preparation that minimalizes the appearance of both oxidative and reductive artifacts. A crucial point in sample preparation is lysis or disruption of cells that is a first risk point of artificial oxidation. A commonly used method to minimize artificial oxidation is via trichloroacetic acid (TCAH) oxidative reactions quenching followed by free thiols alkylation under denaturing conditions (Duan et al., 2017). TCAH works by quickly lowering the pH to acid-trap free thiols.

Subsequent alkylation agents like N-ethylmalemide (NEM) or iodoacetamide (IAM) are often used in denaturing buffer to allow covalent binding with free thiols, thus preserving cysteines in their native state for analysis. NEM is much more frequently an alkylation agent of choice when compared to IAM, being more specific, faster and less pH dependent (Ying et al., 2007). Another point to be aware of during sample preparation is that the presence of active metal ions can also catalase thiol oxidation, therefore, addition of chelating agents like diethylenetriaminepentaacetic acid (DTPA) or neocuproine is beneficial. When focusing on specific redox modification it is also important to be aware that each of them has specific properties e.g. SNO are labile in high temperatures or UV (Forrester et al., 2009). A short overview of methods applied for studying oxPTMs is presented in Table 1. In the next two chapters, selected methods for a targeted study approach and global approach will be described in more detail.

Table 1 An overview of methods applied for studying ox-PTMs
(Chung et al., 2013 , modified)

Mediator	PTM	Reaction	Methods	Comment
GSNO	Nitrosylation (SNO)	P-SH + RSNO → P-SNO + RSH N_2O_3 + RSH→P-SNO + HNO	Biotin switch style *Biotin-HPDP SNO-RAC*	HPDP-Biotin is a pyridyldithiol-biotin compound for labeling protein cysteines and other molecules that contain sulfhydryl groups
N_2O_3			*ICAT*	Resin-assisted capture (SNO-RAC)
				Isotope-coded affinity tag (ICAT) reagent with specificity toward sulfhydryl groups
			SNOCAP	SNOCAP (SNO capture) reagents based on biotin-HPDP, selectively labels SNO
				Cysteine reactive tandem mass tag (cysTMT)
			CysTMT	Organomercury reagents react directly, efficiently, and specifically with S-nitrosocysteine
			Organomercury	
H_2O_2	Sulfenylation (SOH)	P-SH + H_2O_2 → P-SOH + H_2O	Biotin switch style *Biotin-HPDP with arsenite*	Arsenite specifically reduces sulfenic acids
			OxICAT	
			Dimedone chemistry	ICAT label that consists of the IAM-moiety
			Yap1 probe	Dimedone selectively tags sulfenylation
				Yap1 transcription factor in *S. cerevisiae* functions as a trap for proteins that form cysteine sulfenic acid in vivo
H_2O_2	Sulfinic acid (SO_2H)	P-SOH + H_2O_2 → P-SO_2H + H_2O	Direct detection by MS	
H_2O_2	Sulfonic acid (SO_3H)	P-SO_2H + H_2O_2 → P-SO_3H + H_2O	Direct detection by MS	
H_2S	Sulfhydrylation (SSH)	Not known	Biotin switch style	
GSSG	Glutathionylation (SSG)	P-SH + GSSG → P-SSG+GSH	Biotinylated reagent	
			Antibody-based assay	
				Requires specific antibodies
	Disulfide bond formation (RSSR)	P-SOH + P'SH → PSSP' + H_2O	2D gel analysis	performic acid oxidation method for cleaving disulfide bonds

1.7.1. Targeted approaches

A targeted *in vitro* approach to characterize the oxidation sensitivity of cysteine containing proteins is possible by performing cysteine alkylation, often by applying malemide-containig reagents, which specifically bind thiol groups. The cysteine derivatization will result in a mobility shift on non-reducing SDS-PAGE. The agent used for alkylation can vary in size and other properties, widely used is 4-acetamido-4′-maleimidylstilbene-2,2′-disulfonic acid (AMS) which induces change of ~0.5k Da per free thiol group. For proteins with higher molecular weight a malemide linked with polyethylele glycol (PEG) can be used, with size ranging from 1 to 30 kDa. PEG-polymerization likely generates a heterogenous mixture that often results in obtaining many bands of different sides on SD-PAGE. These polymers are also not charged, which prevents linear mobility in SDS-PAGE (Zannini et al., 2017). Redox Western blots allow oxidation measurements of individual proteins in cell or tissue extracts. After alkylation and separation an immunoassay is performed with use of specific antibodies (Go and Jones, 2013).

1.7.2. Global, non-targeted approaches

Mass spectrometry-based methods can be used to obtain a global insight into the redoxome. For this, labelling approaches and immunoassays are combined with MS/MS techniques. Together, this allows for the detection of or selection of peptides depending on the presence of reduced cysteines (thiols) (Go and Jones, 2013). The biotin-switch technique (BST) has widely been used for studies on reversible redox modification (Forrester et al., 2009). It was initially developed for the detection of S-nitrosylated proteins in a complex protein mixture such as the cytosol. S-nitrosylation is an ox-PTM that occurs through the reaction of cysteines with NO. In this method, the protein is unfolded in the presence of SDS and thiols are blocked by the addition of the methyl-thiolating agent methyl methane-thiosulfonate (MMTS). Subsequently, nitrosothiol bonds are selectively decomposed by addition of ascorbate. The newly formed thiols are labeled with biotin (*N*-[6-(biotinamido) hexyl]-3′-(2′-pyridyldithio) propionamide (biotin-HPDP)). After labelling, the proteins can be detected via anti-biotin antibodies or purified using immobilized streptavidin, a biotin-binding protein (Jaffrey and Snyder, 2001). The BST method can be modified in order to identify other oxidative cysteine modifications.

The OxICAT is a similar thiol-trapping technique as BST but it utilizes the ICAT label that consists of the IAM-moiety, a cleavable biotin affinity tag, and a 9-carbon linker, which exists

in an isotopically light ^{12}C-form (herein referred to as light ICAT) and a 9-Da-heavier isotopically heavy ^{13}C-form (herein referred to as heavy ICAT). First, the light ICAT is used to irreversibly label all the reduced cysteines under denaturing conditions to allow access to buried amino acids, next all reversibly oxidized csteines are reduced with use of tris(2-carboxyethyl)phosphine (TCEP). The newly accessible Cysteines are subsequently labelled with heavy ICAT. The assay results in chemically identical proteins that differ by mass, thus the heavy ICAT add 9kDa per each modified moiety. Important for later identification steps in MS/MS, the ICAT labelled peptides are chemically identical therefore they ionize in the same way (Leichert et al., 2008). Although OxICAT is a suitable method for studying complex mixtures of reversibly oxidized proteins and can be modified with use of specific reductants and many downstream protein identification methods, the ICAT reagents have not been commercially available since 2017 (https://sciex.com/products/consumables/cleavable-icat-reagent). In recent years a quantitative method coupled with LC-MS/MS was developed for redoxome studies. Tandem mass tags (TMT) have been successfully used in quantitative protein measurements for many proteomic studies (Liang et al., 2015), the quantification is achieved in tandem MS by reporter ion intensity comparison. Recently, cysteine-specific iodoacetyl isobaric tandem mass tags (iodoTMT) have been developed. Free thiols of trichloroacetic acid (TCAH) captured proteins are first blocked with IAM, next all the oxidized residues are reduced and labelled with iodoTMT. Differentially labelled proteins can be than mixed and digested, by adding the mixture to anti-TMT resin a specific enrichment is carried out (Shakir et al., 2017)

1.8. Aim

An adapted approach for studying the light- and dark-dependent redoxosome of *Arabidopsis thaliana*.

Reversible protein thiol oxidations govern key regulatory processes of photosynthesis, metabolism, and gene expression in all photosynthetic organisms. The principle aim of the project was to obtain a comprehensive understanding of the redoxome of *Arabidopsis thaliana* in response to light vs dark. It was decided to utilize a novel chemical labelling method and combine it with the identification of proteins by tandem mass spectrometry. The method used in this study was adapted from Guo and colleagues (2014) (Guo et al., 2014). For the confirmation of a candidate at the single protein level, thiols and disulfides were differentially labelled and the protein was detected with a specific antibody using protein blot analysis. Additionally, CSP41 proteins, which emerged from this study as potential targets of redox-regulation, were further analyzed. These proteins had previously been described as players in chloroplast gene expression (Qi et al., 2012) and were thus further analyzed by ribosome profiling (Chotewutmontri and Barkan, 2018).

2. Materials and Methods

2.1. Materials

2.1.1. Chemicals and consumables

Standard chemicals were ordered from Amersham (Amersham Pharmacia Biotech EuropeGmbH, Freiburg, Germany), Eppendorf (Hamburg, Germany), Invitrogen (Karlsruhe, Germany), Merck (Darmstadt, Germany), Promega (Mannheim, Germany), Roche Biochemicals (Basel,Switzerland), Roth (Karlsruhe, Germany), Sigma-Aldrich (Sigma-Aldrich Chemie, Munich,Germany), Thermo Fisher Scientific (Schwerte, Germany) in the quality pro Analysis (p.a.).

2.1.1.1. Special consumables

Comsumables	Company
Microcon-10kDa Centrifugal Filter Unit with Ultracel-10 membrane	Merck
Amicon® Ultra-4 and Amicon® Ultra-15 with Ultracel-10 membrane	Merck
C_{18} SEP-Pak	Tecknokroma
Acclaim PepMap RSLC reversed-phase column (bead size 2 µm, 15 cm long, 75 µm inner diameter)	Thermo Fisher Scientific

2.1.1.2.

2.1.1.2. Equipment

Instrument	Company
Centrifuge 5804R	Eppendorf
EASY-nLC 1000	Thermo Fisher Scientific
Laboport Vacuum pump	KNF, Sigma-Aldrich
Mini-PROTEAN® System	GE Healthcare

Power PAC 1000	BioRad
Q Exactive Plus Orbitrap	Thermo Fisher Scietific
Q Exactive HF Orbitrap	Thermo Fisher Scietific
QIAvac 24 Plus	QIAGEN
Savant SPD131DDA SpeedVac concentrator	Thermo Fisher Scientific
Thermomixer comfort	Eppendorf

2.1.1.3.

2.1.1.3. Antibodies

Primary antibodies

Name	Species	Dilution	Company / Origin
Anti-FBPase	rabbit polyclonal IgG	1:10 000	custom
Anti-AGPase	rabbit polyclonal IgG	1:10 000	custom
Anti-MDH	rabbit polyclonal IgG	1:5000	custom and Agrisera
Anti-CS	rabbit polyclonal IgG	1:10 000	custom
Anti-ACO	rabbit polyclonal IgG	1:10 000	custom
Anti-CSP41a	rabbit polyclonal IgG	1:5000	custom

2.1.1.4.

2.2. Methods

2.2.1. Plant material and protein extraction

2.2.1.1. Arabidopsis thaliana

Growth conditions, chamber with LED (for light emitting diode) light intensity 150 µmol $m^{-2}s^{-1}$, short day (8 h light/16 h dark photo period), constant 20°C. *Arabidopsis thaliana* accession Col-0 was used as the wild type.

The triple thioredoxin (trx) *m1*(AT1G03680), *m2* (AT4G03520), *m4* (AT3G15360) mutants (*trx m124*) were obtained from Motohashi group, Japan (Okegawa and Motohashi, 2015) . Other *trx* (*trf f1*(AT3G02730)), *csp41a* (AT3G63140) and *csp41b* (AT1G09340) mutants were kindly donated by Prof. Dr. Peter Geigenberger and Prof. Dr. Dario Leister, respectively.

2.2.1.2. CN-PAGE

Arabidopsis thaliana WT and mutants were harvested before the end of the dark period (end of night, EON) or the end of the light period (end of day, EOD), and subjected to cross-linking with formaldehyde.

Col-0 plants were grown for 24 days in short day (8 h light/16 h dark photo period), (150 µmol $m^{-2}s^{-1}$, constant temperature 20°C) before harvesting into liquid nitrogen 15 min respectively. Frozen and powdered plant material was suspended in 2:1 v/w native extraction buffer (40 mM Tris, 20% Glycerol, 60 µl ml^{-1} protease inhibitor cocktail (Roche). Following vigorous mixing, clarification of the extract was done by centrifuged for 10 min at 16,000 *g* and subsequent ultracentrifugation at 100,000 *g* for 45 min. The resulting supernatant was collected and protein concentration was measured by BCA assay (PierceTM BCA Protein Assay Kit, Thermo Scientific).

2.2.1.3. Formaldehyde cross-linking

A single 3-week-old rosette was harvested for cross-linking, with exception of mutant *trx m124*due to small size of the plants as many as 4 rosettes were bulked together for cross-linking. The harvested tissue was submerged in 25 ml cross-linking buffer (10 mM sodium phosphate buffer pH 7, 50 mM NaCl, 0.1 M sucrose, 1% formaldehyde), placed on ice in vacuum chamber for 15 min, after this time vacuum was released and tissue was stirred, next vacuum was applied for next 15 min. Fixation was stopped by adding 2.5 ml cold glycine (1.25 M), the solutions were mixed and vacuum was applied for another 2 min. Washing was performed three times each with 25 ml cross-linking buffer. Plants were next air-dried on paper. After drying there were quick-frozen in liquid nitrogen.

2.2.2. Resin-assisted enrichment of thiols

2.2.2.1.1. Trichloroacetic acid (TCAH) precipitation

A single 3-week-old rosette of *Arabidopsis thaliana* was harvested using a homogenizer (Kinematica Polytron Benchtop Homogenizer) in 4 ml of ice-cold 20% TCAH (trichloroacetic acid). Sample was divided into 2 (one sample for NEM alkylation and one as control) 2 ml samples, using cut 1 ml tips. Proteins were precipitated on ice in darkness for 1

h and spun down in microcentrifuge at ~20,000 *g*. Pellets were washed 3 times with ice-cold acetone without disturbance and air dried and moved to 1.5 ml tubes. Next, 1 ml of degassed alkylation buffer (0.1% SDS, 100 mM HEPES pH 7, 0.01 mM EDTA, 0.1 mM neocuproine) was added to samples, pellets were crushed with the buffer using pestles. Samples were spun shortly at high speed to separate the insoluble debris. The soluble sample was used for determination of the protein concentration in solution with Bradford Reagent (Sigma-Aldrich). Average sample concentration was 1 mg/ml

2.2.2.1.2. Coomassie staining on Whatmann paper

In buffers not compatible with Bradford measurement proteins concentration was estimated by Coomassie staining on Whatmann paper. A 1 µl of each protein sample and BSA (bovine serum albumin) standard were pipetted onto Whatmann paper and air-dried. Next the Whatmann paper was soaked in staining solution (0.1% Coomassie Brilliant Blue R-250, 50% methanol and 10% glacial acetic acid) for 5 min with shaking. Next destaining was performed by multiple washes with destaining solution (40% methanol and 10% glacial acetic acid) and the paper was air-dried. Concentration of protein was performed by comparing the intensity of color of each sample with BSA standard.

2.2.2.1.3. Resin assisted enrichment of thiols - protocol

To pellets obtained after TCAH precipitation, 1 ml of degassed NEM alkylation buffer (0.1% SDS, 250 mM HEPES pH 7, 0.01 mM EDTA, 0.1 mM neocuproine with/without 100 mM NEM with addition of protease inhibitor cocktail (Roche)) was added, pellets were crushed with the buffer using pestles, final concentration of protein was adjusted to 1 mg/ml . All samples were incubated for 30 min at 55°C with shaking. Samples were spun shortly at high speed to separate the insoluble debris. The solubilized sample was transferred to a 15 ml falcon tube and precipitated with 4 ml ice-cold acetone. Proteins were precipitated for half an hour, spun down at maximal speed of centrifuge (~16,000 *g*), NEM was washed out with additional 3 washed with ice-cold acetone, and samples were air-dried. Next all pellets were moved to 1,5 ml tube and suspended with 400 µl reducing buffer (250 mM 4-(2-hydroxyethyl)-1-piperazineethanesulfonic acid (HEPES pH 7), 8 M urea, 10 mM dithiothreitol (DTT). Incubation lasted for 1h in 37°C with shaking. Excess of DTT was next removed with Amicon® Ultra-4 centrifugal filters with 10 kDa cut off. First 3 ml of 3 M urea was added to the filter and spun in swing out rotor at 4,000 *g* for 30 min, next 3 ml of enrichment coupling buffer (0.1 M tris-HCl pH 7.5, 0.5 M NaCl, 5 mM EDTA, protease inhibitor cocktail (Roche)) were added and centrifuged 4,000 *g* for 30 min at 4°C. Enrichment

column were prepared at this time or earlier and stored at 4°C. 35 mg of thiopropyl sepharose 6B resin was weight in 1.5 ml tube, water and buffers used for further column preparation were degassed, 1 ml of water was added to the resin and left for 15 min at room temperature (RT). Resin was resuspended with cut 1 ml tip and left for another 10 min RT. 0.5 ml of water from the top of each tube was removed, resin was again resuspended with use of modified tip and transferred to the empty gravity flow columns (Poly-Prep, BioRad). Resin on the column was washed 5 times with 1 ml of water at each time, shortly spun in-between and 5 times with enrichment coupling buffer. For storage (only short term) a cup and bottom plug were put on. Pre-processed samples were transferred to the column and incubated 4 h, RT with shaking. Next the unbound fraction of proteins was collected by centrifugation 1min at 1,500 *g*. Wash was performed with 4 different buffers (1st 8 M urea, 2nd 2 M NaCl, 3rd 80% acetonitril and 0.1% TFA, 4th 25 mM HEPES pH 7). Lastly the enriched proteins were released from the column by incubation with 120 µl 50 mM DTT in enrichment coupling buffer for 1 h and collected to new tube by 1,500 *g* 1min centrifugation. The enriched sample was next used for protein digest.

2.2.3. Protein digestion

Approximately 100 µg protein was mixed with 100 µl 8 M urea in urea-Tris buffer (10 mM Tris-HCl, pH 8) to the top of filter column (Merck, 10 kDa cutoff), spun shortly at 4^{0}C. Subsequently proteins were washed on filter with 100 µl urea-Tris buffer and spun at RT, 40 min, 14,000 *g*. Next reduction with DTT was performed by addition 50 µl 10mM DTT in urea-Tris buffer and spinning at RT, 30 min, 14,000 *g*. Next proteins on filter were modified with iodoacetamide (carbamidomethylation); 50 µl 27 mM iodoacetamide in urea-Tris buffer was added to the filter and incubated with mixing, for 1 min, and 5 min without mixing. Spin at RT for 30 min, 14,000 *g*, followed by one wash with urea-Tris buffer was performed, followed by spinning, RT, 40 min, 14,000 *g*. Afterward peptides were subjected to digest on filters with modified trypsin (Promega) in 100 µl 100 mM ammonium bicarbonate, in proportion 1:25 trypsin : protein. Digest was performed for 14 h in 37^{0}C. Peptides were recovered form filter first by centrifugation for 40 min, RT, 14,000 *g* and next desalting by adding 50 µl 0.5 M NaCl and centrifugation for 20 min, RT, 14,000 *g*.

2.2.4. Peptide clean-up

Peptides were acidified with Trifluoroacetic acid (TFA, 10%) to pH<3.0. The mixture of peptides was subsequently purified and desalted on C18 SEP-Pak columns (Tecknokroma). These columns were used in combinations in combinations with a QIAvac 24 Plus (QIAGEN) vacuum manifold. The columns equilibration was achieved by

washing with 1 ml 100 % methanol, once with 1 ml 60 % acetonitrile (ACN) and twice with 1 ml of 0.1 % TFA. Next peptides were allowed to pass through C18 column. Then washing step was performed on column, twice with 1 ml of 0.1% TFA. Peptides were eluted with 800 µl 60 % ACN, 0.1% TFA, dried in the speed vacuum concentrator and stored at -20°C before LC-MS/MS measurement.

2.2.5. LC MS/MS method

2.2.5.1. LC MS/MS method for enrichment

Instrument type Q Exactive Plus combined with nano LC 1000 with column reverse phase C18 (Acclaim PepMap RSLC, 75 µm x 150 mm, C18, 2 µm, 100 Å) was used to resolve peptides. Equilibration bufor A (3% acetonitrile, 0.1% TFA), elution buffer B (80% acetonitrile, 0.1% TFA) were used. Gradient was run as follows: 65 min from zero to up 28% buffer B with 300 nl/min flow , 10 min up to 40% B with flow 300 nl/min, 5 min up to 80% B with flow 300 nl/min, followed by wash for 5 minutes up to 85% B with flow 500 nl/min, 5min 0% flow 500 nl/min. Q Exactive Plus Full MS scan settings were: resolution 60,000, AGC target 3e6, maximum IT 100ms, scan range 150 to 1600 mz. MS2 scan settings were: resolution 15,000, AGC target 2e5, loop count 15, isolation window 2 m/z, collision energy nce: 30. Data dependent acquisition settings were: apex trigger on, charge exclusion 1.5-8>8.

2.2.5.2. LC MS/MS method for gel excision

2.2.5.2.1. In gel digest

Protein gel was stained with Pierce Silver Stain Kit (Thermo Fisher Scientific) scanned and destained using the same kit destaining components. Next gel pieces were dehydrated by 50% acetonitrile, reduced with DTT (10 mM DTT, 5 mM ammonium bicarbonate) in 50°C for 45min. Next reducing solution was removed and proteins were modified with iodoacetamide (carbamidomethylation) by incubation in 50 mM iodoacetamide, 50 mM ammoniu bicarbonate for 1 h 45min in darkness. After removing iodoacetamide solution, gel pieces were dehydrated with acetonitrile and subjected for digest with modified trypsin (Promega) in 50 mM ammonium bicarbonate for 14 h in 37°C, the amount of trypsin was estimated to be in proportion 1:30 protein : trypsin. To recover the peptides digest mix was acidified to 0.6% TFA content and acetonitrile was added up to 50% concentration and incubated for 20 min. The suparnatatnt was collected to a new tube and the remaining gel piece was further incubated with 300 µl 2% TFA for 30 min, next 400 µl acetonitrile was added and incubated

to 20 min RT. Collected supernatant was combined with the supernatant from the step before, the sample was next dried in speed vac concentrator and proceeded to desalting.

2.2.5.2.2. LC MS/MS method for gel excision

Instrument type Q Exactive Plus combined with nano LC 1000 with column reverse phase C18 (Acclaim PepMap RSLC, 75 µm x 150 mm, C18, 2 µm, 100 Å) was used to resolve peptides. Equilibration bufor A (3% acetonitrile, 0.1% TFA), elution buffer B (80% acetonitrile, 0.1% TFA) were used. Gradient was run with following settings: 5 min from zero to up 10% buffer B with 300 nl/min flow, 30 min up to 20% B with flow 300 nl/min, 8 min up to 40% B with flow 300 nl/min, followed by wash for 2 min up to 80% B with flow 500 nl/min, 1 min 80% B with flow 500 nl/min and 4 min down to 0% flow 500 nl/min. The following scan setting of the

Q Exactive Plus Full MS were used: resolution scan range 150 to 1600 mz, 60.000, AGC target 3e6, maximum IT 100 ms. MS2 scan settings were: resolution 15.000, AGC target 2e5, loop count 15, isolation window 2 m/z, collision energy nce: 30. Data dependent acquisition was applied with following settings: apex trigger on, charge exclusion 1.5-8.>8.

2.2.6. Protein annotation method

Progenesis QI LC/MS software (Nonlinear Dynamics) combined with Mascot search engine was used to annotate peptide sequences using Arabidopsis TAIR10 genome annotation data base. Protein were digested with Trypsin, fixed modification was set as Carbaminomethylation, allowed peptide charges of 2^+ and 3^+ and maximum of two missed cleavages. Additionally, a FDR score below 1% on protein level was esnsured by performing a search of spectra against decoy data base of Arabidopsis thaliana. The peptide identifications with a Mascot score below 25 were excluded. Mascot results were imported into Progenesis QI. Relative quantitation using Hi-N was selected as a protein quantitation option.

2.2.7. Double labelling

A single 3 weeks old rosette of *Arabidopsis thaliana* was harvested using a homogenizer (Kinematica Polytron Benchtop Homogenizer) in 4 ml of ice-cold 20% TCAH (trichloroacetic acid). Sample was divided into 2 after NEM alkylation. The protocol was performed after Peled-Zehavi *et al*., 2010

2.2.8. Ribo –Seq

The Ribo-Seq experiment was performed according to a protocol published in 2018 by Chotewutmontri et al. (Chotewutmontri and Barkan, 2018).

Analysis was done on the *Arabidopsis thaliana* TAIR10 genome and ensembl42 gene annotations (http://plants.ensembl.org/Arabidopsis_thaliana/Info/Index). Sequencing adapters were removed from the reads using flexbar (https://github.com/seqan/flexbar/wiki/Manual), according to "NEXTflex Small RNA-Seq Kit v3" manual. The Unique Molecular Indexes on the 5' and 3' end of reads were removed and tagged to the read name using a custom python script. The libraries were then filtered by aligning to all annotated rRNA, tRNA and snoRNA of TAIR10 using STAR aligner v2.6.0 (Dobin et al., 2013) with the following parameter: *-outFilterMismatchNoverLmax 0.1*. Unaligned reads where then aligned to the TAIR10 genome using the following parameters: *-outFilterMismatchNoverLmax 0.1, -alignIntronMax 6000*. PCR duplications were removed using UMI-tools (Smith et al., 2017). Gene counts were summarized using FeatureCounts (Liao et al., 2014). Differential gene expression was conducted using Deseq2 (Love et al., 2014). Psite and metagene plots were done using a combination of Plastid (Dunn and Weissman, 2016) and RiboseQC (Calviello et al., 2019).

3. Results

3.1. Work flow for resin-assisted enrichment of thiols

The reversible oxidative PTMs are major components of redox signaling involved in the regulation of processes under physiological as well as pathological conditions. Here, a study of the plant light-dependent redoxome was conducted under physiological conditions. As accumulating evidence shows the redox signaling in plants is involved in central physiological processes of energy generation and consumption such as respiration, photosynthesis and photorespiration (Janku et al., 2019). The end of the day (EOD) and the end of the night (EON) time points were chosen for plant harvest. The EOD and EON samples were expected to carry specific redox regulation marks such as S-nitrosylation or disulfide bridge as they have previously been shown to appear at different times in the diurnal cycle. A major bottleneck in most redoxome studies is the preservation of the endogenous redox state of the protein. It is desirable to minimize the occurrence of oxidative and reductive artifacts during preparation of the samples. Thiols can be easily oxidized upon cell lysis and further downstream processing. In the current study, an established protocol minimizing oxidative artifacts was undertaken – quenching in trichloroacetic acid (TCAH) followed by blocking of free thiols with the alkylating reagent N-ethylmaleimide (NEM). After blocking, oxidized forms were reduced by the nonspecific reductant like dithiothreitol (DTT). The reduced form of cysteines can bind to thioprophyl 6B resin columns. All non-thiol-containing proteins cannot bind to the column and are subsequently washed out. Proteins that bind the column via their thiols are eluted by addition of the reductant DTT and subjected to LC-MS/MS. Alternatively, no NEM is added to the sample and all cysteine containing proteins can be reduced by DTT and thus bind to the column. This allows for the identification of all sufficiently abundant proteins that contain cysteine residues. Together, both experiments yield the total sample (NEM) versus the oxidized (Figure 11).

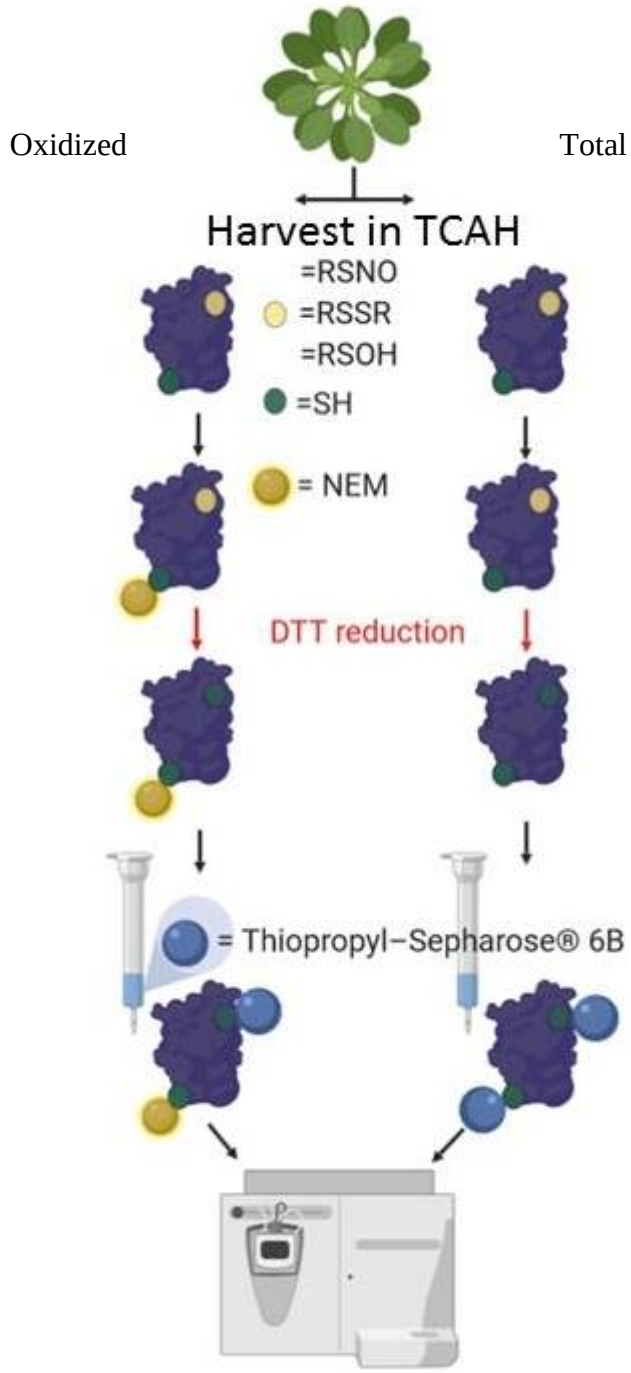

Figure 11 Experimental workflow
After harvest in trichloroacetic acid (TCAH) the sample is divided in two, namely the "Oxidized" and "Total" samples. The green oval corresponds to reduced cysteine and the yellow to oxidized – with different oxidative PTMs. The yellow globe is the NEM moiety that stably attaches to reduced cysteine. The blue column is filled with Thiopropylsepharose 6B, that is able to covalently bind reduced cysteines. After washing the unbound fraction and eluting the bound protein portion the eluate is subjected to LC-MS/MS which is represented on the scheme as a MS machine. Images were constructed for visualistion using BioRender (https://biorender.com/)

3.2. Resin-assisted enrichment of thiols

3.2.1. Pre-column loading evaluation

The aim of this part of a study was to identify differentially modified proteins at the end of the night (EON) and the end of the day (EOD) in the *Arabidopsis thaliana* proteome. The enrichment experiment was conducted based on a previously established protocol (Guo et al., 2014). Here, a novel attempt to study the redoxome in plants was undertaken. It is known that plant species have a complex redox regulation system of processes control (Ferrandez et al., 2012). In the first experiment, a single plant (n=4) was used to assess total (non-alkylated) and oxidized (alkylated) fraction of eluted proteins; the single plant was harvested and divided in two for further steps. This was a simple test conducted by staining on Whatmann paper (Figure 12).

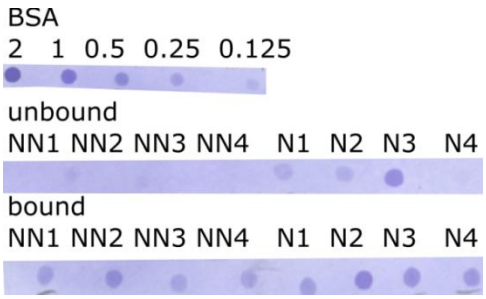

Figure 12 Sepharose 6B binding test
Coomassie staining on Whatmann paper, EON samples treated with NEM (N) and non-treated (NN). This test proves differential binding of alkylated samples (N) and non-alkylated (NN). The unbound fraction was washed out with buffers according to the protocol (2.2.2.1.3 Resin assisted enrichment of thiols - protocol, page 39), the resin-bound protein were eluted with 100 mM DTT

The first enrichment experiment (ENR1) was conducted according to the modified work-flow (Figure 13). Samples of equal volume (named X1) were partitioned before loading to the thiopropyl sepharose 6B column and separated by SDS-PAGE gel to ensure equal loading to the column, X1 samples were also used later for NEM binding evaluation (3.2.1.1 LC-MS/MS analysis of upstream thiopropyl sepharose 6B column loading samples (X1 samples), page 49). Based on the silver stained gel, samples were evaluated in pairs (e.g. “1” was compared to “1NEM”), the loading was almost equal in at least three out of four samples as shown on the gel (Figure 14). The most prominent band on each gel was compared, for gel EOD it was the band corresponding to the PSII oxygen evolving complex protein- (PsbO1)/ Early Response to Dehydration 14 (ERD14) and for gel EON the large subunit of RUBISCO (RBCL) (Figure 15).

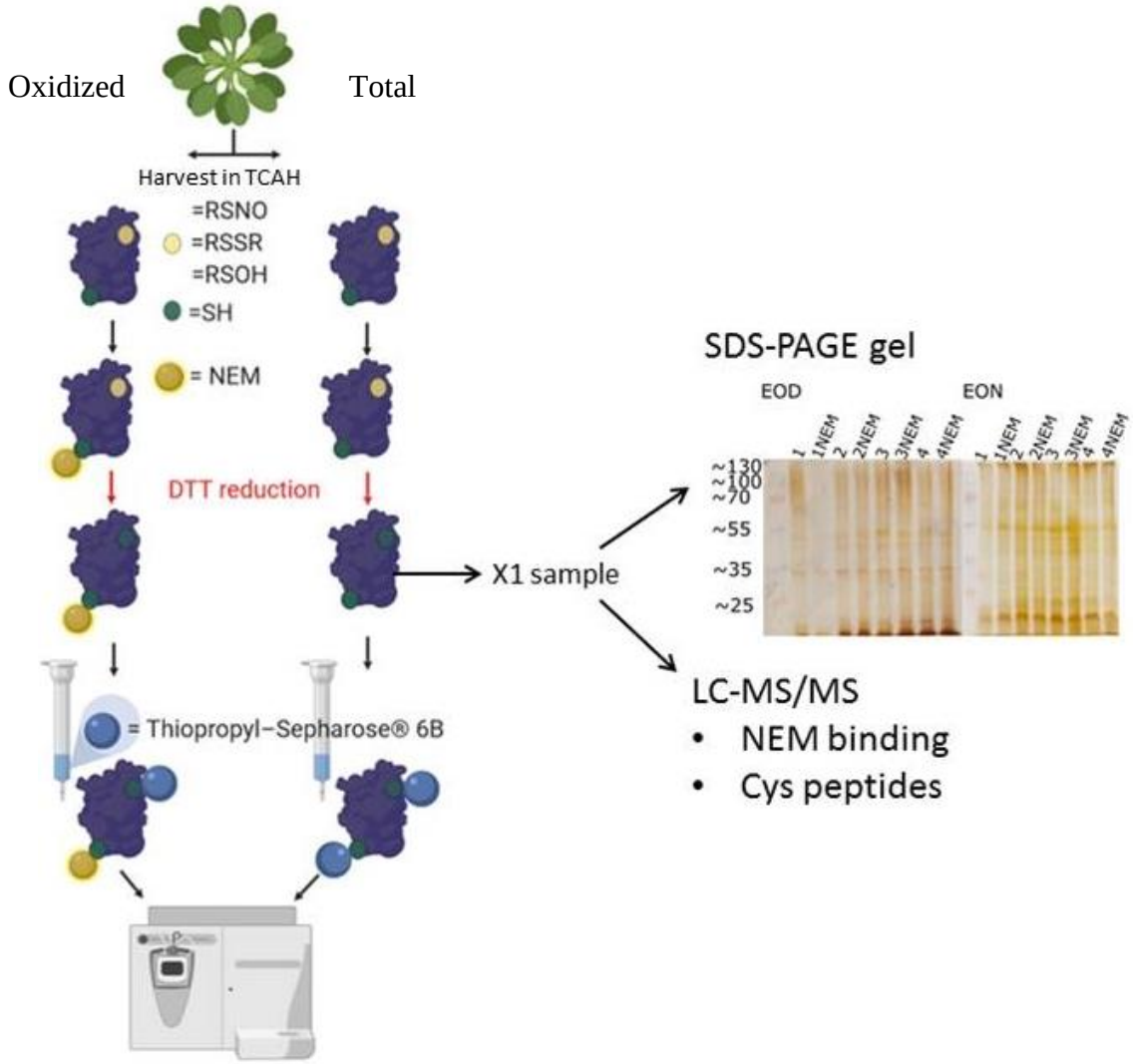

Figure 13 Overview of first Resin-assisted enrichment of thiols experiment
From the first experiment additional samples were partitioned before final elution to ensure equal sample division for "total" and "oxidized", also to evaluate NEM binding and number of peptides containing cysteines before loading on the thiopropyl sepharose 6B column.

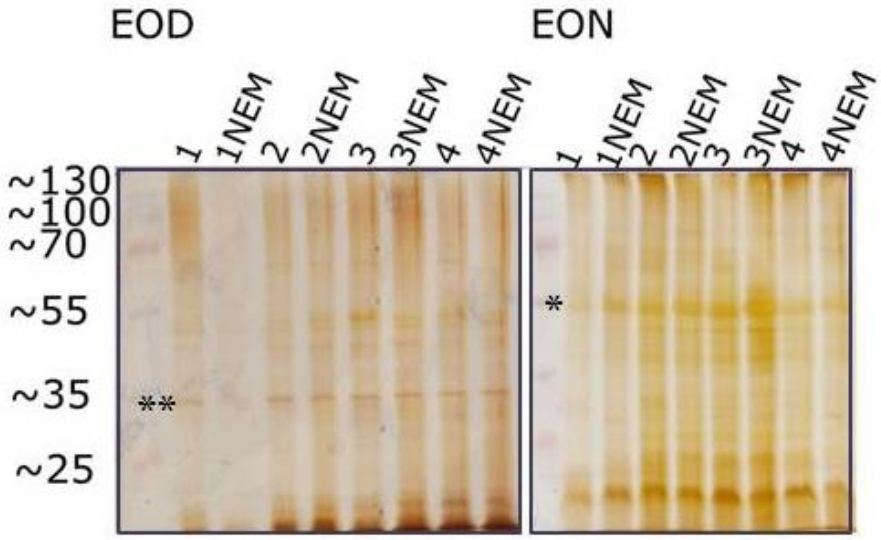

Figure 14 SDS-PAGE before loading on the thiopropyl sepharose 6B column
The denaturing urea SDS-PAGE was stained using silver stain to visualize loading quality. The samples number corresponds to a plant that the material was obtained from. The alkylated sample will be later compared with non-alkylated sample within the pairs holding the same number. It is important that the amount of protein that is loaded onto the column is equal between NEM and non-NEM treated samples. The most prominent band in the end of the night (EON) gel is Rubisco (marked with *), in end of the day (EOD) gel the most prominent band was excised and subjected to LC-MS/MS (marked with **). On the gel for EOD RbcL is not visible; this might be due to the gel quality.

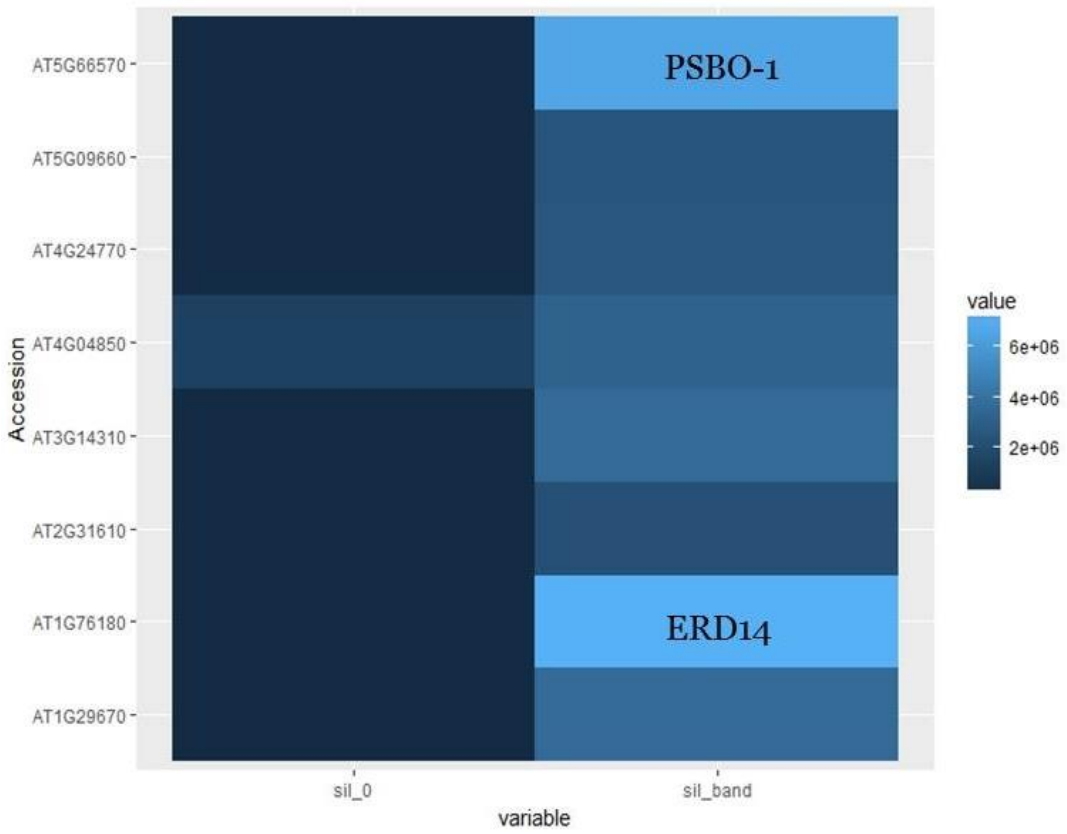

Figure 15 Comparison of signal intensity in excised gel bands

A heat map showing abundance of identified proteins in excised gel pieces. Two bands were excised from the EOD gel, one from a line 4NEM and a corresponding size band from the adjacent place in the gel where no sample was run as a control (see Figure 14). The heat map shows relative protein abundance in both gel pieces, "sil_band" – band excised from line in gel and "sil_0" – control band. The most prominent proteins in the gel are PSBO1 and ERD14. KEA3 protein (AT4G04850) is a technical contaminant present in both samples. All proteins present in the heat map, starting at the top: **AT5G66570** 33 kDa Oxygen Evolving Polypeptide 1, Oxygen Evolving Enhancer Protein 33, PS II Oxygen-Evolving Complex 1, PSBO-1, PSBO1**;** **AT5G09660** Peroxisomal NAD-Malate Dehydrogenase 2, PMDH2**;** **AT4G24770** 31-kDa RNA Binding Protein, *Arabidopsis thaliana* RNA Binding Protein, Approximately 31 kDa, ATRBP31, ATRBP33, CP31, RBP31**;** **AT4G04850** ATKEA3, K+ efflux Antiporter 3, KEA3**;** **AT3G14310** ATPME3, Overly Zinc Sensitive 2, OZS2, Pectin Methylesterase 3, PME3**;** **AT2G31610** Ribosomal Protein S3 Family Protein**;** **AT1G76180** Early Response to Dehydration 14, ERD14**;** **AT1G29670** GDSL1, GDSL-motif esterase/acyltransferase/lipase

3.2.1.1. LC-MS/MS analysis of upstream thiopropyl sepharose 6B column loading samples (X1 samples)

3.2.1.1.1. EOD vs EON

After the treatment with or without NEM and subsequent reduction with DTT, the samples were separated and analyzed by MS. This was done to monitor labelling of proteins with NEM. On the other hand, samples that were not treated with NEM were used to assess proteomes obtained from the end of the day and end of night. The samples were collected directly before thiopropyl sepharose 6B column loading (X1 samples; see Figure 13) The identified peptides between samples in X1 shared common sequence in 74.68%, specific peptides identified in EOD were 8.77%; EOD treated with NEM were 5.16%; EON were 3.98% and EON treated with NEM 7.41%. Nonetheless, on the protein identification level it was possible to identify proteins specific for EON and EOD as well as proteins with different levels of expression between the two conditions. Among proteins that were expressed at similar level in both conditions were proteins belonging to photosynthesis such as Rubisco Activase - RCA (AT2G39730), Ribulose Bisphosphate Carboxylase Small Chain 1A - RBCS1A (AT1G67090), RBCL large subunit of RUBISCO (ATCG00490) and other housekeeping genes such as those those involved in regulation of actin filament-based processes like the costars family protein (AT4G33640).

Among identified proteins there were proteins of the photosynthetic apparatus present in conditions EON and EOD, yet their abundance was different. Some of these have previously been shown to be subjected to a rapid turnover in darkness, such as Photosystem I Light Harvesting Complex Gene 3 - LHCA3 (AT1G61520) (Bennett, 1981), or otherwise involved in photosynthesis regulation like Thioredoxin - Dependent Peroxidase 1 - TPX1(AT1G65980) and a Thioredoxin superfamily protein (AT1G60740). Although the proteasome was shown to be stable between night and day here we see a shift towards higher levels at EOD for protein Proteasome Alpha Subunit A1 - PAA1 (AT5G35590), consistent with data shown in previous studies (Gorka, 2017) (Figure 16). Proteins identified only in one condition amounted to 268 and 122, for EOD and EON respectively. Among those, 243 and 104, respectively, were proteins containing cysteines, so potentially regulated via redox signaling pathway (Figure 16). The proteins were grouped by biological processes (https://www.arabidopsis.org/tools/go_term_enrichment.jsp) (Figure 17, Figure 18). Proteins involved in other then photosynthesis processes are not excluded as candidates and still are interesting for further verification and comparison with results from final experiments.

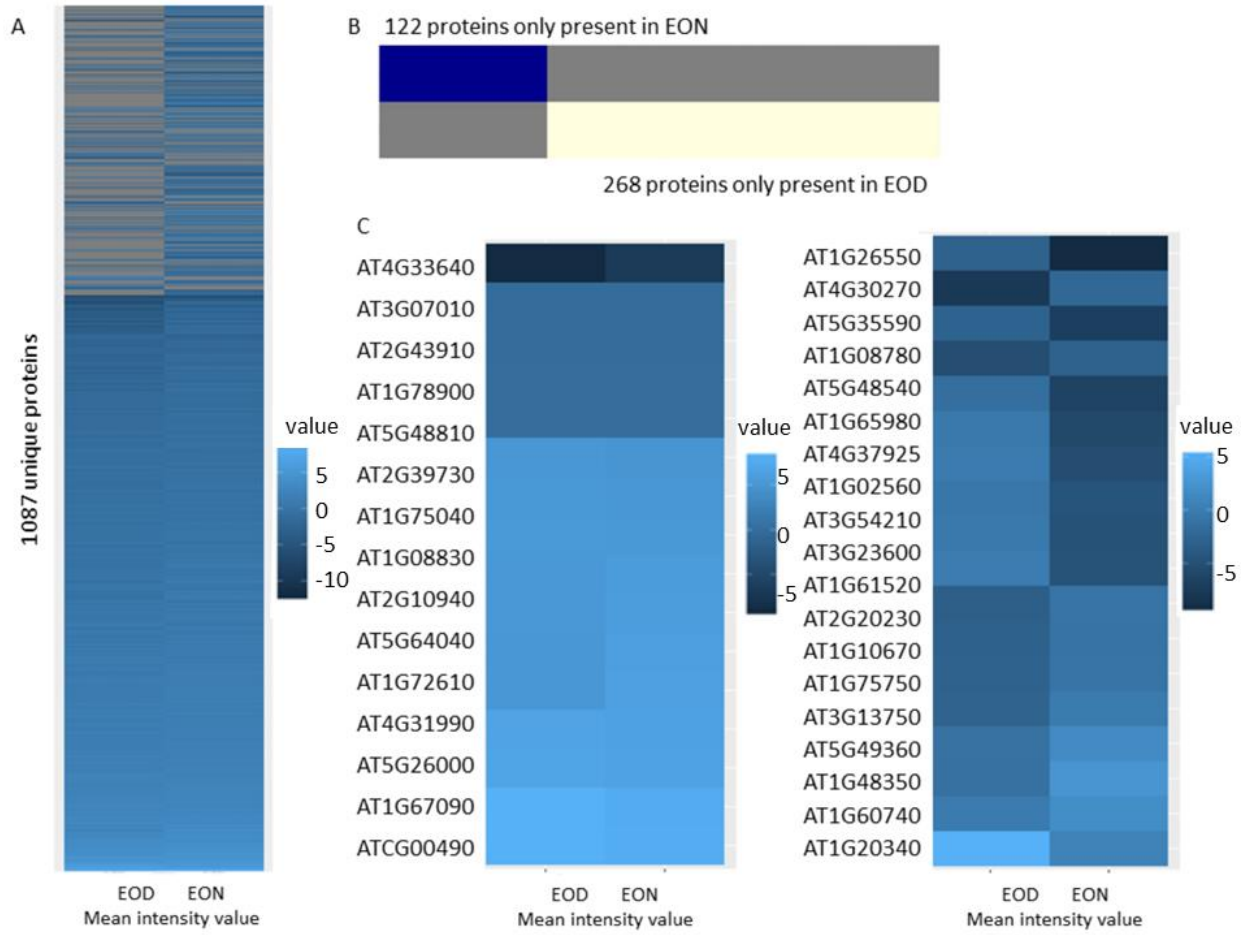

Figure 16 EOD and EON proteins

A. Heat map showing expression of 1087 proteins identified in EOD and EON.
B. Proportion of protein expressed solely in one condition.
C. Left panel, selected examples of proteins similarly abundant in EOD and EON.

Right panel, selected examples of proteins differentially abundant in EOD and EON.
EOD n=3; EON n=2

The heat maps were generated by comparing fold change values of mean (EOD vs EON) and displaying the mean values for each chosen protein. For display the top 15 most similar proteins were chosen and the top 19 most differing proteins. Presence of previously described proteins characterized by differential abundance at morning and evening timepoints was observed among proteins found in the timepoint samples of X1 (see the paragraph text).

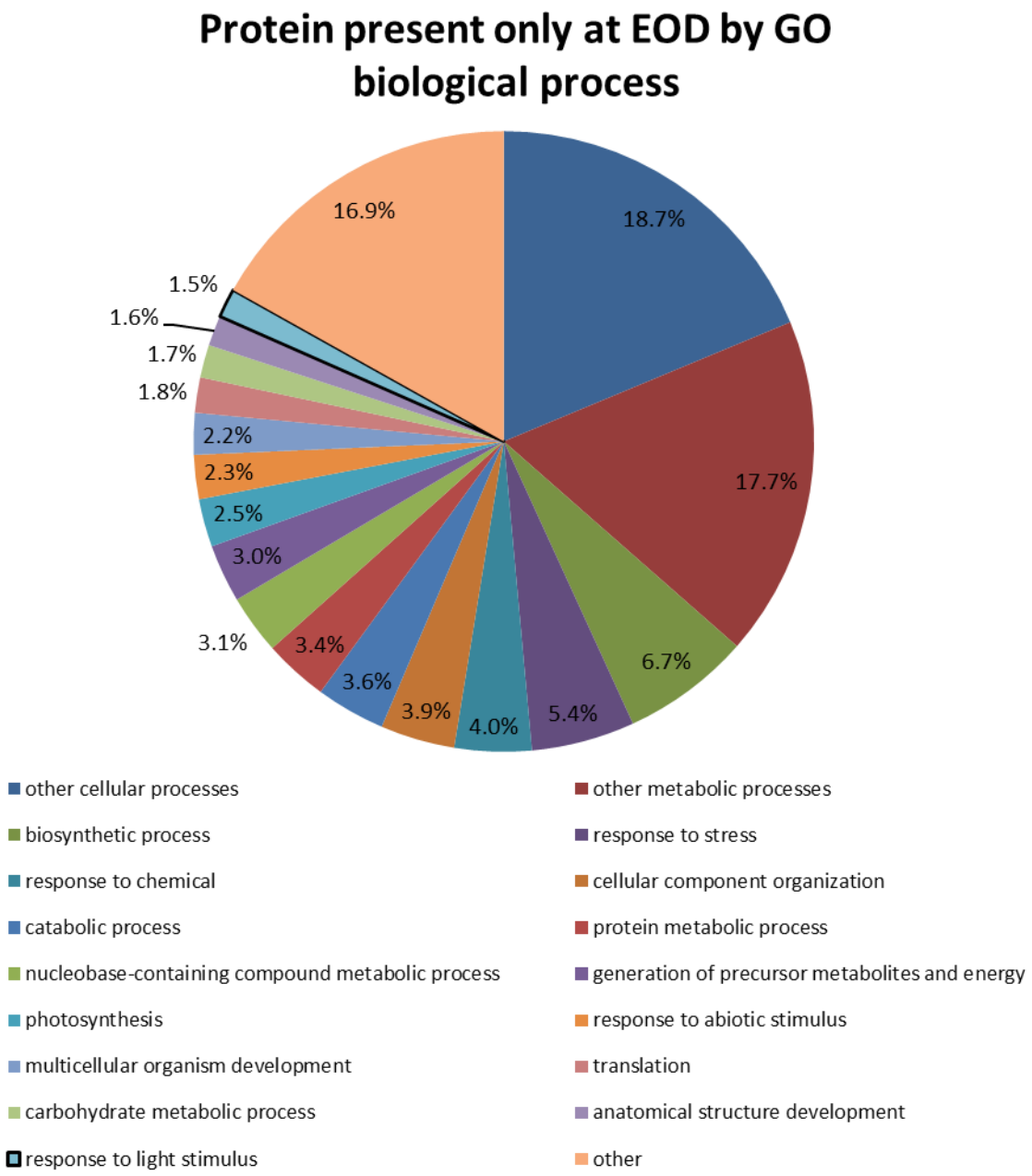

Figure 17 GO annotation of proteins identified specifically at the end of the day (EOD) in the non-enriched samples, by biological processes

There were three main groups dominating by the annotation percentage – unspecified processes as "other", "other cellular processes" and "other metabolic processes". There was no one process specifically enhanced at EOD (light), yet proteins annotated as involved in photosynthesis were present in the plot only in EOD (and not in EON see Figure 21). The identified proteins could be ascribed to a wide range of functions.

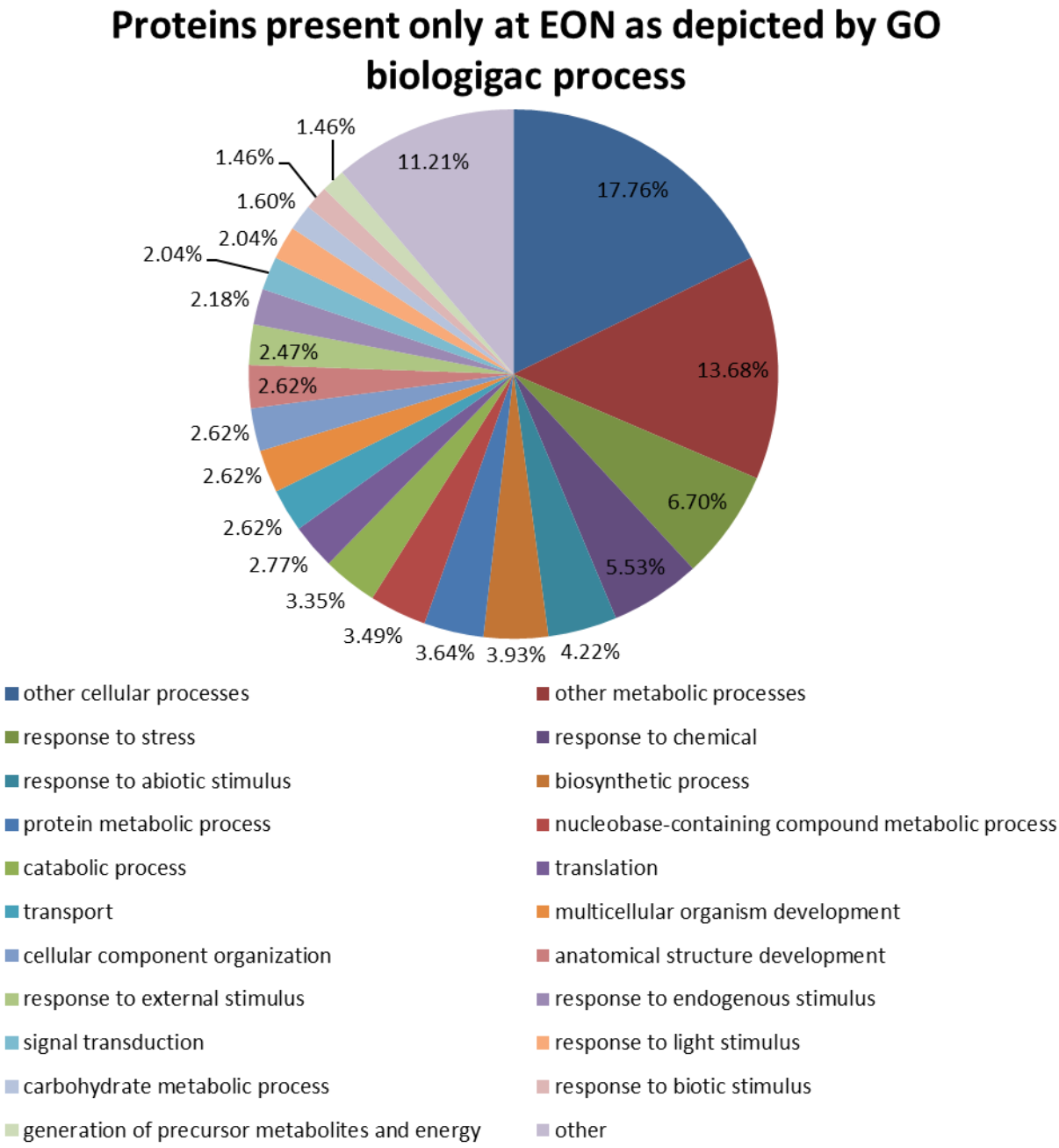

Figure 18 GO annotation of proteins identified specifically at the end of the night (EON) in the non-enriched samples, by biological processes

There were three main groups dominating by the annotation percentage – unspecified processes as "other", "other cellular processes" and "other metabolic processes". Several processes were annotated only to proteins identified at EON – transport, response to external stimuli, signal transduction, response to endogenous stimuli, and response to biotic stimuli. The increase in the expression of signaling proteins as well as stress and defense proteins is consistent with previous research (Wang et al., 2016).

3.2.1.1.2. NEM binding

Initially, NEM binding was compared on a peptide level separately in EOD and EON conditions. The NEM binding occurs at "oxidized" samples and occurred in 7 unique peptides detected in EOD samples and 6 in EON in the "total" samples, in which NEM was not applied. The upstream thiopropyl sepharose 6B column loading samples (X1 samples) were prepared for LC-MS/MS measurement according to standard procedure without any modification (with use of iodoacetamide causing carbamidomethylation). The carbamidomethylation was the most frequently occurring modification whereas NEM alkylation was less frequently occurring. At the peptide level, the unique number of peptides and their modifications were considered (Figure 19, Figure 20).

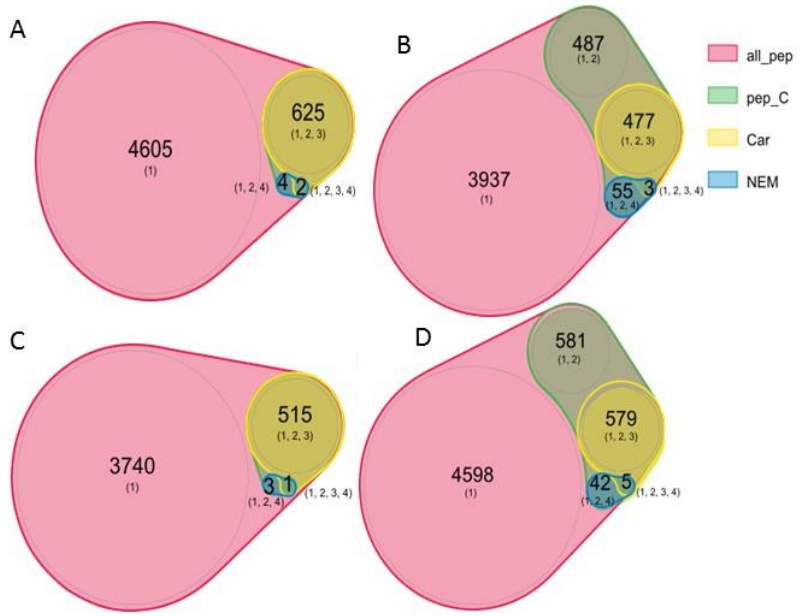

Figure 19 Venn diagrams of unique peptides, X1

A. EOD – total, without NEM treatment. Among all 4605 peptides (all_pep), 625 contained cysteines and all of them were carbamidomethylated (pep_C = Car). 2 were carrying carbamidomethylation as well as NEM alkylation and 4 were modified by NEM (NEM).
B. EOD_NEM - oxidized, with NEM treatment among all 3937 peptides, 487 had cysteines and among those 477 were carbamidomethylated, 55 were carrying only modification by NEM and 3 were carrying both modifications.
C. EON - total, without NEM treatment among all 3740 peptides (all_pep) 515 were containing Cysteines and all of them were carbamidomethylated (pep_C = Car). 1 was carrying carbamidomethylation as well as NEM alkylation and 3 were modified by NEM (NEM).
D. EON_NEM - oxidized, with NEM treatment among all 4598 peptides 581 had cysteines and among those 579 were carbamidomethylated, 42 were carrying only modification by NEM and 5 were carrying both modifications.

A, B, C, D - EOD n=3; EON n=2

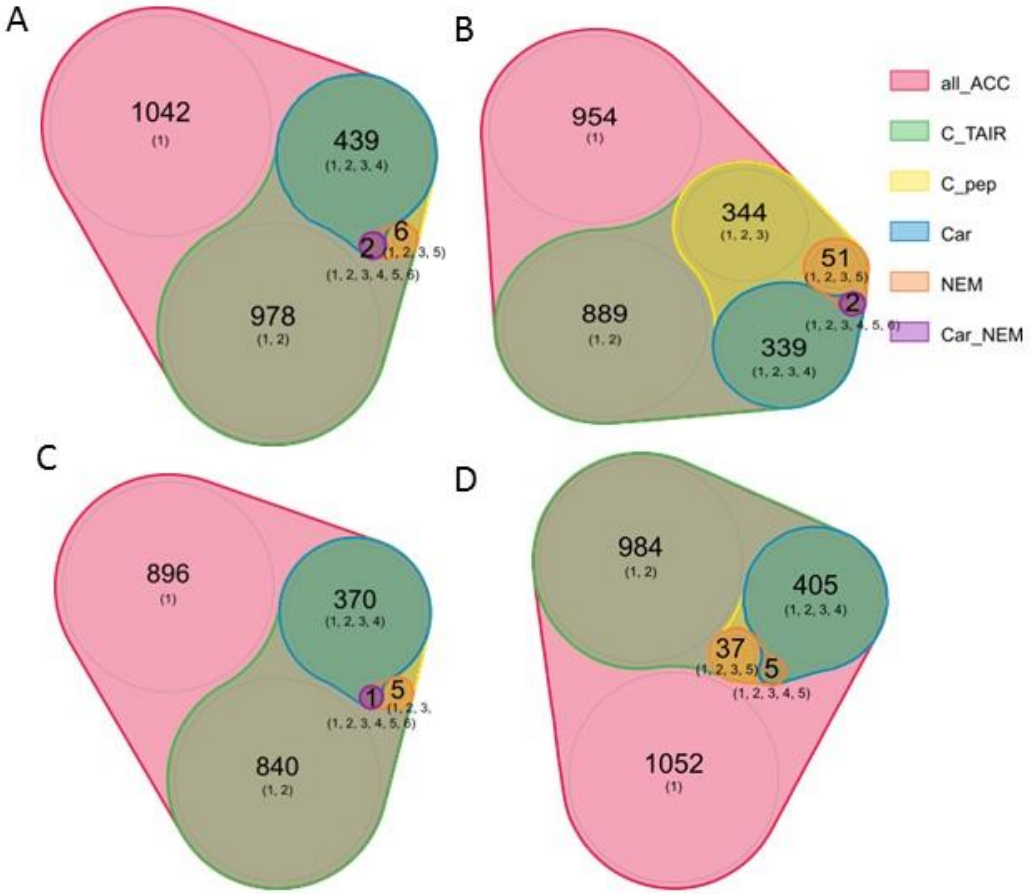

Figure 20 Venn diagram of proteins, X1 proteins containing cysteines overlapping with identified proteins that contain cysteines according to TAIR database

A. EOD – total. The total number of annotated proteins was 1042 (all_ACC). Among those proteins, 978 contain cysteines according to TAIR database (C_TAIR), this group overlaps with a smaller group of 439 proteins that contain peptides that have cysteines in their identified peptide sequence (C_pep) and are carbamidomethylated (Car), 2 proteins contained NEM(NEM) and 2 contained both NEM and carbamidomethylation (Car_NEM).
B. EOD_NEM - oxidized, all annotated proteins were 954 (all_ACC) among those proteins, 889 are containing cysteines according to TAIR data base (C_TAIR), this group overlaps with smaller group of 344 proteins that were containing peptides that have cysteines in their identified peptide sequence (C_pep), proteins containing NEM were 51 (NEM) and containing both NEM and carbamidomethylation were 2 (Car_NEM), 339 proteins were containing peptides with carbamidomethylation (Car).
C. EON – total, all annotated proteins were 896 (all_ACC) among those proteins, 840 are containing cysteines according to TAIR data base (C_TAIR), this group fully overlaps with smaller group of 370 proteins that were containing peptides that have cysteines in their identified peptide sequence (C_pep) and are carbamidomethylated (Car), proteins containing NEM were 5 (NEM) and containing both modifications one protein.
D. EON_NEM - oxidized, all annotated proteins were 1052 (all_ACC) among those proteins, 984 are containing cysteines according to TAIR data base (C_TAIR), this group overlaps with smaller group of 405 proteins that were containing peptides that have cysteines in their identified peptide sequence (C_pep), proteins containing NEM were 37 (NEM) and containing both NEM and carbamidomethylation were 5 (Car_NEM), 405 proteins were containing peptides with carbamidomethylation (Car).
A, B, C, D - EOD n=3; EON n=2

3.3. Resin-assisted enrichment of thiols

3.3.1. Oxidation ratio calculation – redox state verification

The resin-assisted enrichment of thiols was performed in three independent experiments, for each experiment four plants per condition were used. The first experiment (ENR_1) was also used for NEM evaluation and comparison of proteome during day and night (see Chapter 2.3). This experiment was followed by two repetitions (ENR_2 and ENR_3). For all three experiments the same analysis principle was applied, the processed samples were subjected to LC-MS/MS in order to measure proteins relative abundancies, based on abundances the oxidation ratio was calculated for each protein in each replicate as follows. First, the oxidation ratio of EOD was calculated by division of the total fraction (NO NEM LIGHT) by the oxidized fraction (NEM LIGHT). Next, the oxidation rate of EON was calculated by division of the total fraction (NO NEM DARK) by the oxidized fraction (NEM DARK). Finally, by division of the EOD oxidation ratio by the EON oxidation ratio the final oxidation ratio was calculated (Ratio Light_Dark).

Equation:

(NEM LIGHT/NO NEM LIGHT)/(NEM DARK/NO NEM DARK) = Ratio Light_Dark oxidation ratio

The critical threshold values were chosen based on a previously published data on redox-sensitive proteome in another organism (Rosenwasser et al., 2014). A final oxidation ratio above 1.2 (high) was considered as representing proteins oxidized in light (EOD). Yet, for this type of experiment the higher ratio might be interpreted as no change in oxidation and not necessarily points to higher oxidation. A final oxidation ratio below 0.8 (low) was considered to represent proteins more reduced in the light. Thus, the oxidation ratio as regarded as a qualitative measure for the existence of redox response rather than a quantitative measure.

3.3.2. Statistical analyses of protein redox state

The results were analyzed using as first analysis of variance (ANOVA) followed by Tukey's test. Statistical tests were performed to identify proteins characterized by significant abundance difference in total fraction (NO NEM) as compared to the oxidized fraction (NEM), separately in dark and light conditions. The subsequent step involved comparison of *p*-values per protein identified in dark as well as in light to identify proteins characterized as significantly reduced or oxidized in light but not in dark and vice versa (as reflected by abundance in the total and oxidized fractions). For most of the proteins the *p*-value was neither calculated nor turned to be significant, this is due to the variation between replicates.

This approach was tested on the experiment ENR_1, but not on pooled values for all three experiments (ENR_1, ENR_2 and ENR_3). Results of this analysis were not further used for the thesis. A second approach exploited Gaussian error propagation for calculation of confidence intervals. For each group of replicates per protein (oxidized (NEM) in dark, oxidized (NEM) in light, total-control (no NEM) in dark, total-control (no NEM) in light) the average and standard error were calculated. Next, confidence intervals (based on a t-student distribution) of the average, using propagated error were calculated. Finally, overlaps between confidence intervals were tested as an assessment of differences in redox status of a given group in light compared to dark. Using this approach only a few proteins were identified as redox regulated (further discussed in the Discussion section 4.2 Analysis approaches for candidate's identification). The MS data outcome typically contains large number of missing samples (Nas). These values may indicate the absence or an abundance below detection limit of peptides used for the certain protein identification. Ignoring the NAs may lead to a biased outcome as well as imputing these values that mostly are not normally distributed (Li et al., 2019), which makes the statistical analyses difficult to carry out.

Alternative experimental approach, the double labelling approach identified light-reduction of FBPase (Figure 21). This protein is well-known to be reduced under light.

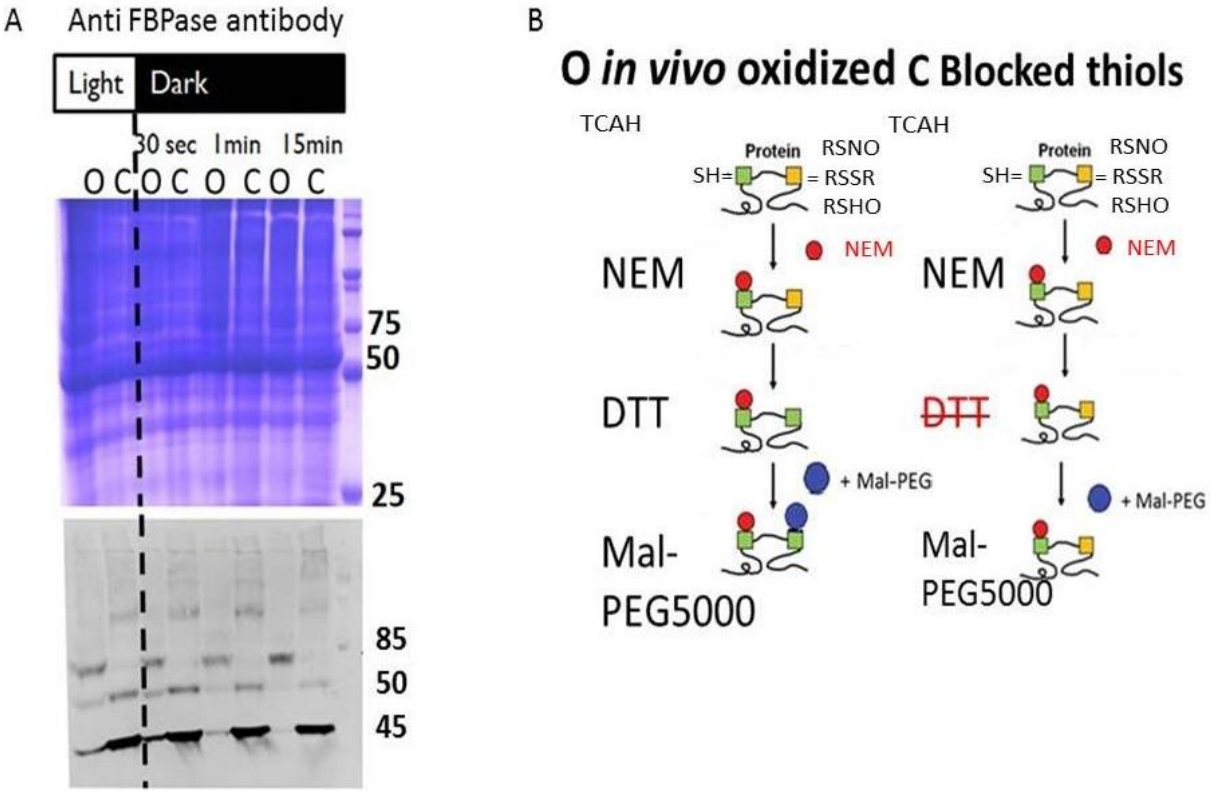

Figure 21 A double labelling approach to confirm FBPase as a redox regulated proteins
A. FBPase (45kDa) has eight Cysteines thus by adding Mal-PEG5000, ~40kDa increase of protein size can be observed by western blot. In light in both *in vivo oxidized* "O" and blocked thiols "C" both sizes can be recognized – 45kDa as well as 85kDa which corresponds with the reduced and oxidized state of protein. In light, the intensity of the lower band is stronger than the higher band. With increased time of dark incubation of the plant it can be seen that the band of 85kDa increases in intensity and at the same time the band of 45kDa decreases in intensity in samples "O". This shows that as the dark period prolongs more of the oxidized version of protein accumulates in the plants, while the reduced version becomes depleted. The sample "C" does not show the fully oxidized version in any of the conditions. An unspecific band is also present on the blot in all the conditions, probably due to Mal-PEG5000 application.
B. The double labelling approach explained. Material was collected in TCAH to preserve redox state of the protein. Proteins containing thiols are labelled with NEM, which due to its low molecular weight does not increase the proteins size appearance on subsequent SDS-PAGE and immunoblot. In next step, proteins get reduced by DTT in the sample "O" – *in vivo* oxidized while in sample "C" – blocked thiols they are not reduced. After this step Mal-PEG5000 can attach to newly formed thiols in sample "O", but not in sample "C", since no thiols were formed there. Mal-PEG5000 adds to the size of protein ~5kDA per cysteine.

3.3.3. Comparison of resin-assisted thiol enrichment experiments

The protein identification in the first replica experiment, ENR_1 was 1262 individual proteins, among which 1196 contained cysteines (95%). In ENR_2, total protein number was 1148 and 1076 contained cysteines (94%), while in ENR_3 the total number was 1886 with 1772 containing cysteines (94%). In all cases, the proteins not containing cysteines were identified as the ones characterized by a high oxidation ratio (Light_Dark ratio above 1.2),

thus were not redox regulated depending on light (EOD) conditions or oxidized in light (EOD). On average, 419 (27%) proteins were reduced in light as characterized by a Light_Dark oxidation ratio lower than 0.8. On average, the ratio higher than 1.2 was found to be applicable for 173 (11%) proteins, while steady were 938 (61%) (Figure 22).

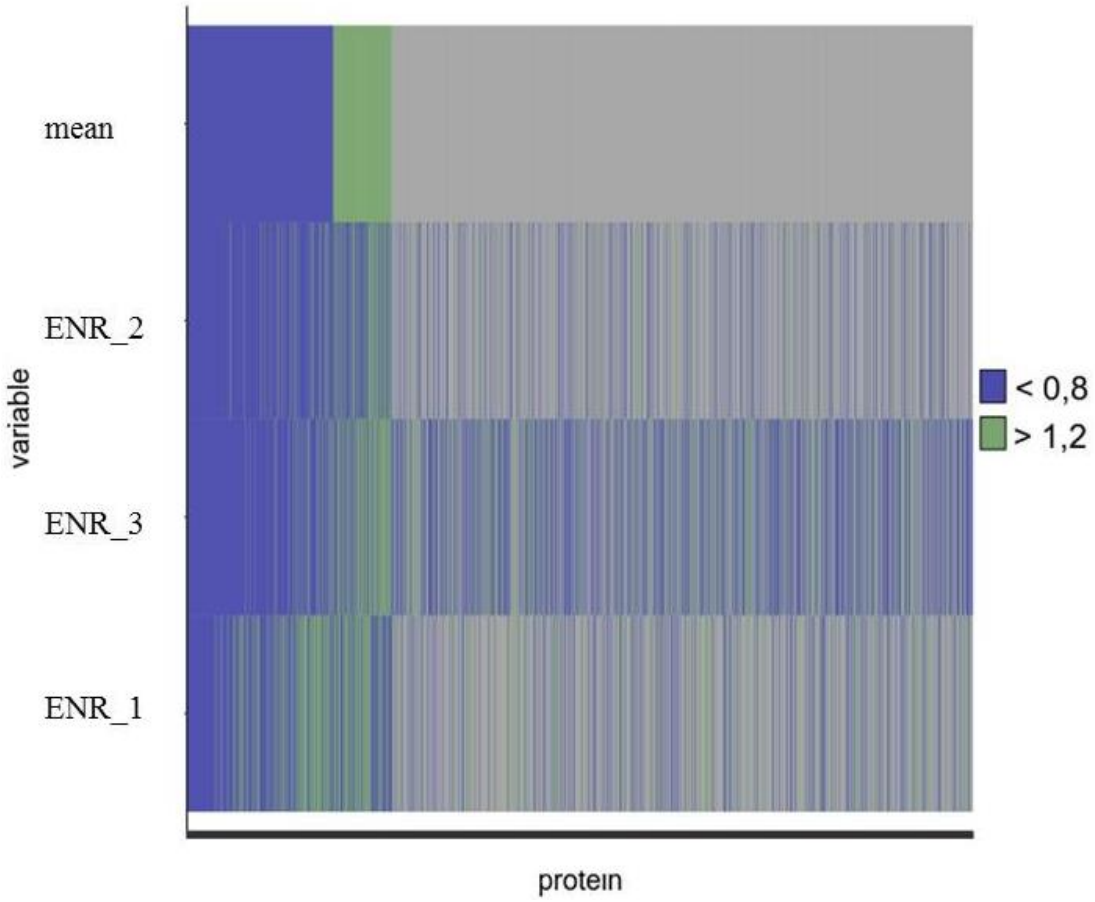

Figure 22 The visual comparison of ENR_1, ENR_2 and ENR_3 experiments
The blue bar was annotated for each protein reduced in light (Light_Dark ratio lower than 0.8), green bar was annotated to possibly oxidized or non-redox regulated in light, i.e., proteins with high ratio (Light_Dark ratio), the grey bar was annotated to steady state interval proteins (oxidation Light_Dark ratio in the range 0.8-1.2). Particularly in ENR_1presence of proteins characterized by steady state ratio was high, as compared to ENR_2 and ENR_3. The bar "mean" represents a mean number of proteins occurring in each repetition.
ENR_1 n=4; ENR_2 n=4; ENR_3 n=4

When analyzing qualitatively results of all three experiments, the overlapping proteins were considered as results that could be regarded with high confidence (Figure 23).

The light-reduced overlapping proteins were subjected to bulk Gene Ontology GO Annotation analysis (https://www.arabidopsis.org/tools/bulk/index.jsp) to reveal their localization in the cell (Figure 24), function of the protein (Figure 25) and its involvement in biological

processes (Figure 26). Since the group of overlapping light-reduced proteins in all three thiol-enrichment experiments was just 22 proteins, and as comparison between identified proteins in all three enrichment experiments showed that experiments ENR2 and ENR3 shared more identifications than any of those two with experiment ENR1, a comparison between ENR2 and ENR3 was also conducted. The GO annotation of experiment ENR2 and ENR3 by localization resulted in a similar outcome as compared with the comparison of all three experiments. Proteins identified localized to a wide range of organelles and compartments with highest number of annotations belonging to cytoplasm (12%), other intracellular compartment (11%), chloroplast (10%), plastid (8%) and thylakoid (5%) (Figure 26).

A. B.

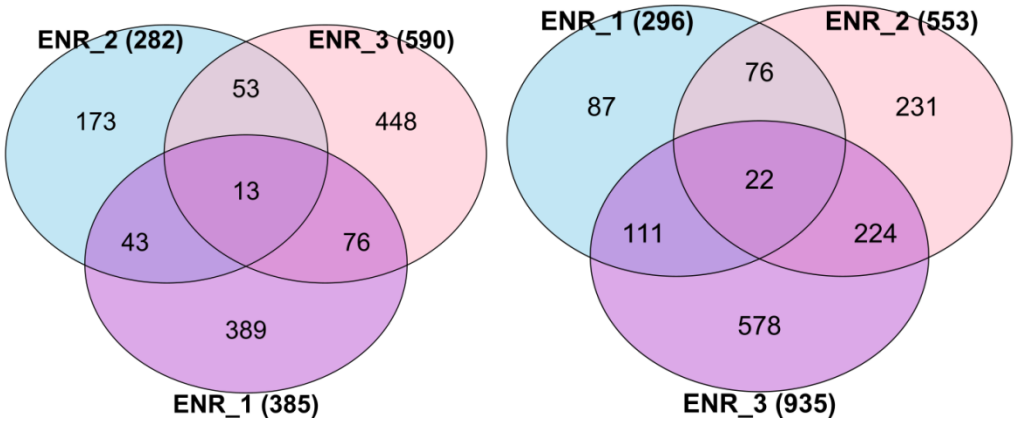

Figure 23 Comparison of overlapping proteins in experiments ENR_1, ENR_2 and ENR_3

A. Overlapping proteins characterized by high oxidation ratio (above 1.2). The overlap between all three thiol-based enrichment experiments (ENR1, ENR2 and ENR3) was 13 proteins.

B. Overlapping proteins reduced in light, characterized by lower than 0.8 Light_Dark ratios. Among all three thiol-based enrichment experiments (ENR1, ENR2 and ENR3), 22 proteins were identified. Between ENR1 and ENR2 76 proteins were shared, in ENR1 and ENR2 it was 111 and between ENR2 and ENR3 224 proteins. ENR2 and ENR3 were also shown to be more consistent in Figure 22.

A, B - ENR_1 n=4; ENR_2 n=4; ENR_3 n=4

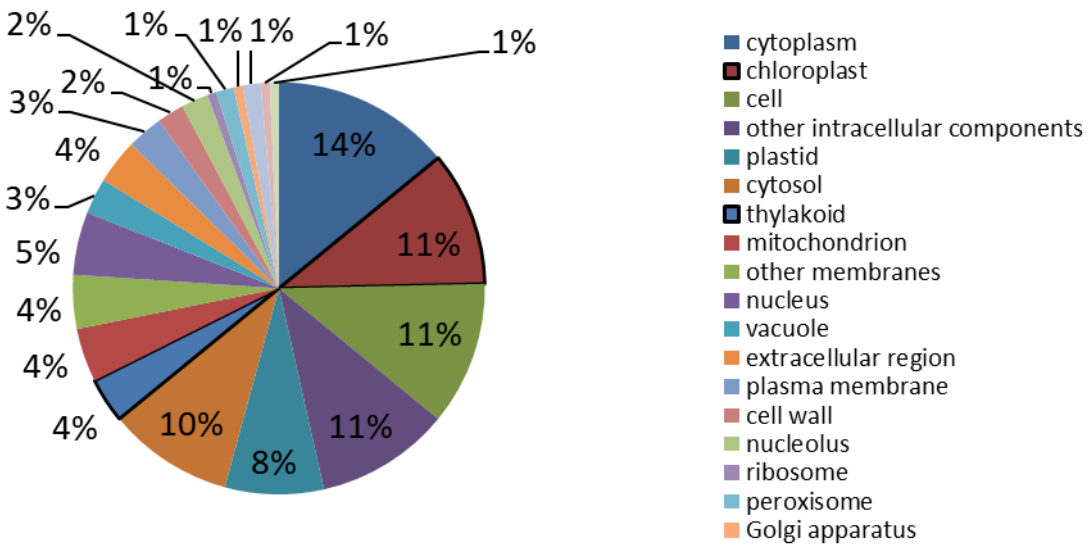

Figure 24 GO annotation – localization for common reduced in light proteins identified in ENR1, ENR2, and ENR3 (22 proteins)

The highest percentage of proteins reduced in light and shared between all three enrichment data sets were localized in the cytoplasm and chloroplast. Proteins that might be directly linked to light-dependent photosynthetic processes were localized in chloroplast (11%), plastid (8%), and thylakoid (4%). Only proteins that were consistently reduced in light proteins, according to the calculation of the oxidation ratio in all three experiments (ENR_1, ENR_2, ENR_3) are represented here.

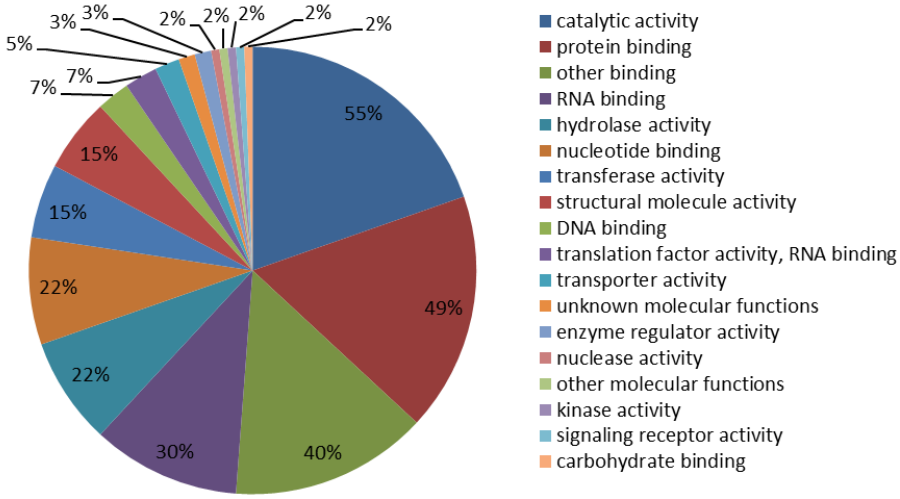

Figure 25 GO annotation – function for common reduced in light proteins identified in ENR1, ENR2, and ENR3 (22 proteins)

The highest percentage of proteins reduced in light and shared between all three enrichment data sets had a function described as catalytic activity (55%). Protein binding (49%) and other binding (40%) or RNA binding (30%) were also high in number in this data set, importantly proteins can play more than one role in cell. Function of enzyme regulator activity was found for only 3% of identified proteins. Only proteins that were consistently reduced in light proteins, according to the calculation of the oxidation ratio in all three experiments (ENR_1, ENR_2, ENR_3) are represented here.

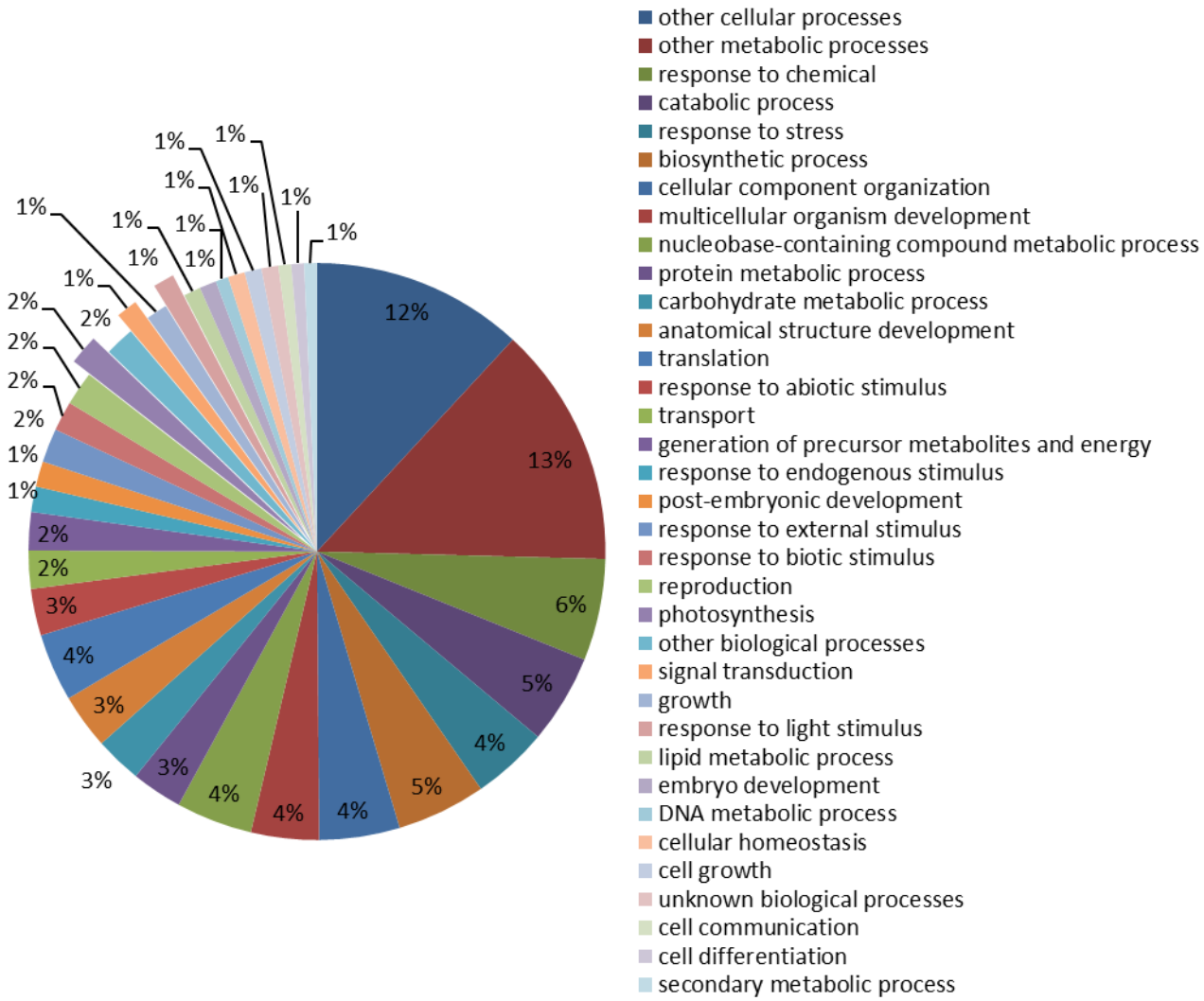

Figure 26 GO annotation – process for common reduced in light protein identified in ENR1, ENR2, and ENR3

The highest percentage of identified proteins belonged to a group annotated as “other cellular process” by GO annotation (12%) and “other metabolic processes” (13%) by GO annotation. Only proteins that were consistently reduced in light proteins, according to the calculation of the oxidation ratio in all three experiments (ENR_1, ENR_2, ENR_3) are represented here.

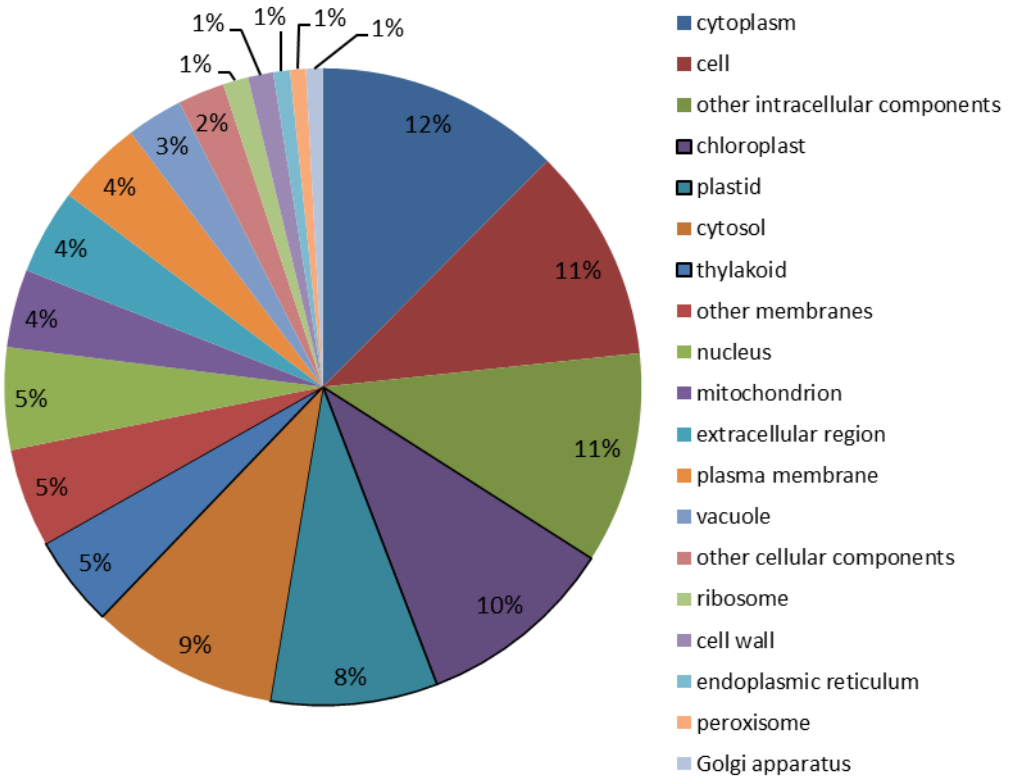

Figure 27 GO annotation analysis by localization of two enrichment experiments (ENR2 and ENR3) common light- reduced proteins

The highest overlap of identified proteins was found between ENR2 and ENR3 rather than in ENR1, ENR2, and ENR3. Nevertheless the localization of identified proteins is very similar as when all three experiments were compared. The localization of the proteins was identified as cytoplasm (12%), cell (11%) and other intracellular components (11%). Interestingly proteins localized in chloroplast were 10%, plastid 8% and thylakoid 5%. Only proteins that were consistently reduced in light proteins, according to the calculation of the oxidation ratio in all three experiments (ENR_1, ENR_2, ENR_3) are represented here.

For further analysis several proteins were chosen that appeared to be reduced in light in at least two out of three experiments. Those proteins are CSP41B, AtRabE1b elongation factor Tu with GTPase activity, proteinase FtsH2. Additionally, CSP41A was included despite it was identified only in ENR_2 as reduced in light. It was chosen beacause it is know that this protein forms complex with CSP41B (Qi et al., 2012). CSP41A and CSP41B proteins are known to be light regulated but their characterization is not complete (Bollenbach et al., 2003; Beligni and Mayfield, 2008; Bollenbach et al., 2009; Qi et al., 2012). None of these were previously reported to be a redox regulated in light. AtRabE1b protein also known as SVR11 (Suppressor of Variegation 11) has homologues in *Populus trichocarpa* x *deltoides* and *Pisum sativum* that have been postulated to be GRX targets (Rouhier et al., 2005), while the FtsH metalloprotease residing at thylakoid membrane was found to be involved in O_2 dependent

signaling *via* proteolysis of EXECUTER1 (EX1) protein that mediates stress responses (Dogra et al., 2017) (Figure 28, Table 2).

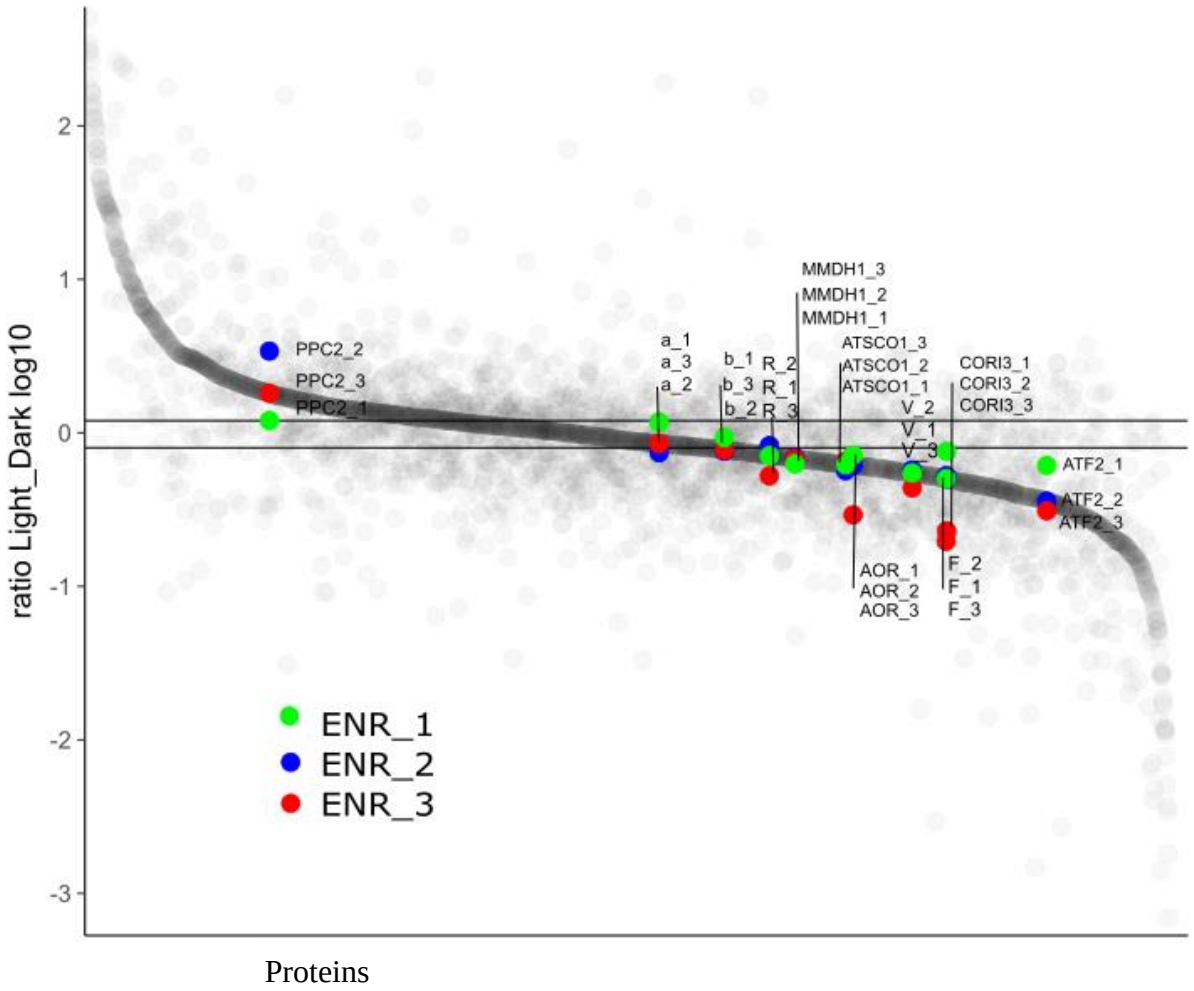

Figure 28 Distribution of proteins identified in enrichment experiments (ENR1, ENR2, ENR3)

Proteins identified in all three enrichment experiments (green –ENR1, blue – ENR2, red – ENR3) distributed according to the $\log_{10}$ of their Light_Dark ratio on *y* axis, thresholds chosen according to Rossenwesser et al.2014, marked with black lines at 0.8 ($\log_{10}$ = -0.09691) and 1.2 ($\log_{10}$ = 0.079181). Proteins with a ratio lower than 0.8 are reduced in light (EOD) according to enrichment experiments. Detailed description of proteins marked on this graph can be found in Table 3.

ENR_1 n=4; ENR_2 n=4; ENR_3 n=4

Table 2 Detailed description of candidates shown in Figure 25
The Light_Dark ratio was used as a proxy indicator of protein reduction in light. A ratio value below 0.8 indicates that the protein of interest is reduced in the data set described (ENR_1, ENR_2 or ENR_3), while a ratio above 1.2 indicates that the protein is not reduced in light. All candidates reduced in light, except CSP41A, were, were shown to be reduced (ratio value below 0.8) in at least two out of three enrichment data sets. One protein not reduced in light with ratio value above 1.2 in all data sets was chosen to be highlighted for all enrichment data sets (PPC2).

			ENR_1			ENR_2			ENR_3		
Protein	Description	Graph name		Ratio Light_Dark	log10		Ratio Light_Dark	log10		Ratio Light_Dark	log10
AT3G63140	CSP41A, encodes a protein with ribonuclease activity that is involved in plastid rRNA maturation.	a_1		1.173	0.069	*	0.742	* -0.130		0.852	-0.069
AT1G23740	AOR, ALKENAL/ONE OXIDOREDUCTASE, this protein localizes to the chloroplast where it is likely helping to maintain the photosynthetic process by detoxifying reactive carbonyls formed during lipid peroxidation.	AOR_1	*	0.717	* -0.145	*	0.614	* -0.212	*	0.292	* -0.535
AT5G16400	TRXF2, encodes an f-type thioredoxin (Trx-f2) localized in chloroplast stroma.	ATF2_1	*	0.613	* -0.212	*	0.359	* -0.445	*	0.311	* -0.508
AT1G62750	ATSCO1, This ptrotein localizes to nucleus, it consists of the five domains conserved in EF-G proteins, with two GTP-binding sites.	ATSCO1_1	*	0.619	* -0.208	*	0.567	* -0.246	*	0.654	* -0.185
AT1G09340	CSP41B, encodes CHLOROPLAST RNA BINDING (CRB).	b_1		0.933	-0.030	*	0.759	* -0.120	*	0.773	* -0.112
AT4G23600	CORI3, JR2, encodes cystine lyase which is expected to be involved in amino acid metabolism, providing the plant with cysteine and the generation of precursors of ethylene biosynthesis.	CORI3_1	*	0.757	* -0.121	*	0.503	* -0.299	*	0.230	* -0.639
AT3G54050	CFBP1, encodes a chloroplastic fructose 1,6-bisphosphate phosphatase.	F_1	*	0.503	* -0.298	*	0.526	* -0.279	*	0.197	* -0.706
AT1G53240	mMDH1 encodes a mitochrondrial malate dehydrogenase.	MMDH1_1	*	0.627	* -0.202	*	0.693	* -0.159	*	0.681	* -0.167
AT2G42600	Encodes one of four Arabidopsis phosphoenolpyruvate carboxylase proteins.PPC1 and PPC2 are crucial for balancing carbon and nitrogen metabolism	PPC2_1	**	1.203	** 0.080	**	3.406	** 0.532	**	1.811	** 0.258
AT4G20360	SVR11, it is eferred to as AtRabE1b, GTP-ase activity	R_1	*	0.711	* -0.148	*	0.826	-0.083	*	0.524	* -0.281
AT2G30950	FTSH2, VAR2,it is a metalloprotease that functions in thylakoid membrane biogenesis.	V_1	*	0.548	* -0.261	*	0.573	* -0.242	*	0.437	* -0.359
				*	<0.8		**	>1.2			
				*	<0.09691		**	>0.079181			

3.4. Redox regulated candidates

3.4.1.1. CSP41A (AT3G63140), CSP41B (AT1G09340)

The CSP41B protein was identified as a redox-regulated, reduced in light protein in ENR2 and ENR3, and was chosen for further studies. The protein CSP41A was included as a candidate for further studies even though in was identified as reduced in EOD only in ENR2. In ENR3 the ratio value for CSP41A was 0.852, thus only 0.052 higher than an arbitrarily chosen threshold (Table 2). Both proteins CSP41A and CSP41B are unique to photosynthetic organisms; they are nuclear encoded and chloroplast localized. Studies of CSP41A function showed that the protein is a non-specific RNA binding ribonuclease (Qi et al., 2012). It was

postulated that this protein initiates RNA degradation based on decrease in turnover of certain RNA transcripts in tobacco mutants (Bollenbach et al., 2003). CSP41B mutants in *Arabidopsis* were reported to accumulate precursors of 23S RNA, leading to the conclusion that this protein plays a role in the final step of maturation of 23S RNA (Beligni and Mayfield, 2008). The endonucleolytic function of CSP41 proteins shown *in vitro* contradicts the studies of CSP41A and CSP41B complexes *in vivo* where the rRNA and mRNA of certain targets was stabilized during the night (Figure 29 , Qi et al., 2012). These findings indicate that observed defects in translation and transcription are rather secondary effects due to transcripts stability drop off (Qi et al., 2012). The visual and molecular phenotype of the *csp41b* mutant in *Arabidopsis* is much more severe than that of the *csp41a* mutant. The *csp41a* mutant is able to accumulate CSP41B protein to wild type plant level, whereas *csp41b* mutants were shown to accumulate very little CSP41A protein (Bollenbach et al., 2009). Plants of the mutant line *csp41b* are visibly paler and develop to be smaller than WT plants, while *csp41a* plants resemble WT. Furthermore, the phenotype of *csp41b* can vary dependent on the growth conditions, while *csp41a* plants resemble WT under all tested conditions (Qi et al., 2012).

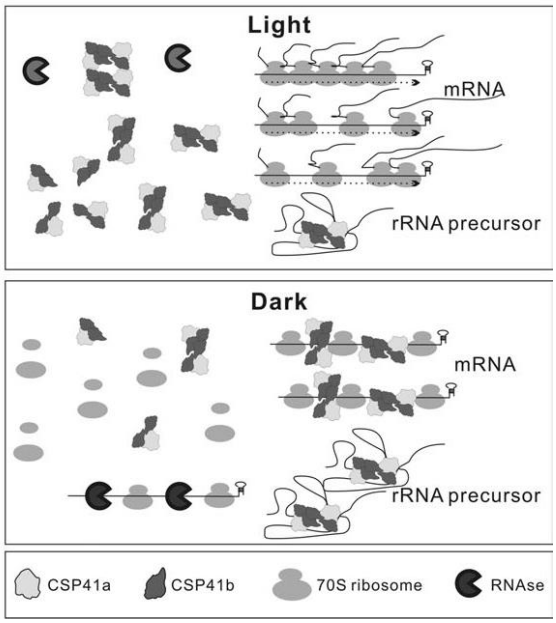

Figure 29 Postulated mode of mRNA and rRNA complex formation with CSP41 proteins
Proteins CSP41 occupy mRNA during the night preserving it from degradation and making them inaccessible for ribosomes at the same time, during the day they do not bind the transcript making it accessible for translation (after Qi et al. 2012).

3.4.1.2. Variegated 2 (VAR2, FtsH2 (AT2G30950))

The candidate VAR2 was categorized as redox-regulated and light-reduced in all three ENR experiments.

Variegated 2 (VAR2, also known as FtsH2) is a metalloprotease localized to the thylakoid membrane. Proteolysis is an important process in the chloroplast affecting photosynthesis at several different levels. Massive protein degradation is required for the development of proplastids and etioplasts into chloroplasts. Proteolytic processing is required for sorting nuclear-encoded chloroplast proteins (Figure 30) (Zaltsman et al., 2005). FtsH is a conserved in many species among kingdoms; it is a membrane bound metallo-protease with an ATPase domain and a catalytic zinc-binding site. While most prokaryotes have a single FtsH, photosynthetic organisms have multiple isoforms organized in heterocomplexes. Arabidopsis has 12 FtsHs with FtsH2 being the most abundant (Sakamoto et al., 2003). FtsHs are known to be involved in D1 protein degradation during the photosystem II repair cycle (Lindahl et al., 2000). Additionally, the *var2* mutant shows a unique pattern of variegation, suggesting that FtsH2 plays another role in chloroplast development (Chen et al., 2000). FtsH2 mediated post translational regulation is involved in chloroplast translation (Adam et al., 2011). Regulation of FtsHs is vastly unknown, yet recent studies have shown that EngA, a protein homolog of the universally conserved GTPase protein, interacts with FtsH. Overexpression of EngA positively influences stability of FtsH, yet it was not verified if that is due to specific effect on FtsH or a pleiotropic effect of EngA overexpression (Kato et al., 2018).

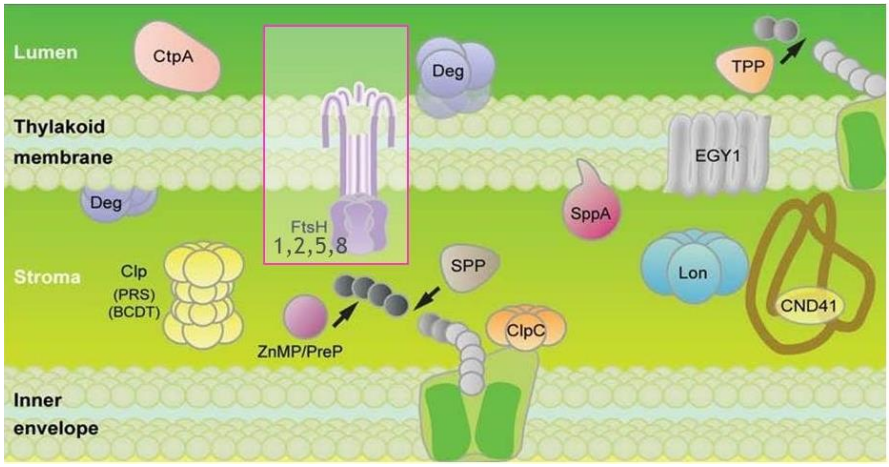

Figure 30 The proteolytic machinery of chloroplasts
FtsH members form a complex embedded in thylakoid membrane (FtsH 1,2,5,8). Other members of the proteolytic machinery: ATP-dependent proteases – Clp, FtsH, Lon; Deg family proteases; SppA - ATP-independent serine protease possibly regulated by light; EGY – ATP-independent metalloprotease involved in chloroplast development; CND41 – less known protease; SPP – stroma processing peptidase and TPP – thylakoid processing peptidase are involved in cleavage and degradation of transit peptides (after .

3.4.1.3. RAB GTPase HOMOLOG E1b (RABE1b, SUPPRESSOR OF VARIEGATION11, SVR11 (AT4G20360))

This candidate appeared as redox-regulated and light dependent in two out of three ENR experiments (ENR1 and ENR 3).

RAB GTPASE HOMOLOG E1B is a nuclear transcribed, plastid localized putative EF-Tu translation elongation factor. The protein has several activities: GTP binding, GTPase, protein binding and translation elongation factor activity (Li et al., 2018). It was shown that *svr11* mutant is a suppressor of var2 mutant. Furthermore, studies of *svr11-1* and *svr9-1* double mutants have shown a phenotype of serrated leaf margin and altered cotyledon venation, this was associated with SVR roles in regulating chloroplast and leaf development in *Arabidopsis(Liu et al., 2019).*

3.5. Further studies of selected candidates

3.5.1. CSP41A as a thioredoxin target

To further verify if CSP41A is redox regulated, formaldehyde crosslinking was performed on shaded plants of several genotypes followed by native extraction, CN-PAGE and Western blot with anti-CSP41A antibody. Plant genotypes used for this experiment were: wild type plants Col-0, thioredoxin (trx) mutant *trxm4*, double mutant *trxm1m2*, *csp41a*, and *csp41b* mutant, *trxf1* mutant and the triple *trxm124*. CSP41A stabilized by cross-linking with its interaction partner has an increased size when compared to a mutant absent with the interaction partner. From the experiment it could be concluded that indeed CSP41A interacts with thioredoxin but in an unspecific manner, or at least with several types of thioredoxins, since the molecular size appeared to be bigger in single and double mutants and lower forms could be only observed in a triple *trxm124* mutant (Figure 31).

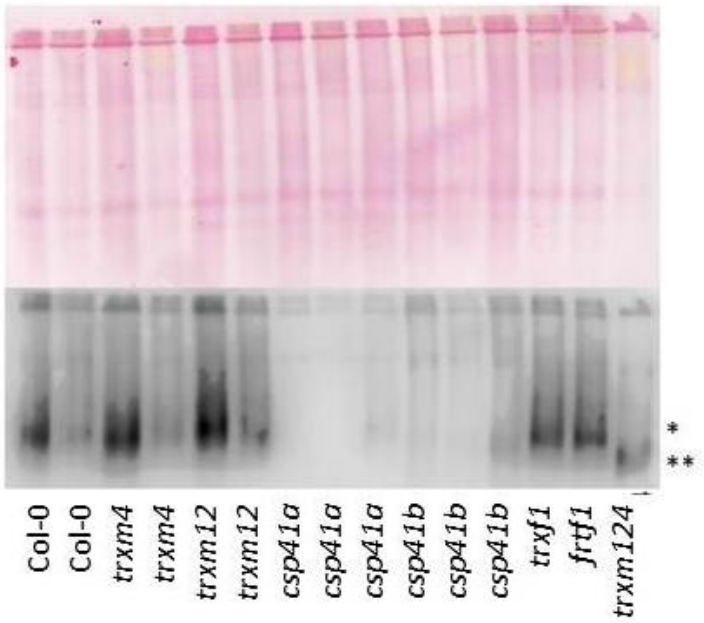

Figure 31 CSP41A as a thioredoxin putative target
Plant samples (Col-0, *trxm4, trxm12, csp41a, csp41b, trxf1 and trxm124*) underwent *in vivo* cross-linking with formaldehyde, native protein extraction and were separated by CN-PAGE. WB with antiCSP41A was performed to verify a complex formation of CSP41A protein with thioredoxins. A higher molecular weight of a putative complex is visible in lines Col-0, *trxm4, trxm12, csp41a, csp41b* and *trxf1* indicating non-disrupted complex presence even in the absence of respective thioredoxins as marked with single star (*). By contrast, in the triple mutant *trxm124*, the molecular weight is smaller than the size appearing in Col-0 indicating disruption of a putative complex, marked with double star (**). This points to interaction of Trx M1, M2 or M4 with CSP41A. Since in single mutants the size change did not occur it is possible that CSP41A is able to interact with several thioredoxins due to their redundant function. The main Trx interactor is yet to be further studied.

3.5.2. Further study of CSP41a and CSP41b candidates by Ribo-Seq

3.5.2.1. Ribo-seq concept validation

CSP41A and CSP41B were chosen as redox regulated candidates, which are reduced in light. Previous studies have shown that those proteins form a complex with RNA specifically in the light or in a mutant with low photosynthetic electron transport capacity (Qi et al., 2012). To further investigate the role of CSP41A and CSP41B in differential light conditions a Ribo-Seq experiment was conducted with *csp41a* and *cps41b,* with harvest points at EOD and EON. The Ribo-Seq method grants insight into active translation, as only the mRNA actively processed by ribosomes (so called ribosome footprints) are extracted and sequenced. The Ribo-Seq study of mutants and WT plants was performed to gain insight into translatome changes dependent on CSP41A and CSP41B proteins at EOD and EON. Since light-regulated transcriptional networks are well documented (Bailey-Serres and Juntawong,

2012), the results of Ribo-Seq obtained from WT at EON and EOD were initially compared. The data obtained from controls (WT EOD and WT EON) were consistent with previously published data (Chotewutmontri and Barkan, 2018). It was shown in previous studies that the *psbA* mRNA (encoding photosystem D1 protein) exhibits gain of ribosome occupancy under light conditions and the opposite is observed in the dark (Chotewutmontri and Barkan, 2018). Here, the same trend was observed when footprint abundance in samples WT EOD were compared with WT EON (Figure 32). This tendency is preserved when samples *csp41a* or *csp41b* EOD were compared to EON samples. Nevertheless, when comparing EOD WT to EOD *csp41a,* the difference remains significant. Although, there is less ribosome occupancy on the D1 protein transcript in *csp41a* than WT plant in EOD conditions. Low but not significantly altered abundance at EON when compared to WT EON also occurs in *csp41a*. However, since this experiment is not accompanied with the transcript level, it is unclear whether this is due to lower transcript levels (reduced transcription or degradation: i.e., when the transcript was not protected by CSP41 during the night), or due to lower levels of the ribosome-incorporated forms of rRNA, which were shown to be lower in plants lacking CSP41 (Pesaresi et al., 2001; Qi et al., 2012).

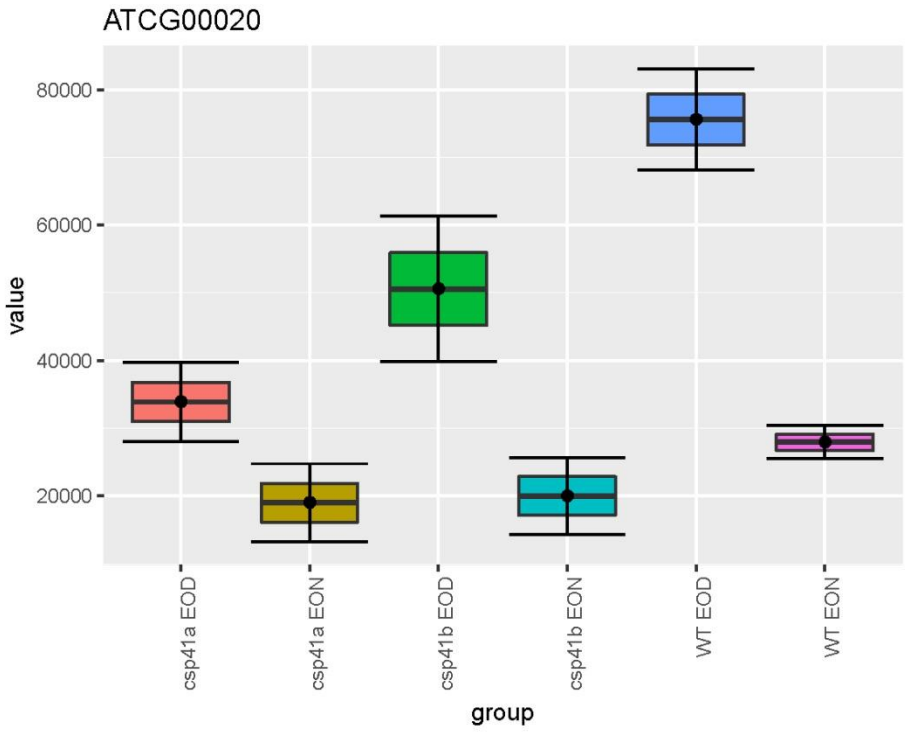

	Protein.ID	comparison	p_value
304112	ATCG00020	WT:EOD-csp41a:EOD	0.03415481
304120	ATCG00020	csp41a:EON-WT:EOD	0.00798216
304121	ATCG00020	csp41b:EON-WT:EOD	0.00871365
304122	ATCG00020	WT:EON-WT:EOD	0.01852537

Figure 32 psbA footprints abundance across the mutants and conditions in Ribo-Seq experiment
On the *X*-axis of the box plot, the mutants of the different conditions are displayed, on the *Y*-axis the abundance of identified *psbA* transcript fragments protected by ribosome binding are displayed. Table below shown significant comparisons between mutants and conditions, WT EOD: *csp41a* EOD, *csp41a* EON: WT EOD, *csp41b* EON: WT EOD and WT EON: WT EOD. The *psbA* transcript was used as a proxy for data validation, presented data goes in concert with previously published evidence about *psbA* transcript ribosomal occupancy discrepancy during the night and day.

WT EOD n=2; *csp41a* EOD n=2; *csp41b* EOD n=2; WT EON n=2; *csp41a* EON n=2; *csp41b* EON n=2

3.5.2.2. End of the Day vs End of the Night in csp41a and csp41b mutants

In total there were 20,401 transcripts identified in the Ribo-Seq experiment; out of those 2841 exhibited significant difference of the ribosome occupancy between EOD and EON in WT. Among those, 1520 were significantly more occupied by ribosomes at EON, and 1321 at EOD (Figure 33). The highest number of significantly altered footprints abundance was observed when samples from EON and EOD were compared in WT, *csp41a* and *csp41b*. By these comparisons it was possible to tackle diurnal cycle dependent footprints shared across the tested genotypes. Interestingly, there was also a sub-group of footprints that acted

in the reverse trend in mutants and also in WT plants. There were 1,687 genes concluded to be under diurnal control because they change significantly and overlapped between EON and EOD in WT as well as in the *csp41a* mutant. Among those overlapping genes, 19 genes were more translated at EOD in WT while the same genes were more translated at EON in *csp41a* plants, in the same comparison genes of opposite trend occurred in number of 46 for *csp41b*, 17 were consistent in both mutants. In *csp41b* five genes with significantly more footprints in EON WT were more abundant in EOD *csp41b* (Figure 34). Within the group of 17 genes mentioned before, 7 are located in the chloroplast according to GO annotation (https://www.arabidopsis.org/tools/bulk/go/index.jsp), among those are for example: AT2G39730 which encodes Rubisco activase – which is known to be under redox regulation and a target of thioredoxin f (Zhang and Portis, 1999) and thioredoxin H3, which mRNA is cell-to-cell mobile (Jung et al., 2013). Interestingly, among the 46 genes differentially translated in *csp41b* and WT at EON was AT3G27160, which encodes plastid ribosomal protein S21, the mRNA is cell-to-cell mobile (Pulido et al., 2018), *ATCG00770* which encodes ribosomal protein S8 (Ascencio-Ibanez et al., 2008), among others. Nevertheless, the CSP41 proteins reside in the chloroplast: how they would influence transcripts outside chloroplasts remains unclear.

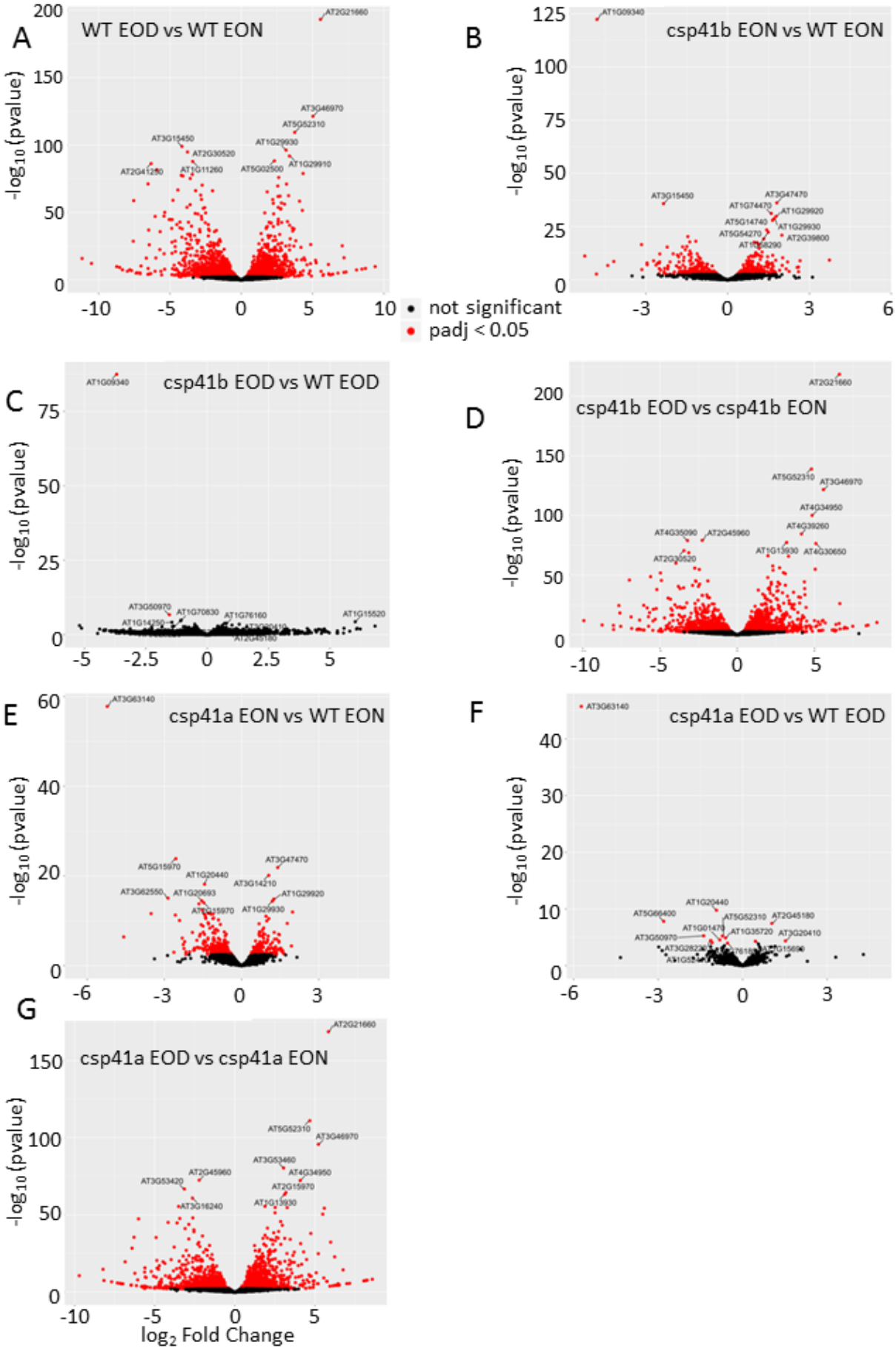
A
WT EOD vs WT EON
B
csp41b EON vs WT EON
C
csp41b EOD vs WT EOD
D
csp41b EOD vs csp41b EON
E
csp41a EON vs WT EON
F
csp41a EOD vs WT EOD
G
csp41a EOD vs csp41a EON
-log10(pvalue)
log2 Fold Change
not significant
padj < 0.05

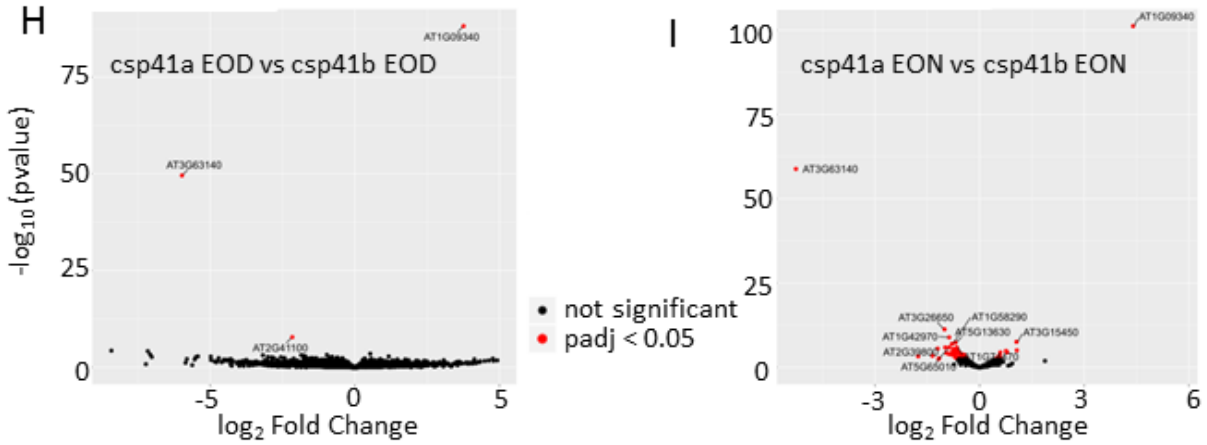

Figure 33 Volcano plots displaying the result of Ribo-Seq experiment
Volcano plots show the statistical significance ($-\log_{10}$ P value on *y* axis) versus magnitude of change ($\log_2$ fold change on *x* axis). On the plots – red dot marks a significantly altered footprint (P value adjusted – padj <0.05), black dots for not significantly altered footprint. AGI codes are displayed for the ten most significantly altered footprints. Genotypes: WT – wild type plant, csp41a – CSP41A mutant plant, csp41b – CSP41B mutant plant. Conditions: EON – End Of the Night, EOD – End Of the Day. **A. WT EOD vs WT EON** – most of the identified footprints were altered when EON and EOD conditions were compared for WT, including genes known to be under light control and circadian clock genes.
B. *csp41b* EON vs WT EON – the top altered gene in this comparison is AT1G09340 (CSP41B), as expected from the mutant being depleted of the transcript, this comparison highlights footprint likely altered in absence of csp41B and dependent or its difference in activity at night.
C. *csp41b* EOD vs WT EOD – a very low number of transcripts in plant lacking CSP41B were altered as compared to WT, the top altered gene in this comparison is AT1G09340 (CSP41B), as expected from the mutant being depleted of the transcript
D. *csp41b* EOD vs *csp41b* EON - a high number of changed footprints is identical as in comparison A. and G. due to identification of light dependent genes and circadian clock – regulated genes, not dependent on CSP41.
E. *csp41a* EON vs WT EON – the top altered gene in this comparison is AT3G63140 (CSP41A), as expected from the mutant being depleted of the transcript, this comparison highlights footprint likely altered in absence of csp41A and dependent or its difference in activity at night.
F. *csp41a* EOD vs WT EOD– a very low number of transcripts in plant lacking CSP41A was altered as compared to WT, the top altered gene in this comparison is AT3G63140 (CSP41A), as expected from the mutant being depleted of the transcript
G. *csp41a* EOD vs *csp41a* EON - a high number of changed footprints is identical as in comparison A. and D. due to identification of light dependent genes and circadian clock – regulated genes, not dependent on CSP41.
H. *csp41a* EOD vs *csp41b* EOD – nor CSP41A neither CSP41B influence footprint abundance during the EOD, see also C. and F.
I. *csp41a* EON vs *csp41b* EON – this comparison highlights the footprints belonging to genes that are under differential regulation depending on CSP41A or CSP41B at EON.

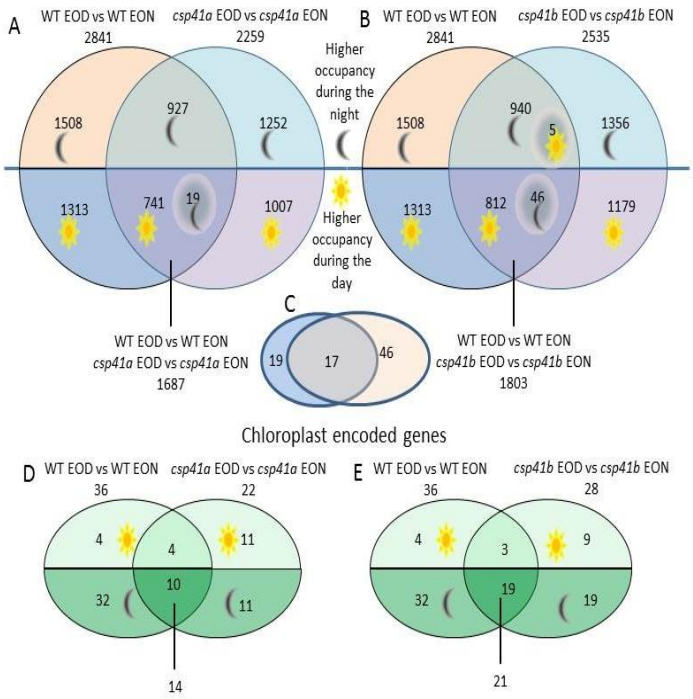

Figure 34 Comparison of genes attributed to footprints from Ribo-Seq between the EON and EOD conditions for WT and csp41 mutants

A. A Venn diagram of WT EOD vs WT EON overlapping with *csp41a* EOD vs *csp41a* EON. Genes considered for the graph were significantly changed in footprint abundance (P value adjusted – padj <0.05). Top part of the graph, above blue line separates genes assigned to footprints characterized by higher ribosomal occupancy in the nigh (EON) while the bottom part higher occupancy during the day (EOD). Consistent in the diurnal change genes were 1687, yet within this group 19 genes were more translated at EOD in WT while the same genes were more translated at EON in *csp41a*. A group of 325 genes was characterized by higher ribosomal occupancy at night (EON) in *csp41a*. A group of 266 genes was characterized by higher ribosomal occupancy at day (EOD) in *csp41a*.

B. A Venn diagram of WT EOD vs WT EON overlapping with *csp41b* EOD vs *csp41b* EON. Genes considered for the graph were significantly changed in footprint abundance. The top part of the graph, above the blue line separates genes assigned to footprints characterized by higher ribosomal occupancy in the nigh (EON) while the bottom part higher occupancy during the day (EOD). Consistent in the diurnal change genes were 1803, yet within this group 46 genes were more translated at EOD in WT while the same genes were more translated at EON in *csp41a;* 5 genes were more translated at EON in WT while the same genes were more translated at EOD in *csp41b.* A group of 416 genes was characterized by higher ribosomal occupancy at night (EON) in *csp41b*. A group of 367 genes was characterized by higher ribosomal occupancy at day (EOD) in *csp41b*. **C.** A Venn diagram of genes more translated at EOD in WT yet more translated at EON both mutants, showing an overlap of 17 genes. **D.** A Venn diagram of chloroplast encoded genes significantly changed between conditions EOD and EON. There were 36 identified and significantly altered in abundance of footprints genes in WT EOD vs WT EON, among those 4 were characterized by higher ribosomal occupancy at EOD and 32 in EON. There were 22 identified and significantly altered in abundance of footprints genes in *csp41a* EOD vs *csp41a* EON, among those 11 were characterized by higher ribosomal occupancy at EOD and 11 in EON. The specific genes for *csp41a* higher occupancy in EOD were 7 and higher in EON 1 gene. **E.** A Venn diagram of chloroplast encoded genes significantly changed between conditions EOD and EON. There were 28 identified and significantly altered in abundance of footprints genes in *csp41b* EOD vs *csp41b* EON, among those 9 were characterized by higher ribosomal occupancy at EOD and 19 in EON. The specific genes for *csp41a* higher occupancy in EOD were 6 and higher in EON no gene.

Significantly altered footprints displayed in fig. 34 (in all panels) are consistent and based on the same analysis as fig. 33.(P value adjusted – padj <0.05).

3.5.2.3. csp41a and csp41b End of the Night vs Wild Type End of the Night, csp41a and csp41b End of the Day vs Wild Type End of the Day

The Ribo-seq analysis revealed a sizeable fraction of genes differed in their expression, especially in EON condition. The counts of 481 gene transcripts were significantly differently occupied by ribosomes in *csp41b* EON and WT EON, for *csp41a* EON and WT EON it was 370. In both mutants there were present genes significantly more occupied by ribosomes during the night as well as significantly less. To focus on genes that might be targets of CSP41A and CSP41B genes specifically altered in the respective mutants were identified. Additionally, chloroplast encoded specific genes that might be involved in photosynthesis regulation were also identified (Figure 35). In *csp41a* among specific genes encoded in the chloroplast there were five ribosome associated transcripts. All of them were significantly lower in footprints abundance in *csp41a* EON *vs.* WT EON (RPL20, RPL36, RPS8, RPL14, and RPL22). RPL22, RPL36, RPL14 and RPS8 are among 11 proteins that belong to same interaction network (https://version-11-0.string-db.org/cgi/network.pl?networkId=T2LYFYMTHzYR). RPS8, RPL14, PRL20, RPL22 were shown to be essential ,thus the knockout is lethal (Shoji et al., 2011), RPL36 is non-essential, the knockout generates plethora of phenotypes in tobacco (Baba et al., 2006). Another gene specific for mutant *csp41a* is TIC214 that encodes a translocation protein. It is a member of photosynthetic-type TIC complex, in its absence alternative minor complex can partially replace its function, yet in absence of both complexes plants cannot grow (Kikuchi et al., 2018). Involvement of CSP41A protein with TIC214 transcript could provide a link for CSP41A role in communication of chloroplast with outside chloroplast. In the Ribo-seq experiment a higher number of genes were specific for the *csp41b* mutant at EON, although less chloroplast encoded genes were identified. Interestingly among specific putative CSP41B targets was CP12, a known redox regulated protein and key regulator of light dependent activation of CBB (Calvin-Benson-Bassham cycle) enzymes (Trost et al., 2006). CP12 forms a complex with phosphoribulokinase (PRK) and glyceraldehyde-3-phosphate dehydrogenase (GAPDH) in darkness or low light conditions, and this complex dissociates within 1 min after exposure to light, facilitating activation of PRK and NADP-GAPDH. Redox modification in all identified CP12 proteins occurs via the reduction of two cysteine pairs (Marri et al. 2009). In the Ribo-Seq in *csp41b* mutant, the CP12 footprint was accumulated two times more during EON than EOD. Also increased was GapA-1that is known to be coordinately expressed by light with PRK and CP12 (Del Giudice et al., 2015), GapA-1 footprint was two

and half times more abundant in EON than EOD. TOC159 is not encoded in the chloroplast but it is a protein required for import of protein necessary for chloroplast biogenesis (Chang et al., 2017). The specific and chloroplast encoded footprints identified for *csp41b* mutants were seven in total but only three had significant difference between EON and EOD- RPS14, NDHJ and NDHG, none of those overlapped with csp41a chloroplast encoded and significantly altered footprints. In the mutant *csp41b* there were two genes significantly differently occupied by ribosomes when compared to WT EOD, they were both significantly less occupied than WT EOD. One of these was CSP41B and the second gene was shared with *csp41a* mutant - AT3G50970, XERO2, a cold responsive protein located in the cytosol and membrane whose RNA is cell-to-cell mobile (Gupta et al., 2019).

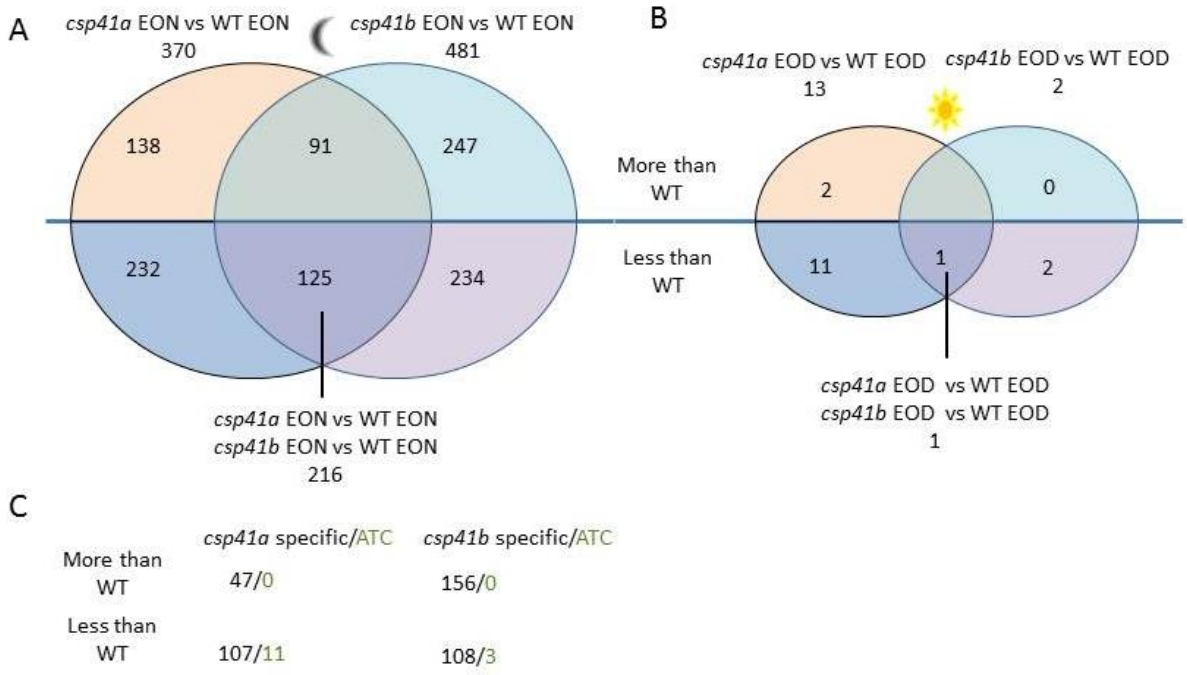

Figure 35 Comparison of genes attributed to footprints from Ribo-Seq, EON mutants vs EON WT and EOD mutant vs EOD WT

A. A Venn diagram showing overlap of genes annotated to footprints of *csp41a* EON vs WT EON and *csp41b* EON vs WT EON. The total overlap of genes identified was 216. The specific genes identified only in *csp41a* EON vs WT EON were 154, among those 47 were up regulated and 107 were down regulated, in *csp41b* EON vs WT EON specific genes were 264, among those 156 were up regulated and 108 down regulated. **B.** A Venn diagram showing overlap of genes annotated to footprints of *csp41a* EOD vs WT EOD and *csp41b* EOD vs WT EOD. The comparison in EOD condition showed a minimal difference in footprint analysis. **C.** A table showing chloroplast encoded genes occurrence identified to be specifically changed in *csp41a* EON vs WT EON and *csp41b* EON vs WT EON comparisons. Significantly altered footprints displayed in fig. 35 are consistent (fig. 33-35) and based on the same analysis as fig. 33.(P value adjusted – padj <0.05).

3.6. Multi-omics analysis reveals mechanisms of complete resistance to extreme illumination levels in a green alga isolated from desert soil crusts - collaboration

The redox enrichment protocol optimized as a part of this thesis was next applied for a study of the alga *Chlorella ohadii* (Treves et al. 2020). The collaborative work included redox proteomics, transcriptomics, metabolomics and lipidomics. For the purpose of this thesis the main findings of the research in the area of redoxome study will be summarized.

3.6.1. *Chlorella ohadii* as a subject of study - introduction

The recently characterized alga *C. ohadii* was isolated from desert biological sand crusts (BSC) (Treves et al., 2013). This organism exhibits the remarkable capacity to tolerate an extremely high light up to 3000 µmol photons m^{-2} s^{-1}, which is six times higher than required to saturate photosynthesis. The study was designed to dissect the cellular response of this alga to extreme irradiation levels (EIL, 3000 µmol photons m^{-2} s^{-1}) using a multi-omics approach.

3.6.2. Experimental design

Algal material. Batch cultures of *C. ohadii* for inoculum were grown in Erlenmeyer flasks, on a shaker, in Tris, acetate, phosphate (TAP) medium (Tris, acetate, phosphate buffer), or TAP without acetate, at 35°C, 100 g, 100µmol photonsm^{-2} s^{-1}.

Photobioreactor cultures. *Chlorella ohadii* was grown in a flat glass bioreactor vessel (20×3×24 cm^3) (FMT-150, PSI), as previously described (Červený et al. 2013). Two bioreactors were used to allow parallel culture of cells under both LL and EIL. Unless specified otherwise, the experiments were initiated at low cell density corresponding to optical density (OD)735 nm =0.02 and the culture temperature was stabilized at 35.0±0.3 °C. Irradiance levels included three regimes: 100µmol photonsm^{-2} s^{-1} (LL), 3,000 µmol photonsm^{-2} s^{-1} (continuous EIL) and transfer from LL to EIL. In parallel cultures, when density had reached the value at which EIL transfer was applied (OD735 nm =0.73), the lid of the reactor was opened and penetrating light was measured using a universal light meter (ULM500, Walz) placed inside the bioreactor vessel either on the side adjacent to or on the side opposite the light-emitting diode (LED) panel, as ~80 and ~30µmol photons m^{-2} s^{-1} under LL and as 2,300 and 800 µmol photonsm^{-2} s^{-1} under EIL. Air for bubbling was

supplied using an air-pump at ~100mlmin^{-1}. Dissolved oxygen concentration and pH were monitored in situ every 1min, and OD680 nm and OD735 nm were monitored every 1min. All cultures were grown starting from the same inoculum density. Bioreactors were autoclaved with medium and electrodes, and axenic inoculum was added on a sterile bench, together with 0.22-µm filters on all air inlets/outlets of the system. The cultures were axenic, as validated by light microscopy and Luriana broth plating/incubation before the first sampling point in each replica. Cell counting and contamination control were performed using a light microscope (Eclipse E200, Nikon) and a haemocytometer; for each data point, we counted ten squares containing up to 30 cells.

Redox proteome. *Chlorella ohadii* cells for proteome analysis were quenched by the addition of 40ml of culture to 10ml of ice-cold 100% TCAH under a light level corresponding to that of the treatment, and the mixture was then put on ice. Thereafter, quenched cells were harvested by centrifugation for 5 min, 4,000 rpm, 4°C and the pellet was washed with 10% TCAH-acetone and stored at −80 °C. Thiol-based enrichment was performed as described for *Arabidopsis* in this thesis with certain modifications. Each sample was split into two subsamples, for either alkylation or control. All buffers from this point on were de-gassed before use. Alkylation was performed using 100mM N-ethylmaleimide (NEM) in buffer (0.05% SDS, 250mM HEPES, 0.1mM EDTA, 0.1mM neocuproine, pH 7.5), followed by acetone precipitation and three washing steps of both control and subsamples. Thereafter, all subsamples were reduced with DTT in mild denaturing buffer (250mM HEPES, 8M urea, 0.1% SDS, 10mM DTT). Excess DTT was removed using 10 kDa centrifugal filters (Amicon Ultra-4 Centrifugal Filter Units) before loading of samples onto self-made thiopropyl sepharose 6B columns conditioned with water and enrichment buffer (0.1M Tris-HCl pH 7.5, 0.5M NaCl, 5mM EDTA). Enrichment was performed by shaking (600 rpm.) in a table-top Eppendorf thermo-mixer at room temperature for 4h. To minimize non-specific binding, unbound proteins were removed by rigorous washing including five cycles of each of the following: 8M urea, 2M NaCl, 80% acetonitrile with 0.1% trifluoroacetic acid (TFA) and 25mM Hepes. Lastly, the bound fraction was eluted from the column by incubation with 50mM DTT and was further subjected to tryptic digest LC–MS analysis. We used QExactive Plus combined with nano LC1000 in column reverse phase C18 (Acclaim PepMap RSLC, 75 µm×150mm, C18, 2 µm, 100Å) to resolve peptides. Equilibration buffer A (3% acetonitrile, 0.1% TFA) and elution buffer B (80% acetonitrile, 0.1% TFA) were used. The gradient was run as follows: 50min from 0 to 28% buffer B at a flow rate of 300nlmin^{-1} , 8 min to 40% buffer B at 300nl min^{-1}, 2min to 80% buffer B at 300nl min^{-1} , followed by a 5-min wash

with 80% buffer B at 500nl min^{-1} and 4-min 0% buffer B at 500nl min^{-1}. QExactive Plus Full MS scan settings were: resolution 60,000, AGC target 3×106, maximum IT 100 MS, scan range 150–1,600 m/z. MS2 scan settings were: resolution 15,000, AGC target 2×105, loop count 15, isolation window 2m/z, collision energy nce:30. Data-dependent acquisition settings were: apex trigger on, charge exclusion 1, 5–8, >8. MaxQuant v.1.4.1.2 (https://www.maxquant.org/), in combination with the Andromeda search engine79, was used to annotate peptide sequences (PRIDE dataset identifier: PXD015681) using the *C. ohadii* genome. Proteins were digested with trypsin, and fixed modification was set as carbaminomethylation. Further settings were as follows: false discovery rate 1% with decoy mode: revert; score cut-off 25 for unmodified peptides. For quantification, unique and razor peptides were used and label-free quantification was on, with a maximum of two mis-cleavages allowed. The experiment was repeated four times, and only proteins that were identified and found as redox sensitive in at least two experiments were considered as redox sensitive. The difference in degree of reduction between cells at t3EIL and under continuous EIL to LL was calculated for each peptide.

Calculation of redox index RI (compared resin-bound blocked thiol and control subsamples in each treatment and calculated the relative change in reduction state, in the *Arabidopsis* related part this comparison was called ratio Light_Dark) was defined as the quotient of NEM alkal by control subsamples per replica and was averaged for each peptide per treatment (LL, t3EIL and continuous EIL). We defined peptides as redox sensitive if their calculated RI average at t3EIL or under continuous EIL was at least 20% higher than under LL, and thus change in RI was regarded as a qualitative measure of the existence of redox response rather than as a quantitative measure of its extent. Over 3% of identified proteins did not contain cysteine in their sequence and were removed from our analysis, indicating the specificity of our approach.

3.6.3. Main findings in the area of redoxome study. *C. ohadii* proteome illustrates a highly dynamic redox response to EIL

The rapid alterations of photosynthesis and growth in *C. ohadii* cells exposed to EIL, together with the absence of any detectable effect of EIL on productivity (Treves et al., 2016) suggest that rapid sensing and adjustment of redox state in the alga plays a crucial role in EIL tolerance. The analysis of redox enrichment was done as presented in the thesis in chapter 3.3.1 Oxidation ratio calculation – redox state verification, page 57. The oxidation ratio was calculated for LL, t3EIL and continuous EIL. The total identification was 1061 proteins. Of these, 175 proteins (~16% of the thiol-enriched proteome) exhibited a considerable change in

oxidation ratio compared to LL at t3EIL and/or continuous EIL (a candidate redox sensitive protein is shown as such in at least two out of four experiments). Of these 148 (~85% of the detected redox-responsive proteins) exhibited a significant response at t3EIL. This emphasizes the importance of post-translational modification in the early response to EIL.

The 175 redox-responsive proteins of interest were further investigated in search of known redox-regulated homologs from other species. Among identified homologs were thioredoxins (four), glutaredoxin (one) and plastidic FBPase. Additionally, two known redox-regulated heat-shock proteins were identified (HSP70 and HSP33), and constitutively expressed in *C. ohadii* heat-shock transcription factor (HSF).

The list of *C. ohadii* redox-responsive proteins included 11 serine-threonine kinases, three predicted transcription factors, three RNA-interacting and two TPR-domain containing proteins. Functional enrichment analysis highlighted the terms phosphotransferase/kinase activity-associated proteins, translation, oxidation/reduction and lipid metabolism.

Additionally, two enzymes with potential role in NADPH removal in EIL were identified, a cytosolic non-phosphorylating glyceraldehyde-3-phosphate dehydrogenase (NADP-GAPDH) homolog and a predicted mitochondrial NADP-dependent malic enzyme (NADP-ME).

Moreover, the *C. ohadii* proteome is more rich in cysteines as homologs in other species comparison reveled. The redox-proteome of *C.ohadii* has 8-18% higher cysteine abundance as compared to homologs from *C. sorokiniana*, *C. vulgaris*, *C. variabilis* and *C. reinhardtii.* This implies even larger potential of redox-regulation in *C. ohadii* than this study revealed.

3.6.1. Main findings in the area of redoxome study – discussion

Photosynthesis and growth increased within the very few first minutes of shift to EIL (data not presented here) - long before de-novo protein synthesis can alter protein abundance. The 3 min shift to EIL was enough to initiate rapid post-translational redox response reflected in modification of many protein kinases/phosphatases, which are themselves likely to provide the potential for further rapid amplification of regulation at the post-translational level. Post-translational redox regulation also affected pathways involved in redox-signaling, Heat Shosck responses, lipid biosynthesis, and translation. *C. ohadii* grown in LL maintains the capacity to cope with the high light excess of 3000 µmol photons m^{-2} s^{-1}, this remarkable

feature might be associated with evolutionary adaptation to optimize growth in this non-classical diurnal cycle.

4. Discussion

Cysteine residues in proteins contain a highly reactive thiol sidechain. This sidechain can potentially react with a plethora of oxidants and undergo various redox-based modifications. Possible PTMs are intra- and intermolecular disulfide bridges, and formation of mixed disulfides with glutathione (S-glutathionylation) or S-nitrosylation (Mieyal and Chock, 2012). Conformational changes that occur along with the modifications can regulate the protein activity or protect against irreversible hyperoxidation to sulfonic acid (SO_3H) (Brandes et al., 2009; Konig et al., 2012). Higher oxidation forms like sulfenic (SOH) or sulfinic acid (SO_2H) can be reversed by specific cellular reductants such as thioredoxin or glutathione or sulfiredoxin (Liu et al., 2016). Those PTMs occurring via cysteine are involved in numerous cellular activities, including immediate metabolic regulation and control of transcriptional and translational activities in development and defense pathways (Muthuramalingam et al., 2013). Therefore, studies of such PTMs are crucial for understanding plant adaptation to external stimuli such as light. Optimizing methods suitable for studying plants redox PTMs is of high importance in the development of the redox-proteome field.

4.1. Yield of affinity enrichment

In this study a published method for resin-assisted thiol enrichment of proteins (Guo et al., 2014) was adapted for use in *Arabidopsis thaliana*. This study consists of three independent biological repetitions (using independently grown sets of plants in growth chambers) of the whole work flow from growing plants to mass spectrometric measurements and analysis (ENR1, ENR2, and ENR3). The main interest of the presented experiments was to gain a global insight into oxidative post translational modifications (ox-PTMs) in physiological conditions for the plant at the end of the night (EON) and at the end of the day (EOD). To do so a relative abundance of proteins in different light conditions (EON and EOD) was measured for the control and NEM-alkylated samples (see workflow 3.1Work flow for resin-assisted enrichment of thiols experiments, page 43). In Guo et al. 2014 following protein enrichment on the affinity resin, an on-resin digestion was performed followed by isobaric labelling, thereby only the labelled and enriched peptides were measured. In the modification used in this study, the intact enriched proteins were eluted from the resin and followed by a digest and MS preparation in the standard manner used at MPI (Takahashi et al., 2019). Due

to reaction with iodoacetamide (IAM), carbamidomethylation is the most frequently occurring modification in the NEM binding evaluation (see 3.2.1.1.2 NEM binding, page 53), whereas NEM alkylation occurs less frequently. NEM alkylation is reversible in some conditions (Nishiyama and Kuninori, 1992). Nevertheless, NEM is an alkylating agent of choice for many studies due to faster reaction than e.g. IAM and smaller pH dependence (Hill et al., 2009). NEM binding efficiency is crucial for the success of this method, thus it is important to use optimal pH and an excess of reagent. For all three enrichment experiments (ENR1, ENR2 and ENR3) a molar excess of roughly 500 times per expected protein concentration was used. The starting protein solution used for NEM alkylation was in 1mg/ml concentration, the amount 1 ml, which assuming the average molar weight of a protein 50 kDa suggests a concentration of 0.02 mM while the final NEM concentration was 100 mM. Nevertheless, it is possible that not every accessible cysteine gets alkylated during this step, application of IAM in later step prevents artificial cysteine bridge formation during the sample processing before MS (Gundry et al., 2009). Application of IAM in this full workflow creates a competing environment for the two alkylating agents – NEM and IAM. An experiment verifying NEM binding carried out without IAM (or any other downstream alkylator) application would be beneficial. The relative abundance difference presented for ENR samples with and without NEM suggests that NEM alkylation occurred and the differential binding to thiol-affinity resin was successful, though the second alkylation with IAM being unnecessary.

4.2. Analysis approaches for candidate(s) identification

The protein coding genes of *Arabidopsis thaliana* are only 27,000, yet the number of the protein products are 35,000 (Arabidopsis Genome, 2000). The detectable protein number does not include the post translational modifications (PTMs). The myriad of existing PTMs is studied within the field of ever-expanding proteomics field. However, existing methods and analytic approaches present a number of challenges, with a lack of well-established enrichment strategies for many of PTMs, renders identification challenges due to low number of modified peptides (Olsen and Mann, 2013). This issue was avoided in the presented enrichment study since whole proteins were enriched, thus the peptides used for identification were not only those with modifications. Mass spectrometry (MS) is the method of choice for PTMs studies, yet the full PTM proteome remains undefined. Among other issues, a reason for that is the transient nature of many PTMs, and their occurrence only in very particular conditions and biotic or abiotic stress occurrence (Dix et al., 2008). It was previously postulated that up to 70% of all proteins get phosphorylated at some point (Huttlin et al., 2010; Olsen et al., 2010). A statistical approach to unravel relevant redox modification was

undertaken in this work. The average abundance in replicates and standard error calculation were used for calculation of the abundance ratio for identified proteins of NEM alkylated sample compared to the corresponding control (non-alkylated sample) (see 3.3.1 Oxidation ratio calculation – redox state verification, page 57), at the end of the day and end of the night (EOD – light conditions vs EON – dark conditions). A confidence interval (CI) was identified for light ratio (EOD) and dark ratio (EON) and the overlap between the confidence intervals was tested. If the light CI and dark CI do not overlap, this implies that values are statistically different. Using this approach only a handful of proteins were identified as being redox regulated. It was also not possible to observe a significant change in FBPase behavior in between the light and dark despite this being well characterized (Balmer et al., 2001). The statistical significance could also not be proven for other known redox-regulated protein by this approach, yet an alternative experiment was successfully conducted. A double labelling method performed in parallel to the enrichment experiments was successful in confirming redox regulation of FBPase (see 3.3.1 Oxidation ratio calculation – redox state verification 55). Since comparison of CI did not yield any candidates, yet the light/dark redox regulation mark could be detected by the double labelling approach, the enrichment data were subjected to a simpler analysis. The ratio of alkylated sample to control in the light was compared to the same ratio obtained in the dark. By experiment dividing the former by the latter a value range from 0 to ~200 was obtained, with a threshold of 0.8 being chosen; below the threshold value proteins with cysteines reduced in light were located. The threshold value was chosen motivated by a publication by Rosenwasser (Rosenwasser et al., 2014). The mentioned paper applied OxICAT method which is not commercially available. The OxICAT allows calculation of the percentage of oxidized cysteines in different conditions. The arbitrary chosen oxidation percentage difference between H_2O_2 treated and steady-state sample was 10 % for proteins that are under redox control. A number of candidates studied validated this method (Rosenwasser et al., 2014). Analysis of the redoxome in *E.coli* also utilized the percentage of oxidized cysteines before and after stress as a threshold followed by calculation of the fold change of respective percentages, an arbitrary threshold of 1.5 was used. This manner of narrowing-down the results highlighted a number of known redox regulated proteins and as well unraveling new candidates (Leichert et al., 2008). The relevance of candidates in the enrichment studies presented in this thesis was verified by dedicated experiments, double labelling, thioredoxin target verification and Ribo-seq (3.5 Further studies of selected candidates, page 67).

4.3. Candidates emerging from enrichment experiments

Enrichment experiments presented in the current study were replicated three times (ENR1, ENR2, and ENR3) according to the protocol modified from Guo et al. 2014. Results were filtered by applying a threshold of fold change (0.8) abundance difference between end of the day and end of the night conditions (END and EON, respectively) (see 3.3.1 Oxidation ratio calculation – redox state verification 57). By this, proteins that were reduced in light were selected. This list contains well studied redox-regulated proteins like fructose 1,6-bis-phosphatase (FBPase) that was the first described as thioredoxin targeted enzyme (Wolosiuk and Buchanan, 1977). Further studies confirmed this finding and provided proofs that thioredoxins have high specificity towards their targets (Collin et al., 2003), supporting the use of this protein as a control for enrichment experiments. To assess how many new redox regulated proteins were found in the current study the list of light reduced proteins that were present in at least two out of three experiments (ENR1, ENR2 and ENR3) were compared to several published, independent results showing redox regulated proteins. These proteins were excluded as potential new candidates, but prove the enrichment experiments to be effective (Supplemental Table 1, Supplemental Table 2, Supplemental Table 3, Supplemental Table 4, Supplemental Table 5).

4.3.1. Comparison of enrichment results with known and putative redox regulated proteins in *Arabidopsis thaliana* leaves

The enrichment results were compared with results from a publication that utilized three different techniques to reveal redox regulated protein targeted by thioredoxin. In the first method a mixture of cytosolic leaf proteins were reduces with TRX H3 and the newly formed thiols were labelled with radioactive iodoacetamide allowing specific detection. In the second approach another label was used, a biotinylated thiol-specific compound allowing selective elution from avidin column. The third method utilized a chromatography technique with mutated TRX H3 column. By the above-described three different methods 73 putative thioredoxin targets were detected (Marchand et al., 2006), out of these 49 were found in at least two out of three enrichment experiments (ENR1, ENR2 and ENR3) (Supplemental Table 1).

One example is the small protein CP12 (*AT2G47400*), a well-studied regulator of the Calvin–Benson–Basham cycle (CBB). CP12 is a small, redox-sensitive protein present in chloroplast. It interacts with glyceraldehyde-3-phosphate dehydrogenase (GAPDH) and phosphoribulokinase (PRK) to form a complex. The complex formation and dissociation is regulated by the redox state of Trx, as two pairs of cysteines present in CP12 were found out

to be redox regulated (Liu et al., 2015). A homolog of this protein was also found in alga *Chlorella ohadii*. Although the full importance of CP12 protein in CBB is not yet known, in light of recent findings in this alga it is hypothesized that it functions in forming a dynamic equilibrium between ROS-induced complex formation and reduction-based dissociation. It was suggested that both forms of CP12 are needed (in complex, as well as free), allowing high photosynthetic rates upon high light conditions where ROS scavenging and protection against oxidation damage are needed (Treves et al. 2019 - unpublished). CP12-like protein (AT3G62410) shares function with CP12. Recent studies of both proteins have shown specificity of thioredoxin f1 towards both of CP12 and CP12-like (Sugiura et al., 2019).

Another example of a protein found in the previously published work and this sturdy is sedophulose 1,7-bisphosphatase (*AT3G55800*) (SBPase). SBPase and FBPase are related enzymes with high level of homology. FBPase is organized as tetramer and SBPase as dimer, the biggest difference between those two enzymes is the position of redox regulated disulphides – in FBPase they are located at the outer edges of the protein while in SBPase they are more hidden and less accessible for thioredoxins (Gutle et al., 2017).

Finding the 49 known redox regulated proteins demonstrates the ability of the enrichment method to capture redox regulated proteins. In the study presented here the main interest was to explore the light-regulated redoxome, thus, complete coverage of all known redox-regulated proteins was not expected, as they might be responsive to different stimuli than light.

4.3.2. Comparison of enrichment results with known and putative-redox regulated proteins in *Arabidopsis thaliana* mitochondria

The enrichment method included no organelle fractionation, thus the results were compared with targeted approaches to find proteins regulated by thioredoxins in plant mitochondria. Redox state in mitochondria primarily depends on the respiratory chain, but in photosynthetic tissues it is also dependent on light, due to organellar cross-talk (e.g. photorespiration) (Yoshida and Noguchi, 2011). The result of enrichment was compared with results of a published work, where mitochondrial extracts (*Arabidopsis* shoots, spinach leaves and potato tubers) were applied to affinity column immobilizing *Arabidopsis* mitochondrial TRX O mutant protein (Yoshida et al., 2013). In this experiment, 95 proteins were identified as putative redox regulated candidates and 31 of those were also present in enrichment results in at least two out of three experiments (Supplemental Table 2).

Among the overlapping proteins were well studied tricarboxylic acid cycle (TCA) enzymes such as isocitrate dehydrogenase (IDH) (*AT5G03290*) and mitochondrial malate dehydrogenase (mMDH) (*AT1g53240*). IDH was suspected to be a redox regulated enzyme since it was shown in *E. coli.* Only recently *Arabidopsis* IDH was shown to be inactivated by oxidation and reactivated by subsequent reduction (Yoshida and Hisabori, 2014). MDH in mitochondria is NAD-dependent,as are MDH isoforms from peroxisomes, cytosol and plastids. Alternatively, the MDH localized in the chloroplast is NADP-dependent and is a crucial part of "light malate-valve". Its activity is strictly regulated by theferredoxin-thioredoxin system and finetuned via the $NADP^+$/NADP (H) ratio. The regulation system of many MDH isoforms, including mitochondrial MDH, is not known yet, nevertheless redox regulation is a possibility that needs more detailed investigation (Selinski and Scheibe, 2019). Moreover, NADP-linked TRX system was identified as a regulator of mitochondrial TCA cycle as well as regulator of root and plants growth. The multi-level analysis of TRX system in mitochondria pointed TRX to be a master regulator of TCA cycle itself and the citrate shunt pathway which exports the intermediates to the cytosol. Yet the remaining question is what the mechanism is by which the redox status of mitochondria influences the cytosol (Daloso et al., 2015).

The enrichment experiment pointed to one third of all mitochondrial proteins proposed in the paper by Yoshida et al. (2013) as light dependent. Although in enrichment experiment there was no organellar enrichment and the tissues compared in all considered experiments were different, this work identified many interesting proteins that should be considered in future studies of redox regulated proteins in mitochondria.

4.3.3. Comparison of enrichment results with known and putative redox-regulated proteins in *Arabidopsis thaliana* roots

In the enrichment experiments the whole plant was harvested, possibly with part of the root, therefore it is possible that part of the identified proteins were root-localized. For this reason, the results were compared to a study of TRX targeted proteins specifically in the root of Arabidopsis. The root proteins from crude extract were applied to a proteomic approach based on affinity chromatography with use of mutated plastidal TRX Y (Marchand et al., 2010).

The 72 proteins identified in roots by Marchand et al. in 2010 overlapped with 26 proteins identified in the enrichment approached discussed here (Supplemental Table 3). Among those appeared mitochondrial MDH (*At1g53240*). The cytosolic putative fructose bisphosphate aldolase (cALD2) (*At2g36460*) was also co-identified in the enrichment studies

and root studies from 2010. It was shown that this protein harbors two different cysteine modifications on separate residues–glutathionylation and nitrosylation. Modifications led to partial deactivation of the enzyme, incubation with glutathione disulfide (GSSG) and diamide (also creating oxidizing environment) led to fast and almost complete deactivation (van der Linde et al., 2011).

The enrichment experiment pointed to over one third of all root proteins proposed in the paper by Marchand et al. 2010 as light dependent, despite no tissue specific approach. It is known that hypocotyl responds to dark/light treatments and that an extra endoduplication cycle is triggered in the dark (Berckmans et al., 2011). There is also accumulating evidence that cell proliferation and shoot and root meristem activities are influenced by the redox state inside the cell. Lateral root development and root hairs are also under redox regulation. It is generally assumed that most of ROS production originates from mitochondrial respiration in roots (Considine and Foyer, 2014). Communication between cells of a plant and its distant organs is crucial for its balanced development. Plasmodesmata (PD) are channels enabling synplastic communication between cells, it was shown that TRX m3 is necessary and sufficient to control intercellular PD transport. It was proposed that sucrose transported from source to sink organs by phloem activates reduction of TRX m3, thus influencing communication by PD in sink organs (Benitez-Alfonso et al., 2009). There are still many unknowns about redox regulation in the root, and especially what has driven the changes in root redox regulated proteins in light-dependent experiment requires further studies.

4.3.4. Comparison of enrichment results with known and putative-redox regulated by S-nitrosylation proteins in *Arabidopsis thaliana*

In the work-flow of enrichment experiments a general reductant was used – DTT. By use of this chemical all the oxidative PTMs are reduced. The oxidative modification remains unknown; because of this the results were compared with a list of identified S-nitrosylated proteins, to get an insight in the spectrum of modifications on captured proteins.

S-nitrosylated proteins were detected by biotinylation of modified cysteines, next biotinylated protein were purified and analyzed by LC/MS. This approach allowed identifying 161 S-nitrosylated proteins (Lindermayr et al., 2005). Among those 20 proteins were also present in at least two out of three enrichment experiments (Supplemental Table 4). S-nitrosylation is one of the modifications occurring due to reaction with NO. NO in land plants is produced from nitrate *via* enzymatic or non-enzymatic pathways. Once NO reacts with a protein to S-nitrosylate it, the modification can be transferred to another protein in a process called

transnitrosylation. Transnitrosylation can be done via a transition metal (e.g. $Fe^{2+,}$ Cu^{2+}) complex or another S-nistrosylaed protein. Some transnitrolases have been identified, including cytochrome c, cyclin dependent kinase, caspase3, thioredoxin and glycerol-3-phospahatase-dehydrogenase (Turkan, 2018). In the enrichment data the cytochrome c (*AT1G22840*) was identified (Supplemental Table 5, position 161). The data published by Lindermayr et al. 2005 contained only one of these proteins – thioredoxin (AT3G24730 - thioredoxin-like).

An important protein that was found in the Lindermayr et al. 2005 approach and enrichment was a S –adenosylmethionine synthetase (SAMS3) (AT3G17390). So far there is no direct study of this protein in plant showing its S-nitrosylated residue or pointing the role of the modification. Nevertheless the possibility is speculated and its function could be in ethylene biosynthesis (Lindermayr et al., 2006).

Interestingly, another protein was present in the Lindermayr data set and enrichment: CSP41B, AT1G09340 (CRB). This protein was also suggested to be S-nitrosylated in the hyper sensitive response (HR), a type of plant response to pathogens. Proteins from leaves undergoing HR were subjected to biotin-switch method, purified by affinity chromatography and subjected to a two dimensional electrophoresis (2DE). Selected spots were excited from the gel and analyzed by mass spectrometry. Among 16 proteins identified was *CSP41B*, nevertheless no follow-up experiments were performed to prove the modification, nor its function was discussed (Romero-Puertas et al., 2008). CSP41B was also chosen for further studies, as a follow-up study to the enrichment.

4.4. New redox regulated candidates

By applying the modified method for resin-assisted thiol enrichment of proteins (Guo et al., 2014) for studying the redoxome of *Arabidopsis thaliana*, new potentially redox regulated candidates have emerged. The enrichment experiment has been repeated three times (ENR1, ENR2 and ENR3). Known or potential candidates that have appeared in chosen publications from the field (Lindermayr et al., 2005; Marchand et al., 2006; Marchand et al., 2010; Yoshida et al., 2013) were excluded from the list of potential novel candidates emerging from enrichment studies. The final catalog of candidates contains 230 proteins (Supplemental Table 5). The proteins present is this catalogue are reduced in light, at the end of the day (EOD) while oxidized in dark, at the end of the night (EON), they were captured by the enrichment method due to carrying on or more oxidative post translational modifications (Ox-PTMs). It is possible that some of the proteins are known to be involved in reduction-oxidation processes,

but their Ox-PTMs were not studied in details. There are 7 proteins directly involved in signal transduction based on their GO annotation (AT1G09210 - calreticulin, AT1G10840 - translation initiation factor, AT1G22300 - 14-3-3 protein a general regulatory factor, AT2G25110-endoplasmic reticulum protein SDF2, AT2G44100-GDP dissociation inhibitor involved in vesicular membrane traffic, AT5G07340 - calreticulin and AT5G61790-calnexin), 8% of annotations belonged to stress response, 7% to biosynthetic function, 4% belonged to response to abiotic stimuli. The proteins belong to a wide range of annotated biological processes and localizations, proving that redox regulation and signaling are not exclusive for chloroplast, mitochondria or peroxisome. It is more widespread signaling pathway, influencing processes on inter- and intracellular level. A remaining challenge is to tackle spatiotemporal triggers for redox signaling (Geigenberger and Fernie, 2014). A global study comparing two conditions (day and night) provided over 200 candidates, yet they remain to be characterized individually. Understanding at which cysteine the modification occurs can be ndertaken using a labelling method combined with MS approaches (see 1.7 Methods for oxidative PTMs study 30, (Chung et al., 2013)) To verify functionality of the ox-PTM of certain cysteine residue in candidate protein, redox regulated cysteines in question can be substituted with alanine.

Alanine cannot undergo any of the Ox-PTMs. The protein 3′-phosphoadenosine 5′-phosphate (PAP) phosphatase SAL1 (AtSAL1) has four cysteines, the protein is known to be downregulated by the process oxidation: following Cys residues substitution to Ala the oxidative down-regulation was lost. Combinatorial analysis of Cys to Ala mutations leads to identification of Cys pairs forming cysteine bridges in the protein (Chan et al., 2016). Ala is a hydrophobic amino acid, usually buried inside the protein, Cys is a special amino acid, Cys that engages in disulfide bridge formation is surfaced exposed, Ser is a hydrophylic amino acid also surfaced exposed (Lodish H et al., 2000). Serine is a commonly used substitution for Cysteine. In 2Cys Prx (PRX) A site directed mutations of various Cys residues to Ser were performed in order to detect source of variation in its enzymatic activity and chaperone activity among other properties (Lee et al., 2015).

An interesting follow up to enrichment study is using selective reduction to target single types of Ox-PTM. Instead of using DTT which reduces unselectively, ascorbate could be used for selective reduction of S-nitrosylation, glutaredoxin for S-glutationylation and hydroxylamine for S-acylation. For facilitating LC-MS/MS runs and allowing relative and absolute quantification iTRAQ isobaric label can be used (Unwin, 2010; Guo et al., 2014).

4.5. Ribo-Seq

The biggest changes in footprint abundances were observed when mutants were compared to the wild type at the End of the Night (EON). The previously studied function of CSP41A and CSP41B proteins in stabilizing transcripts during the night (Qi et al., 2012) might not be associated with mutants phenotypes. Nevertheless, more genes specifically changed (up or down regulated footprints) in *csp41b.* Up regulated footprints specific for *csp41a* were 47, down regulated 107, in *csp41b* 156 and 108 respectively. As mentioned, the *csp41a* plants are able to accumulate the CSP41B protein to WT level, while the *csp41b* mutants have lower than WT level of protein CSP41A (Bollenbach et al., 2009). The *csp41b* plant threfore suffers effects of depletion in both CSP41 proteins (3.4.1.1 CSP41A (AT3G63140), CSP41B (AT1G09340) page 64), thus changes observed in the mutant are not solely specific to a lack of CSP41B protein. On the other hand *csp41a* changes that are attributed to lack of CSP41A protein solely are not associated with a severe phenotype. Thus, among genes identified in *csp41b* mutant might be involved in causing the phenotype as targets of signal coming from lack of CSP41B protein. However, observed changes were not associated with chloroplast encoded genes. Only three identified genes encoded in chloroplast and specific for *csp41b* (*ATCG00330* – Chloroplast Ribosomal Protein S14, RPS14; *ATCG00420* - NADH Dehydrogenase Subunit J, NDHJ; *ATCG01080* - NADH dehydrogenase ND6, NDHG) were up regulated and none were down regulated. The changes on level of translation observed in the mutants probably are no enough to cause the photosynthetic, sever phenotype of *csp41b,* thus another function of CSP41B might be involved in its genesis. Likely, CSP41B is involved in a signalling pathway between chloroplast and cytosol that indirectly regulated photosynthesis.

5. Conclusion and outlook

In photosynthetic organisms redox regulation via light and dark modulation plays a crucial role in the control of photosynthesis, metabolism and gene expression. Despite the significance of redox regulation the overall knowledge about it, especially in physiological conditions, is limited due to restraint of measurement technologies.

This thesis provides an insight into the *in vivo* redoxome of *Arabidopsis thaliana* in response to light vs dark, by capturing thiol modifications occurring in the plant. This was achieved by utilizing a resin-assisted thiol enrichment approach. In this study, over 1100 proteins on average were identified in three replications. Amongst these, on average 419 proteins were

identified as redox regulated and reduced in light. Many of these were previously described as redox regulated thus confirming successful conduct of the method. New redox regulated candidate proteins emerged from the study. These 230 proteins have not been identified in any publications presented in the discussion of this thesis.

CSP41A as one of the emerging candidates was chosen for further characterization. The CSP41A protein is a possible target of thioredoxins of the m group. It was demonstrated by *in planta* cross-linking and subsequent protein capturing on a native immunoblot of clear native gel. The decreased protein band size on the immunoblot only occurred in *trxm124* mutant as compared to wild type plant and single thioredoxins m and f mutants. This indicates a possible evolvement of thioredoxins of group m as interactors of CSP41A.

The light-dictated function of CSP41A and CSP41B was further studied by Ribo-Seq as a part of work presented here. Since it was previously shown that these proteins are able to form an mRNA stabilizing complex in the night, and release the transcript during the day (Qi et al. 2012). Single mutants of both proteins (*csp41a* and *csp41b*) and wild type plants were used for that experiment. The time points chosen were the same as for redox studies (EON vs EOD). Results have shown most significant differences between the mutants and wild type at the end of the night. Nevertheless, the link between the plant phenotypes, described as possibly derived from disordered photosynthesis, remains elusive. Since, most of the significantly altered ribosomal footprints do not belong to chloroplast-encoded genes, yet CSP41A and CSP41B are both chloroplast localized proteins. Thus, it is possible that the transcript-stabilizing function previously attributed to these proteins is not causing the phenotype, but another yet unknown function. A complementation of Ribo-Seq with microarray RNA-sequencing focused on chloroplastic transcripts would provide needed data about total transcripts levels in *csp41a* and *csp41b* vs wild type at EOD/EON conditions. A further characterization of CSP41A and CSP41B as well as other candidates by means of site-mutagenesis and biochemical studies is needed in order to provide evidence of functional relevance of their redox modifications.

Furthermore, deciphering specific types of Ox-PTM of candidates could be obtained by modifying the method by use of specific reductants, such as ascorbate for specific reduction of S-nitrosylation, glutaredoxin for S-glutathionylation and hydroxylamine for S-acylation. However, none of proposed above work-flow modifications can provide information about irreversible thiol modifications.

Since redox modifications are known to be dynamic, a great deal of information could be obtained by changing plant sampling time points. A scheme of sampling used for the double-labelling approach, presented in this study as an alternative study method of single protein could be used. In this scheme plants were harvested in light conditions, after shading for 30 seconds, 1 minute and 15 minutes.

In future studies, technical variation in the data could be reduced by applying TMT labelling. This method allows pooling of the samples after tryptic digestion, thus degreasing the number of samples to be handled and facilitating downstream LC-MS/MS measurements and analysis. Furthermore, it would enable quantitative and site-specific analysis of light/dark modulated Ox-PTMs.

Supplemental Table 1 List of TRX targets in *Arabidopsis* leaves

List of TRX targets summarized in paper by Marchand *et al.* 2006 present in at least two out of three Enrichment data sets (ENR1, ENR2, ENR3)											
protein	Light_Dark. ENR1	ENR1	Light_Dark. ENR2	ENR2	Light_Dark .ENR3	ENR3	Proteins	present.with. method	process	not present in ENR1/2/3	
AT1G20340	0.80537551	ENR1	0.1917734	ENR2	0.2290634	ENR3	Plastocyanin	3	PHOTOSYNTHESIS	0	
AT1G32470	0.48850562	ENR1	0.4062241	ENR2	0.3960225	ENR3	Probable Protein H	2	PHOTORESPIRATION	0	
AT1G43670	0.95552151	ENR1	0.6997953	ENR2	0.1436432	ENR3	Putative fructosebisphosphate phosphatase	1	CALVIN CYCLE	0	
AT1G53240	0.627746397	ENR1	0.6932889	ENR2	0.6808539	ENR3	Mitochondrial NAD-malate dehydrogenase	3	METABOLISM (C,N,S)	0	
AT1G78380	0.97500309	ENR1	0.3501501	ENR2	0.3147451	ENR3	Glutathione-S-transferase 8 (tau class)	3	OXIDATIVE STRESS RESPONSE	0	
AT2G15620	0.81142919	ENR1	0.9430802	ENR2	0.4641773	ENR3	Fd nitrite reductase	1	METABOLISM (C,N,S)	0	
AT2G21170	0.86327818	ENR1	0.8472832	ENR2	0.9974339	ENR3	Chloroplastic triosephosphate isomerase	1, 3	CALVIN CYCLE	0	
AT2G35370	0.86472261	ENR1	0.3246351	ENR2	0.5081709	ENR3	Protein H	1, 3	PHOTORESPIRATION	0	
AT2G37220	0.73573302	ENR1	0.2824734	ENR2	0.5020799	ENR3	RNA binding protein	1, 3	NUCLEOTIDE BINDING	0	
AT2G47400	0.60390614	ENR1	0.0199663	ENR2	0.1682349	ENR3	CP12	1	CALVIN CYCLE	0	
AT3G11630	0.5317422	ENR1	0.2810641	ENR2	0.5910121	ENR3	Peroxiredoxin BAS1	2, 3	OXIDATIVE STRESS RESPONSE	0	
AT3G12780	0.99326825	ENR1	0.3182551	ENR2	0.6206175	ENR3	PGK	3	METABOLISM (C,N,S)	0	
AT3G55800	0.82495651	ENR1	0.4364753	ENR2	0.6552518	ENR3	Sedoheptulose 1-7 bisphosphatase	1	CALVIN CYCLE	0	
AT3G60750	0.87630456	ENR1	0.9561439	ENR2	0.4788998	ENR3	Transketolase	1, 3	CALVIN CYCLE	0	
AT3G62410	0.92413457	ENR1	0.3748798	ENR2	0.2580479	ENR3	CP 12-like	1	CALVIN CYCLE	0	
AT4G23600	0.75725062	ENR1	0.5025372	ENR2	0.2297666	ENR3	Tyrosine transaminase like	2, 3	DEFENSE AGAINST PATHOGENS	0	
AT4G26530	0.97352316	ENR1	0.8573467	ENR2	0.8042792	ENR3	Fructose bisphosphate aldolase-like	1	METABOLISM (C,N,S)	0	
AT5G06290	0.5317422	ENR1	0.3711489	ENR2	0.2402469	ENR3	PRX-like	2	OXIDATIVE STRESS RESPONSE	0	
AT5G53490	0.70512387	ENR1	0.5246346	ENR2	0.3732531	ENR3	17.4 kDa protein	1	UNKNOWN FUNCTIONS	0	
AT5G58330	0.3319825	ENR1	0.4296705	ENR2	0.3131863	ENR3	NADP-malate dehydrogenase	1	METABOLISM (C,N,S)	0	
ATCG00490	0.78069952	ENR1	0.7109713	ENR2	0.5694181	ENR3	RubisCo LSU	1*, 2, 3	CALVIN CYCLE	0	21
AT1G06680	NA	NA	0.9639346	ENR2	0.8181503	ENR3	OEE2-1	3	PHOTOSYNTHESIS	1	
AT1G09310	NA	NA	0.6586976	ENR2	0.7046722	ENR3	Hypothetical protein (19.9 kDa)	1	UNKNOWN FUNCTIONS	1	
AT1G17290	NA	NA	0.3560271	ENR2	0.3373625	ENR3	Alanine aminotransferase	1	METABOLISM (C,N,S)	1	
AT1G21750	NA	NA	0.1337192	ENR2	0.5010496	ENR3	Protein disulfide isomerase	1, 2	FOLDING	1	
AT1G32060	0.49581661	ENR1	0.380133	ENR2	NA	NA	Phosphoribulokinase	1, 2, 3	CALVIN CYCLE	1	
AT1G65930	NA	NA	0.7659673	ENR2	0.1463936	ENR3	NADP-isocitrate dehydrogenase	1, 3	METABOLISM (C,N,S)	1	
AT1G65980	0.86731086	ENR1	0.6683323	ENR2	NA	NA	Peroxiredoxin TPX1	3	OXIDATIVE STRESS RESPONSE	1	
AT1G75040	NA	NA	0.906293	ENR2	0.0581693	ENR3	PR5 protein	1	DEFENSE AGAINST PATHOGENS	1	
AT2G24270	NA	NA	0.6953095	ENR2	0.2568259	ENR3	NADP-glyceraldehyde 3P dehydrogenase	1	CALVIN CYCLE	1	
AT2G39730	NA	NA	0.8183835	ENR2	0.1388049	ENR3	RubisCO activase (long isoform)	1	CALVIN CYCLE	1	
AT2G43560	0.32722386	ENR1	NA	NA	0.2453299	ENR3	FKBP peptidylprolyl cis-trans isomerase	1	FOLDING	1	
AT3G01500	NA	NA	0.615996	ENR2	0.5604971	ENR3	Chloroplastic carbonic anhydrase	1, 3	CO2/HCO3 EQUILIBRIUM	1	
AT3G04790	NA	NA	0.4570425	ENR2	0.0489007	ENR3	Ribose 5P isomerase	1	CALVIN CYCLE	1	
AT3G22890	0.73803142	ENR1	0.5158618	ENR2	NA	NA	ATP sulfurylase	3	METABOLISM (C,N,S)	1	
AT3G50820	0.7712141	ENR1	NA	NA	0.3748464	ENR3	OEE1-2	1	PHOTOSYNTHESIS	1	
AT3G52960	NA	NA	0.6587575	ENR2	0.319084	ENR3	Peroxiredoxin (type II)	1, 3	OXIDATIVE STRESS RESPONSE	1	
AT3G55440	NA	NA	0.8050548	ENR2	0.7642924	ENR3	Cytosolic triosephosphate isomerase	1*, 3	METABOLISM (C,N,S)	1	
AT3G63140	NA	NA	0.7417231	ENR2	0.8522644	ENR3	mRNA binding protein	3	NUCLEOTIDE BINDING	1	
AT4G25130	NA	NA	0.9077689	ENR2	0.5134942	ENR3	Peptide methionine sulfoxide reductase	1	OXIDATIVE STRESS RESPONSE	1	
AT4G37930	NA	NA	0.7952417	ENR2	0.5902219	ENR3	Serine hydroxymethyltransferase	3	PHOTORESPIRATION	1	
AT5G14740	NA	NA	0.1043884	ENR2	0.6317789	ENR3	Cytosolic carbonic anhydrase	1	CO2/HCO3 EQUILIBRIUM	1	
AT5G26000	NA	NA	0.82215	ENR2	0.365718	ENR3	Myrosinase	1, 2, 3	DEFENSE AGAINST PATHOGENS	1	
AT5G35630	NA	NA	0.6625498	ENR2	0.5054821	ENR3	Glutamine synthetase	1, 3	METABOLISM (C,N,S)	1	
AT5G38430	NA	NA	0.1732593	ENR2	0.7413301	ENR3	RubisCo SSU	1*, 3	CALVIN CYCLE	1	
AT5G60360	NA	NA	0.6047029	ENR2	0.1637813	ENR3	Cysteine protease AALP	1	VARIOUS FUNCTIONS	1	
AT5G61410	NA	NA	0.5256473	ENR2	0.4393282	ENR3	Ribulose 5P epimerase	1	CALVIN CYCLE	1	
AT5G66530	0.91963092	ENR1	NA	NA	0.3588539	ENR3	Apospory-associated protein c-like	1, 3	DEFENSE AGAINST PATHOGENS	1	
AT5G66570	0.8155471	ENR1	NA	NA	0.297166	ENR3	OEE1-1	1	PHOTOSYNTHESIS	1	28
total in the paper 73											49

Supplemental Table 2 List of putative TRX targets in mitochondria

List of TRX targets in mitochondria summarized in paper by Yoshida *et al.* 2013 present in at least two out of three Enrichment data sets (ENR1, ENR2, ENR3)												
protein	Light_Dark. ENR1	ENR1	Light_Dark. ENR2	ENR2	Light_Dark. ENR3	ENR3	Protein identified	cont.	A.t.	process	not present in ENR1/2/3	
AT1G03680	0.63505852	ENR1	0.83401073	ENR2	0.52271467	ENR3	Thioredoxin M1	*		Redox regulation system	0	
AT1G47420	0.89382295	ENR1	0.80382208	ENR2	0.83412531	ENR3	Succinate dehydrogenase subunit 5 (SDH5)			Respiratory chain (electron transport	0	
AT1G53240	0.62746397	ENR1	0.69328893	ENR2	0.68085394	ENR3	Malate dehydrogenase 1 (MDH1)		•	TCA cycle	0	
AT2G35370	0.86472261	ENR1	0.32463509	ENR2	0.50817087	ENR3	Glycine decarboxylase complex H-protein 1 (GDCH1)			Photorespiration	0	
AT3G11630	0.5317422	ENR1	0.28106412	ENR2	0.59101205	ENR3	2-Cys peroxiredoxin BAS1	*		Antioxidant defense	0	
AT4G02930	0.4960946	ENR1	0.36838476	ENR2	0.34365913	ENR3	Elongation factor Tu (EF-Tu)		•	Translation or protein processing	0	
AT4G11600	0.93869716	ENR1	0.21568425	ENR2	0.87737265	ENR3	Glutathione peroxidase 6 (Gpx6)			Antioxidant defense	0	
AT5G03290	0.6477785	ENR1	0.18189292	ENR2	0.942414	ENR3	Isocitrate dehydrogenase (IDH) catalytic subunit			TCA cycle	0	
AT5G50850	0.10323149	ENR1	0.5772384	ENR2	0.37670317	ENR3	Pyruvate dehydrogenase E1 subunit (PDC E1)		•	TCA cycle	0	9
AT1G20620	0.90539382	ENR1	NA	NA	0.77056474	ENR3	Catalase-3			Antioxidant defense	1	
AT1G79230	0.89668205	ENR1	0.17206893	ENR2	NA	NA	3-Mercaptopyruvate			Amino acid metabolism	1	
AT2G33040	0.8268601	ENR1	NA	NA	0.33659397	ENR3	ATP synthase subunit		•	synthase)	1	
AT2G35010	0.26395414	ENR1	NA	NA	0.16541867	ENR3	Thioredoxin O1			Redox regulation system	1	
AT2G43090	0.95751438	ENR1	0.17029871	ENR2	NA	NA	3-Isopropylmalate dehydratase	*		Amino acid metabolism	1	
AT3G06050	NA	NA	0.76926109	ENR2	0.58881089	ENR3	Peroxiredoxin-2F (PrxIIF)			Antioxidant defense	1	
AT3G08580	NA	NA	0.72583245	ENR2	0.44421131	ENR3	ADP/ATP carrier protein 1 (ANT1)		•	Membrane carrier	1	
AT3G14415	0.96020518	ENR1	NA	NA	0.38252304	ENR3	Glycolate oxidase 1	*		Photorespiration	1	
AT3G15660	NA	NA	0.62460505	ENR2	0.35556894	ENR3	Monothiol glutaredoxin-S15			Fe-S cluster biosynthesis	1	
AT3G52960	NA	NA	0.65875754	ENR2	0.31908397	ENR3	Peroxiredoxin-2E (PrxIIE)	*		Antioxidant defense	1	
AT3G61440	0.97384837	ENR1	NA	NA	0.51760516	ENR3	Cysteine synthase C1, l-3-cyanoalanine synthase			Amino acid metabolism	1	
AT4G02580	0.32860682	ENR1	NA	NA	0.81067949	ENR3	NADH dehydrogenase flavoprotein 2 (NDUV2)			Respiratory chain (electron transport complex)	1	
AT4G21860	NA	NA	0.12039745	ENR2	0.25938503	ENR3	Peptide methionine sulfoxide reductase B2 (MsrB2)	*		Antioxidant defense	1	
AT4G25130	NA	NA	0.90776891	ENR2	0.51349417	ENR3	Peptide methionine sulfoxide reductase A4 (MsrA4)			Antioxidant defense	1	
AT4G37930	NA	NA	0.79524171	ENR2	0.59022185	ENR3	Serine hydroxymethyltransferase (SHMT)			Photorespiration	1	
AT5G09590	NA	NA	0.82527002	ENR2	0.86161274	ENR3	Mitochondrial heat shock protein 70-2 (HSP70-2)			Translation or protein processing	1	
AT5G35360	0.4891208	ENR1	0.56222474	ENR2	NA	NA	Acetyl-CoA carboxylase subunit A	*		processes	1	
AT5G35630	NA	NA	0.66254976	ENR2	0.50548215	ENR3	Glutamine synthetase 2 (GS2)			Amino acid metabolism	1	
AT5G49910	NA	NA	0.72776311	ENR2	0.88517753	ENR3	Heat shock protein 70-7	*		processing	1	
AT5G52840	NA	NA	0.50340484	ENR2	0.66898965	ENR3	NADH dehydrogenase 1? subcomplex subunit 5 (NDUA5)			(electron transport complex)	1	
AT5G67500	0.56137709	ENR1	0.79109156	ENR2	NA	NA	Voltage-dependent anion channel 2 (VDAC2)			Membrane carrier	1	
ATMG01190	0.41722986	ENR1	0.39105964	ENR2	NA	NA	ATP synthase subunit		•	synthase)	1	22
total in the paper 95												31

Supplemental Table 3 List of TRX targets in roots

List of TRX targets in roots summarized in paper by Marchand *et al.* 2010 present in at least two out of three Enrichment data sets (ENR1, ENR2, ENR3)

protein	Light_Dark. ENR1	ENR1	Light_Dark. ENR2	ENR2	Light_Dark. ENR3	ENR3	Proteins	function	not present in ENR1/2/3	
AT1G53240	0.627464	ENR1	0.6932889	ENR2	0.68085394	ENR3	Mitochondrial malate dehydrogenase	Carbon metabolism	0	
AT1G78380	0.9750031	ENR1	0.3501501	ENR2	0.31474512	ENR3	Glutathion S transferase 8 (class tau)	Other	0	
AT2G36460	0.8137439	ENR1	0.347176	ENR2	0.30477499	ENR3	Putative fructose bisphosphate aldolase	Carbon metabolism	0	
AT2G41530	0.6952775	ENR1	0.3565386	ENR2	0.31782495	ENR3	S formyl gluthathione hydrolase	Other	0	
AT5G11670	0.8125666	ENR1	0.4030694	ENR2	0.96774505	ENR3	NADP dependent malic enzyme like protein	Carbon metabolism	0	
AT5G17920	0.8172503	ENR1	0.2606273	ENR2	0.56099676	ENR3	Vitamin B12 independent methionine synthase	Metabolism	0	6
AT1G20620	0.9053938	ENR1	NA	NA	0.77056474	ENR3	Catalase 3	Other	1	
AT1G21750	NA	NA	0.1337192	ENR2	0.50104962	ENR3	Probable Protein Disulfide Isomerase 1	Folding	1	
AT1G56070	NA	NA	0.6613294	ENR2	0.70098936	ENR3	Putative elongation factor	Protein biogenesis and degradation	1	
AT1G63940	NA	NA	0.3540456	ENR2	0.15109636	ENR3	Monodehydroascorbate reductase	Other	1	
AT1G65980	0.8673109	ENR1	0.6683323	ENR2	NA	NA	Peroxiredoxin TPx 1	Other	1	
AT1G66200	0.8886621	ENR1	NA	NA	0.48745149	ENR3	Glutamine synthetase	Metabolism	1	
AT2G01140	NA	NA	0.8535781	ENR2	0.77504502	ENR3	Putative fructose bisphosphate aldolase	Carbon metabolism	1	
AT2G05990	NA	NA	0.6633539	ENR2	0.73728181	ENR3	Enoyl ACP reductase	Metabolism	1	
AT2G28190	0.8632527	ENR1	NA	NA	0.19734281	ENR3	CuZnSOD	Other	1	
AT3G14067	0.6969023	ENR1	NA	NA	0.14420879	ENR3	Putative subtilisin like serine protease	Degradation	1	
AT3G16640	NA	NA	0.6792003	ENR2	0.77053042	ENR3	Translationally controlled tumor protein like protein	Signal transduction	1	
AT3G22110	NA	NA	0.4466203	ENR2	0.60794043	ENR3	20S Proteasome subunit C 1	Degradation	1	
AT3G24503	NA	NA	0.5868574	ENR2	0.34042387	ENR3	Aldehyde dehydrogenase REF1	Metabolism	1	
AT3G55440	NA	NA	0.8050548	ENR2	0.76429241	ENR3	Triose phosphate isomerase	Carbon metabolism	1	
AT3G61440	0.9738484	ENR1	NA	NA	0.51760516	ENR3	??cyanoalanine synthase	Other	1	
AT4G13940	0.9829767	ENR1	NA	NA	0.56448608	ENR3	Adenosylhomocysteinase	Carbon metabolism	1	
AT4G33090	0.9331888	ENR1	0.7251925	ENR2	NA	NA	Aminopeptidase M	Degradation	1	
AT5G07460	NA	NA	0.449939	ENR2	0.49114255	ENR3	Peptide methionine sulfoxide reductase?like protein	Other	1	
AT5G10450	NA	NA	0.5249188	ENR2	0.91065662	ENR3	14–3–3 Like protein	Signal transduction	1	
AT5G62530	0.9356457	ENR1	NA	NA	0.30214327	ENR3	Delta 1 pyrroline 5 carboxylate dehydrogenase	Other	1	20
total in the paper 72										26

Supplemental Table 4 List of S-nitrosylated proteins

List of S-nitrosylated proteins in Arabidopsis summarized in paper by Lindermayr *et al*. 2005 present in Enrichment data sets (ENR1, ENR2, ENR3)

protein	Light_Dark. ENR1	ENR1	Light_Dark. ENR2	ENR2	Light_Dark. ENR3	ENR3	Annotation	not present in ENR1/2/3	
AT1G09340	0.93295013	ENR1	0.759051	ENR2	0.77292959	ENR3	Chloroplast RNA binding (CRB)	0	
AT1G72370	0.9778789	ENR1	0.4517318	ENR2	0.44913302	ENR3	40S ribosomal protein SA (RP40)	0	
AT2G21170	0.86327818	ENR1	0.8472832	ENR2	0.99743391	ENR3	Triosephosphate isomerase (TIM)	0	
AT3G59970	0.62362555	ENR1	0.6991446	ENR2	0.32153445	ENR3	Methylenetetrahydrofolate reductase 1 (MTHFR1)	0	
AT4G02930	0.4960946	ENR1	0.3683848	ENR2	0.34365913	ENR3	GTP binding elongation factor Tu family protein	0	
AT5G65010	0.15451623	ENR1	0.8125511	ENR2	0.27623395	ENR3	Asparagine synthetase 2 (ASN2)	0	6
AT1G09310	NA	NA	0.6586976	ENR2	0.70467222	ENR3	Unknown protein	1	
AT1G12270	NA	NA	0.4293241	ENR2	0.72697963	ENR3	Carboxylate clamp (CC)-tetratricopeptide repeat (TPR) protein	1	
AT1G63000	NA	NA	0.0435112	ENR2	0.1847554	ENR3	UDP-4-keto-6-deoxy-D-glucose-3,5-epimerase-4-reductase 1 (UER1)	1	
AT1G74100	0.86725006	ENR1	0.0241845	ENR2	NA	NA	Sulfotransferase 16 (SOT16)	1	
AT2G17390	NA	NA	0.7079923	ENR2	0.65668055	ENR3	Ankyrin repeat-containing 2B (AKR2B)	1	
AT2G30410	NA	NA	0.8872554	ENR2	0.46030347	ENR3	Tubulin folding factor A (TFCA)	1	
AT2G47390	NA	NA	0.3980095	ENR2	0.83675919	ENR3	Prolyl oligopeptidase family protein	1	
AT3G04790	NA	NA	0.4570425	ENR2	0.04890073	ENR3	Embryo defective 3119 (EMB3119)	1	
AT3G17390	0.96879188	ENR1	NA	NA	0.45165306	ENR3	S -adenosylmethionine synthetase 3 (SAMS3)	1	
AT3G59920	NA	NA	0.4955937	ENR2	0.96745896	ENR3	Rab GDP dissociation inhibitor 2 (GDI2)	1	
AT4G24190	NA	NA	0.5596247	ENR2	0.3297739	ENR3	Heat shock protein 90-7 (HSP90.7)	1	
AT4G29840	0.56153337	ENR1	NA	NA	0.24720218	ENR3	Methionine over-accumulator 2 (MTO2)	1	
AT5G36700	0.90446772	ENR1	0.399483	ENR2	NA	NA	2-phosphoglycolate phosphatase 1 (PGLP1)	1	
AT5G47840	NA	NA	0.5042099	ENR2	0.90372322	ENR3	Adenosine monophosphate kinase (AMK2)	1	14
AT1G11660	NA	NA	0.6180333	ENR2	NA	NA	Heat shock protein 70 family protein	2	
AT1G12900	NA	NA	NA	NA	0.27649552	ENR3	Glyceraldehyde 3-phosphate dehydrogenase A2 (GAPA2)	2	
AT1G35420	NA	NA	NA	NA	0.19188045	ENR3	hydrolases superfamily protein	2	
AT1G48850	NA	NA	0.0006932	ENR2	NA	NA	Embryo defective 1144 (EMB1144)	2	
AT1G55490	NA	NA	NA	NA	0.98167568	ENR3	Chaperonin 60 subunit ? (CPN60B)	2	
AT1G62740	NA	NA	0.952816	ENR2	NA	NA	Carboxylate clamp (CC)-tetratricopeptide repeat (TPR) protein	2	
AT1G66430	NA	NA	NA	NA	0.60340741	ENR3	pfkB-like carbohydrate kinase family protein	2	
AT1G67280	NA	NA	0.4725328	ENR2	NA	NA	Dioxygenase superfamily protein	2	
AT1G68010	NA	NA	NA	NA	0.989707	ENR3	Hydroxypyruvate reductase 1 (HPR1)	2	
AT1G70580	NA	NA	NA	NA	0.52687073	ENR3	Glutamate:glyoxylate aminotransferase 2 (GGT2)	2	
AT1G74090	0.72591314	ENR1	NA	NA	NA	NA	Sulfotransferase 5B (ST5B)	2	
AT2G31390	NA	NA	0.0573233	ENR2	NA	NA	pfkB-like carbohydrate kinase family protein	2	
AT2G40490	NA	NA	NA	NA	0.57017985	ENR3	Uroporphyrinogen decarboxylase (HEME2)	2	
AT3G13920	NA	NA	NA	NA	0.60316486	ENR3	Eukaryotic translation initiation factor 4A-1 (eIF4A1)	2	
AT3G48560	NA	NA	0.5262688	ENR2	NA	NA	Acetolactate synthase (ALS)	2	
AT3G54600	0.87866104	ENR1	NA	NA	NA	NA	Class I glutamine amidotransferase-like superfamily protein	2	
AT4G04770	NA	NA	0.636322	ENR2	NA	NA	ATP binding cassette protein 1 (ABC1)	2	
AT4G09320	NA	NA	0.9077837	ENR2	NA	NA	Nucleoside diphosphate kinase 1 (NDPK1)	2	
AT4G26840	NA	NA	0.1840269	ENR2	NA	NA	Small ubiquitin-like modifier 1 (SUMO1)	2	
AT4G35450	NA	NA	NA	NA	0.34539322	ENR3	Ankyrin repeat-containing protein 2 (AKR2)	2	
AT4G37800	0.47474777	ENR1	NA	NA	NA	NA	Xyloglucan endotransglucosylase/hydrolase 7 (XTH7)	2	
AT5G05010	NA	NA	0.5395008	ENR2	NA	NA	Clathrin adaptor complexes medium subunit family protein	2	
AT5G08530	0.96337171	ENR1	NA	NA	NA	NA	51 kDa subunit of complex I (CI51)	2	
AT5G13420	NA	NA	0.5666746	ENR2	NA	NA	Transaldolase 2 (TRA2)	2	
AT5G27380	NA	NA	NA	NA	0.24175503	ENR3	Glutathione synthetase 2 (GSH2)	2	25
total in paper 161									45

Supplemental Table 5 List of new potential redox regulated candidates

The table summarizes all possible candidate proteins emerging from the curent study, for each protein AGI code (columns “protein”) the ratio Light_Dark is stated for each enrichment experiment (columns named as: “Light_Dark.ENR1”, “Light_Dark.ENR2”, “Light_Dark.ENR3”), the column “Cys” contains the number of Cysteines in a given protein, short information about the protein is given in the column “description”, following columns “ENR.1”, “ENR.2”, “ENR.3” are filled if the protein was found in the named enrichment experiment, if the column is filled with “NA”, the column if the column is “not present in ENR1/2/3” gives a total number of NAs per protein, in this the number of NA is no higher than 1, predicted localization of the protein in stated in the column “localization”.

No	Protein	Light_Dark. ENR1	Light_Dark. ENR2	Light_Dark. ENR3	Cys	Description	ENR_1	ENR_2	ENR_3	not present in ENR1/2/3	localization
1	AT1G49240	0.37662659	0.55401305	0.61101674	4	ACT8, actin 8	ENR1	ENR2	ENR3	0	chloroplast
2	AT4G23100	0.44861755	0.10546856	0.21545386	7	ATECS1, ATGSH1, CAD2, CADMIUM SENSITIVE 2, GLUTAMATE-CYSTEINE LIGASE	ENR1	ENR2	ENR3	0	chloroplast
3	AT1G62750	0.61919579	0.5672008	0.65366292	6	ATSCO1 ATSCO1/CPEF-GSCO1Translation elongation factor EFG/EF2 protein	ENR1	ENR2	ENR3	0	chloroplast
4	AT1G29900	0.76989041	0.39383519	0.5947167	21	CARB carbamoyl phosphate synthetase B	ENR1	ENR2	ENR3	0	chloroplast
5	AT3G26740	0.45024127	0.04869074	0.20812044	4	CCLCCR-like	ENR1	ENR2	ENR3	0	chloroplast
6	AT1G22450	0.77487379	0.29242023	0.50485494	4	COX6B ATCOX6B2cyto	ENR1	ENR2	ENR3	0	chloroplast
7	AT3G53460	0.71902596	0.59891462	0.64903018	2	CP29chloroplast RNA-binding protein 29	ENR1	ENR2	ENR3	0	chloroplast
8	AT3G53580	0.65260231	0.35727365	0.53532783	9	diaminopimelate epimerase family protein	ENR1	ENR2	ENR3	0	chloroplast
9	AT3G47470	0.77970411	0.36783289	0.44405503	1	LHCA4 CAB4 light-harvesting chlorophyll-protein complex I subunit A4	ENR1	ENR2	ENR3	0	chloroplast
10	AT3G25860	0.64454768	0.55533827	0.17013981	1	LTA2 PLE22-oxoacid dehydrogenases acyltransferase family protein	ENR1	ENR2	ENR3	0	chloroplast
11	AT1G18500	0.72810103	0.46624733	0.23442129	9	MAML-4 IPMS1methylthioalkylmalate synthase-like 4	ENR1	ENR2	ENR3	0	chloroplast
12	AT1G44575	0.75089423	0.60348941	0.37866074	2	NPQ4 PSBSChlorophyll A-B binding family protein	ENR1	ENR2	ENR3	0	chloroplast
13	AT2G43750	0.50288813	0.72900137	0.62185322	5	OASBO-acetylserine (thiol) lyase B	ENR1	ENR2	ENR3	0	chloroplast
14	AT1G50480	0.75696101	0.64636492	0.56733504	10	THFS10-formyltetrahydrofolate synthetase	ENR1	ENR2	ENR3	0	chloroplast
15	AT5G64300	0.44907235	0.3244909	0.40867847	6	ATGCH, ATRIBA1, GCH, GTP CYCLOHYDROLASE II, RED FLUORESCENT IN DARKNESS 1, RFD1, RIBA1, RIBOFLAVIN A1	ENR1	ENR2	ENR3	0	chloroplast
16	AT4G29350	0.76865776	0.76380808	0.5161364	2	ATPRF2, PFN2, PRF2, PRO2, PROFILIN 2	ENR1	ENR2	ENR3	0	chloroplast
17	AT4G01150	0.67530966	0.35298955	0.54709649	1	CURT1A, CURVATURE THYLAKOID 1A	ENR1	ENR2	ENR3	0	chloroplast

18	AT4G39710	0.47754894	0.62737406	0.63229842	7	FK506-BINDING PROTEIN 16-2, FKBP16-2, PHOTOSYNTHETIC NDH SUBCOMPLEX L 4, PNSL4	ENR1	ENR2	ENR3	0	chloroplast
19	AT4G10340	0.56298043	0.46100812	0.36124213	1	LHCB5, LIGHT HARVESTING COMPLEX OF PHOTOSYSTEM II 5	ENR1	ENR2	ENR3	0	chloroplast
20	AT4G18810	0.30334675	0.4806797	0.13720387	2	NAD(P)-binding Rossmann-fold superfamily protein	ENR1	ENR2	ENR3	0	chloroplast
21	ATCG00270	0.72009931	0.70378287	0.63305744	4	PHOTOSYSTEM II REACTION CENTER PROTEIN D, PSBD	ENR1	ENR2	ENR3	0	chloroplast
22	AT5G08050	0.7465169	0.50332442	0.53365753	1	RIQ1	ENR1	ENR2	ENR3	0	chloroplast
23	AT5G58470	0.49161493	0.60918857	0.32165666	8	TAF15B, TBP-ASSOCIATED FACTOR 15B	ENR1	ENR2	ENR3	0	chloroplast
24	AT5G44340	0.61600768	0.52574501	0.2522752	10	TUB4, TUBULIN BETA CHAIN 4	ENR1	ENR2	ENR3	0	chloroplast
25	AT3G02360	0.45576074	NA	0.182779	5	6-phosphogluconate dehydrogenase family protein	ENR1	NA	ENR3	1	chloroplast
26	AT3G57610	NA	0.10004079	0.6005885	8	ADSSadenylosuccinate synthase	NA	ENR2	ENR3	1	chloroplast
27	AT2G13360	NA	0.51184673	0.22146954	5	AGT AGT1 SGATalanine:glyoxylate aminotransferase	NA	ENR2	ENR3	1	chloroplast
28	AT3G23600	NA	0.38470913	0.68444125	5	alpha/beta-Hydrolases superfamily protein	NA	ENR2	ENR3	1	chloroplast
29	AT3G25660	NA	0.62799638	0.2422711	8	Amidase family protein	NA	ENR2	ENR3	1	chloroplast
30	AT3G63410	0.39839092	0.64206747	NA	4	APG1 VTE3 IEP37 E37S-adenosyl-L-methionine-dependent methyltransferases superfamily protein	ENR1	ENR2	NA	1	chloroplast
31	AT1G27450	0.4463909	0.01404655	NA	4	APT1adenine phosphoribosyl transferase 1	ENR1	ENR2	NA	1	chloroplast
32	AT3G62530	NA	0.65319719	0.31143352	3	ARM repeat superfamily protein	NA	ENR2	ENR3	1	chloroplast
33	AT1G76080	0.38162661	0.76448954	NA	5	ATCDSP32 CDSP32chloroplastic drought-induced stress protein of 32 kD	ENR1	ENR2	NA	1	chloroplast
34	AT1G50320	NA	0.01361254	0.13990871	4	ATHX ATX THXthioredoxin X	NA	ENR2	ENR3	1	chloroplast
35	AT1G77510	NA	0.48544497	0.51466556	5	ATPDIL1-2 PDI6 ATPDI6 PDIL1-2PDI-like 1-2	NA	ENR2	ENR3	1	chloroplast
36	AT3G19170	0.3517551 5	NA	0.501289	13	ATPREP1 ATZNMP PREP1presequence protease 1	ENR1	NA	ENR3	1	chloroplast
37	AT3G52180	NA	0.45786604	0.76553773	9	ATPTPKIS1 DSP4 SEX4 ATSEX4dual specificity protein phosphatase (DsPTP1) family protein	NA	ENR2	ENR3	1	chloroplast

38	AT1G06950	0.26489668	0.58104215	NA	9	ATTIC110 TIC110translocon at the inner envelope membrane of chloroplasts 110	ENR1	ENR2	NA	1	chloroplast
39	AT3G18080	0.78513983	NA	0.26164716	3	BGLU44B-S glucosidase 44	ENR1	NA	ENR3	1	chloroplast
40	AT3G56240	NA	0.33971158	0.47621944	2	CCHcopper chaperone	NA	ENR2	ENR3	1	chloroplast
41	AT3G47860	NA	0.22809836	0.42126887	12	CHLchloroplastic lipocalin	NA	ENR2	ENR3	1	chloroplast
42	AT3G15190	0.73286388	NA	0.3774992	5	chloroplast 30S ribosomal protein S20 putative	ENR1	NA	ENR3	1	chloroplast
43	AT1G11750	NA	0.64029478	0.26810658	3	CLPP6CLP protease proteolytic subunit 6	NA	ENR2	ENR3	1	chloroplast
44	AT1G12410	NA	0.62167393	0.36571917	2	CLPR2 NCLPP2 CLP2CLP protease proteolytic subunit 2	NA	ENR2	ENR3	1	chloroplast
45	AT1G15730	0.72599276	NA	0.38707223	6	Cobalamin biosynthesis CobW-like protein	ENR1	NA	ENR3	1	chloroplast
46	AT3G52380	0.39503573	NA	0.4696304	3	CP33 PDE322chloroplast RNA-binding protein 33	ENR1	NA	ENR3	1	chloroplast
47	AT2G04030	0.71394862	0.7863025	NA	8	CR88 EMB1956 HSP90.5 Hsp88.1 AtHsp90.5 Chaperone protein htpG family protein	ENR1	ENR2	NA	1	chloroplast
48	AT1G09210	NA	0.19763901	0.43204748	4	CRT1b AtCRT1bcalreticulin 1b	NA	ENR2	ENR3	1	chloroplast
49	AT3G54900	NA	0.38076996	0.03488143	4	CXIP1 ATGRXCPCAX interacting protein 1	NA	ENR2	ENR3	1	chloroplast
50	AT3G23490	NA	0.69796751	0.52547803	1	CYNcyanase	NA	ENR2	ENR3	1	chloroplast
51	AT1G05190	NA	0.55923466	0.32945113	1	emb2394Ribosomal protein L6 family	NA	ENR2	ENR3	1	chloroplast
52	AT1G34430	0.46767428	NA	0.09841995	1	EMB30032-oxoacid dehydrogenases acyltransferase family protein	ENR1	NA	ENR3	1	chloroplast
53	AT3G14210	0.66225144	NA	0.4362944	6	ESM1epithiospecifier modifier 1	ENR1	NA	ENR3	1	chloroplast
54	AT1G42960	NA	0.59552128	0.33604404	2	expressed protein localized to the inner membrane of the chloroplast.	NA	ENR2	ENR3	1	chloroplast
55	AT3G23400	0.58084325	NA	0.51176604	1	FIB4Plastid-lipid associated protein PAP / fibrillin family protein	ENR1	NA	ENR3	1	chloroplast
56	AT1G11840	NA	0.60796898	0.75740969	1	GLX1glyoxalase I homolog	NA	ENR2	ENR3	1	chloroplast
57	AT1G22300	NA	0.25241005	0.78150259	2	GRF10 GF14 EPSILONgeneral regulatory factor 10	NA	ENR2	ENR3	1	chloroplast
58	AT2G42590	NA	0.44539654	0.64389386	2	GRF9 GF14 MUgeneral regulatory factor 9	NA	ENR2	ENR3	1	chloroplast

59	AT1G07920	0.74334384	NA	0.60657601	6	GTP binding Elongation factor Tu family protein	ENR1	NA	ENR3	1	chloroplast
60	AT1G56500	0.76224229	NA	0.76287624	13	haloacid dehalogenase-like hydrolase family protein	ENR1	NA	ENR3	1	chloroplast
61	AT1G69740	0.53870013	0.72085453	NA	8	HEMB1Aldolase superfamily protein |	ENR1	ENR2	NA	1	chloroplast
62	AT3G56490	NA	0.13221091	0.22711239	1	HIT3 HINT1HIS triad family protein 3	NA	ENR2	ENR3	1	chloroplast
63	AT3G16470	NA	0.55139949	0.47843885	1	JR1Mannose-binding lectin superfamily protein	NA	ENR2	ENR3	1	chloroplast
64	AT1G49750	NA	0.76338417	0.37333957	14	Leucine-rich repeat (LRR) family protein	NA	ENR2	ENR3	1	chloroplast
65	AT3G54890	NA	0.55524862	0.30329744	3	LHCA1photosystem I light harvesting complex gene 1	NA	ENR2	ENR3	1	chloroplast
66	AT1G61520	0.5155397	NA	0.5402104	2	LHCA3photosystem I light harvesting complex gene 3	ENR1	NA	ENR3	1	chloroplast
67	AT3G08940	NA	0.02805462	0.02578121	3	LHCB4.2light harvesting complex photosystem II	NA	ENR2	ENR3	1	chloroplast
68	AT2G40100	0.684934	NA	0.16578906	1	LHCB4.3light harvesting complex photosystem II	ENR1	NA	ENR3	1	chloroplast
69	AT2G36530	NA	0.50103321	0.12609959	5	LOS2 ENO2Enolase	NA	ENR2	ENR3	1	chloroplast
70	AT2G20690	NA	0.43312506	0.72296208	6	lumazine-binding family protein	NA	ENR2	ENR3	1	chloroplast
71	AT3G15950	0.65510727	0.38633906	NA	4	NAI2DNA topoisomerase-related	ENR1	ENR2	NA	1	chloroplast
72	AT1G15980	NA	0.54103046	0.31067642	5	NDF1 NDH48NDH-dependent cyclic electron flow 1	NA	ENR2	ENR3	1	chloroplast
73	AT3G44310	NA	0.60305646	0.60471733	7	NIT1 ATNIT1 NITInitrilase 1	NA	ENR2	ENR3	1	chloroplast
74	AT1G75330	NA	0.61372655	0.33041838	5	OTCornithine carbamoyltransferase	NA	ENR2	ENR3	1	chloroplast
75	AT1G63770	0.61792842	NA	0.28792722	12	Peptidase M1 family protein	ENR1	NA	ENR3	1	chloroplast
76	AT4G22890	NA	0.40485048	0.06295306	6	PGR5-LIKE APGR5-LIKE A	NA	ENR2	ENR3	1	chloroplast
77	AT2G05620	NA	0.47094207	0.3269359	2	PGR5proton gradient regulation 5	NA	ENR2	ENR3	1	chloroplast
78	AT3G15840	0.77480673	NA	0.21682026	7	PIFIpost-illumination chlorophyll fluorescence increase	ENR1	NA	ENR3	1	chloroplast
79	AT1G80380	0.63861787	NA	0.47173144	9	P-loop containing nucleoside triphosphate hydrolases superfamily protein	ENR1	NA	ENR3	1	chloroplast
80	AT1G31330	0.74001479	NA	0.63684817	3	PSAFphotosystem I subunit F	ENR1	NA	ENR3	1	chloroplast
81	AT2G38140	0.64511024	NA	0.31720239	2	PSRP4plastid-specific ribosomal protein 4	ENR1	NA	ENR3	1	chloroplast

82	AT2G46820	NA	0.10560589	0.24654273	2	PTAC8 TMP14 PSAP PSI-Pphotosystem I P subunit	NA	ENR2	ENR3	1	chloroplast
83	AT1G71500	NA	0.27871049	0.2564308	3	Rieske (2Fe-2S) domain-containing protein	NA	ENR2	ENR3	1	chloroplast
84	AT1G48860	0.63871854	0.07258226	NA	11	RNA 3'-terminal phosphate cyclase/enol pyruvate transferase alpha/beta	ENR1	ENR2	NA	1	chloroplast
85	AT1G79850	NA	0.66180254	0.32453169	1	RPS17 CS17 PRPS17ribosomal protein S17	NA	ENR2	ENR3	1	chloroplast
86	AT1G54500	NA	0.37001573	0.638839	5	Rubredoxin-like superfamily protein	NA	ENR2	ENR3	1	chloroplast
87	AT2G25110	NA	0.29727913	0.13728978	3	SDF2 ATSDL AtSDF2stromal cell-derived factor 2-like protein precursor	NA	ENR2	ENR3	1	chloroplast
88	AT1G14810	0.69929957	NA	0.77183033	5	semialdehyde dehydrogenase family protein	ENR1	NA	ENR3	1	chloroplast
89	AT2G21530	NA	0.67560963	0.39006102	3	SMAD/FHA domain-containing protein	NA	ENR2	ENR3	1	chloroplast
90	AT1G17100	NA	0.46989014	0.31073143	3	SOUL heme-binding family protein	NA	ENR2	ENR3	1	chloroplast
91	AT1G23820	NA	0.26213791	0.60713637	6	SPDS1spermidine synthase 1	NA	ENR2	ENR3	1	chloroplast
92	AT2G29630	0.39270205	NA	0.63149525	11	THICthiaminC	ENR1	NA	ENR3	1	chloroplast
93	AT2G22230	0.26608171	NA	0.29580724	2	Thioesterase superfamily protein	ENR1	NA	ENR3	1	chloroplast
94	AT2G21160	NA	0.67395664	0.43527019	2	Translocon-associated protein (TRAP) alpha subunit	NA	ENR2	ENR3	1	chloroplast
95	AT1G32900	0.78308466	NA	0.78482388	12	UDP-Glycosyltransferase superfamily protein	ENR1	NA	ENR3	1	chloroplast
96	AT2G24020	NA	0.03962869	0.42246548	1	Uncharacterised BCR YbaB family COG0718	NA	ENR2	ENR3	1	chloroplast
97	AT2G21385	0.55920581	NA	0.75105292	5	unknown protein	ENR1	NA	ENR3	1	chloroplast
98	AT3G04550	0.7476519	NA	0.44585888	2	unknown protein	ENR1	NA	ENR3	1	chloroplast
99	AT3G53900	0.47653722	NA	0.76315452	2	UPP PYRRuracil phosphoribosyltransferase	ENR1	NA	ENR3	1	chloroplast
100	AT1G80600	NA	0.51225087	0.26492591	7	WIN1HOPW1-1-interacting 1	NA	ENR2	ENR3	1	chloroplast
101	AT5G23010	0.28220447	0.63866241	NA	9	2-ISOPROPYLMALATE SYNTHASE 3, GLUCOSINOLATE METABOLISM 1, GSM1, IMS3, MAM1	ENR1	ENR2	NA	1	chloroplast
102	AT5G03940	0.26997249	0.79241582	NA	5	54 CHLOROPLAST PROTEIN, 54CP	ENR1	ENR2	NA	1	chloroplast
103	AT4G25050	NA	0.27241753	0.13025903	1	ACP4, ACYL CARRIER PROTEIN 4, ATACP4	NA	ENR2	ENR3	1	chloroplast

104	AT5G09810	0.6760269	0.53938341	NA	4	ACT7, ACTIN 7, ATACT7	ENR1	ENR2	NA	1	chloroplast
105	AT4G01800	NA	0.31572011	0.76881094	10	AGY1, ALBINO OR GLASSY YELLOW 1, ARABIDOPSIS THALIANA CHLOROPLAST SECA, ATCPSECA, SECA1	NA	ENR2	ENR3	1	chloroplast
106	AT5G48220	NA	0.46039028	0.16549514	3	Aldolase-type TIM barrel family protei	NA	ENR2	ENR3	1	chloroplast
107	AT5G53560	NA	0.48363015	0.4129058	1	ARABIDOPSIS CYTOCHROME B5 ISOFORM E, ATB5-A, ATCB5-E, B5 #2, CB5-E, CYTOCHROME B5 ISOFORM E	NA	ENR2	ENR3	1	chloroplast
108	AT5G51820	NA	0.44591621	0.33721002	2	ARABIDOPSIS THALIANA PHOSPHOGLUCOMUTASE, ATPGMP, PGM, PGM1, PHOSPHOGLUCOMUTASE, STARCH-FREE 1, STF1	NA	ENR2	ENR3	1	chloroplast
109	AT4G26500	0.4997564 1	NA	0.60317481	3	CHLOROPLAST SULFUR E, SUFE1, SULFUR E 1	ENR1	NA	ENR3	1	chloroplast
110	AT5G61790	0.75794	NA	0.27435663	6	ATCNX1, CALNEXIN 1, CNX1	ENR1	NA	ENR3	1	chloroplast
111	AT4G27520	NA	0.60744833	0.5602946	2	ATENODL2, EARLY NODULIN-LIKE PROTEIN 2, ENODL2	NA	ENR2	ENR3	1	chloroplast
112	AT5G45680	0.7891491	NA	0.76575628	7	ATFKBP13, FK506 BINDING PROTEIN 13, FK506-BINDING PROTEIN 13, FKBP13	ENR1	NA	ENR3	1	chloroplast
113	AT5G51720	NA	0.75418587	0.69209557	3	AT-NEET, NEET, NEET GROUP PROTEIN	NA	ENR2	ENR3	1	chloroplast
114	AT5G09650	NA	0.19158691	0.7245861	5	ATPPA6, PPA6, PYROPHOSPHORYLASE 6	NA	ENR2	ENR3	1	chloroplast
115	AT5G26742	0.4748907 2	0.21844046	NA	6	ATRH3, EMB1138, EMBRYO DEFECTIVE 1138, RH3	ENR1	ENR2	NA	1	chloroplast
116	AT4G21210	0.1989321 4	NA	0.18550803	3	ATRP1, PPDK REGULATORY PROTEIN, RP1	ENR1	NA	ENR3	1	chloroplast
117	AT5G16620	NA	0.56559 28	0.26314059	4	ATTIC40, PDE120, PIGMENT DEFECTIVE EMBRYO 120, TIC40, TRANSLOCON AT THE INNER ENVELOPE MEMBRANE OF CHLOROPLASTS 40	NA	ENR2	ENR3	1	chloroplast
118	AT4G02510	NA	0.63049073	0.45234343	5	ATTOC159, PLASTID PROTEIN IMPORT 2, PPI2, TOC159, TOC160, TOC86	NA	ENR2	ENR3	1	chloroplast

119	AT5G16390	NA	0.40835166	0.40359926	2	BCCP, BCCP-1, BCCP1, BIOTIN CARBOXYL CARRIER PROTEIN, BIOTIN CARBOXYL-CARRIER PROTEIN 1, CAC1, CAC1-A, CAC1A, CHLOROPLASTIC ACETYLCOENZYME A CARBOXYLASE 1	NA	ENR2	ENR3	1	chloroplast
120	AT5G07340	0.49529292	NA	0.39200964	5	Calreticulin family protein	ENR1	NA	ENR3	1	chloroplast
121	ATCG00670	0.44409231	NA	0.17462978	1	CASEINOLYTIC PROTEASE P 1, CLPP1, PCLPP, PLASTID-ENCODED CLP P	ENR1	NA	ENR3	1	chloroplast
122	AT4G18480	NA	0.77523173	0.40506 73	5	CH-42, CH42, CHL11, CHLI-1, CHLI1, CHLORINA 42, LOST1, LOW TEMPERATURE WITH	NA	ENR2	ENR3	1	chloroplast
123	AT4G24280	NA	0.72776311	0.65077625	2	CHLOROPLAST HEAT SHOCK PROTEIN 70-1, CPHSC70-1	NA	ENR2	ENR3	1	chloroplast
124	AT5G21430	NA	0.77358935	0.18310761	3	CHLORORESPIRATORY REDUCTION L, CRRL, NADH DEHYDROGENASE-LIKE COMPLEX U, NDHU	NA	ENR2	ENR3	1	chloroplast
125	AT4G14040	0.718734	NA	0.79042255	7	EDA38, EMBRYO SAC DEVELOPMENT ARREST 38, SBP2, SELENIUM-BINDING PROTEIN 2	ENR1	NA	ENR3	1	chloroplast
126	AT5G14320	NA	0.37159231	0.45764022	5	EMB3137, EMBRYO DEFECTIVE 3137, Ribosomal protein S13/S18 family	NA	ENR2	ENR3	1	chloroplast
127	AT5G26830	NA	0.73940678	0.28722121	13	Encodes a dual-targeted threonyl-tRNA synthetase found in both the chloroplast and mitochondrion	NA	ENR2	ENR3	1	chloroplast
128	AT5G19760	NA	0.6068083	0.74059878	8	Encodes a **novel mitochondrial carrie**r capable of transporting both dicarboxylates (such as malate, oxaloacetate, oxoglutarate, and maleate) and tricarboxylates (such as citrate, isocitrate, cis-aconitate, and trans-aconitate).	NA	ENR2	ENR3	1	chloroplast
129	AT4G33520	0.54199654	NA	0.27741105	13	Encodes a putative metal-transporting P-type ATPase PAA1	ENR1	NA	ENR3	1	chloroplast
130	AT4G04020	NA	0.75742466	0.67056254	1	**FIB**, FIB1A, FIBRILLIN, FIBRILLIN 1A, PGL35, PLASTOGLOBULIN 35	NA	ENR2	ENR3	1	chloroplast
131	AT5G02160	NA	0.22890752	0.50543324	4	FIP, FTSH5 INTERACTING PROTEIN	NA	ENR2	ENR3	1	chloroplast

132	AT5G48580	0.70054548	NA	0.7143718	2	FK506- AND RAPAMYCIN-BINDING PROTEIN 15 KD-2, FKBP15-2	ENR1	NA	ENR3	1	chloroplast
133	AT4G09000	NA	0.15687456	0.42755186	2	GENERAL REGULATORY FACTOR 1, GENERAL REGULATORY FACTOR1-G-BOX FACTOR 14-3-3 HOMOLOG ISOFORM CHI, GF14 CHI, GRF1	NA	ENR2	ENR3	1	chloroplast
134	AT4G32915	NA	0.34145735	0.26869087	3	glutamyl-tRNA(Gln) amidotransferase subunit C	NA	ENR2	ENR3	1	chloroplast
135	AT5G57040	NA	0.62348631	0.36460213	3	GLXI-LIKE;11, GLYOXALASE I-LIKE;11	NA	ENR2	ENR3	1	chloroplast
136	AT4G35260	NA	0.14206257	0.49157636	7	IDH-I, IDH1, ISOCITRATE DEHYDROGENASE 1, ISOCITRATE DEHYDROGENASE I	NA	ENR2	ENR3	1	chloroplast
137	AT4G17600	NA	0.41209329	0.26771048	1	LIGHT-HARVESTING-LIKE 3:1, LIL3:1	NA	ENR2	ENR3	1	chloroplast
138	AT4G02530	NA	0.27057042	0.13109113	1	MAINTENANCE OF PHOTOSYSTEM II UNDER HIGH LIGHT 2, MPH2	NA	ENR2	ENR3	1	chloroplast
139	AT5G07020	0.48247228	0.63692975	NA	2	MAINTENANCE OF PSII UNDER HIGH LIGHT 1, MPH1	ENR1	ENR2	NA	1	chloroplast
140	AT1G70830	0.7526048	0.50306958	NA	3	MLP28MLP-like protein 28	ENR1	ENR2	NA	1	chloroplast
141	AT4G20020	NA	0.16525764	0.13022891	3	MORF1, MULTIPLE ORGANELLAR RNA EDITING FACTOR 1	NA	ENR2	ENR3	1	chloroplast
142	AT4G37925	0.74552284	NA	0.29666452	3	NADH DEHYDROGENASE-LIKE COMPLEX M, NDH-M, NDHM, SUBUNIT NDH-M OF NAD(P)H:PLASTOQUINONE DEHYDROGENASE COMPLEX	ENR1	NA	ENR3	1	chloroplast
143	AT4G34090	NA	0.58914154	0.25511886	4	PAB, PROTEIN IN CHLOROPLAST ATPASE BIOGENESIS	NA	ENR2	ENR3	1	chloroplast
144	AT5G60640	NA	0.76410533	0.50251954	4	PDI-LIKE 1-4, PDIL1-4	NA	ENR2	ENR3	1	chloroplast
145	ATCG00540	0.77897728	NA	0.32219165	2	PETA, PHOTOSYNTHETIC ELECTRON TRANSFER A	ENR1	NA	ENR3	1	chloroplast
146	ATCG00020	0.68583632	0.35028336	NA	2	PHOTOSYSTEM II REACTION CENTER PROTEIN A, PSBA	ENR1	ENR2	NA	1	chloroplast
147	ATCG00680	NA	0.58928464	0.63387332	3	PHOTOSYSTEM II REACTION CENTER PROTEIN B, PSBB	NA	ENR2	ENR3	1	chloroplast
148	AT4G13670	NA	0.43040314	0.2408211	10	PLASTID TRANSCRIPTIONALLY ACTIVE 5, PTAC5	NA	ENR2	ENR3	1	chloroplast

149	AT5G02240	NA	0.61528475	0.79063667	1	Protein is tyrosine-phosphorylated and its phosphorylation state is modulated in response to ABA in Arabidopsis thaliana seeds. The mRNA is cell-to-cell mobile.	NA	ENR2	ENR3	1	chloroplast
150	ATCG01060	NA	0.24699683	0.42615108	9	PSAC	NA	ENR2	ENR3	1	chloroplast
151	AT5G40450	NA	0.49839781	0.43773975	11	RBB1, REGULATOR OF BULB BIOGENESIS1	NA	ENR2	ENR3	1	chloroplast
152	AT2G42220	0.61132841	0.50691099	NA	4	Rhodanese/Cell cycle control phosphatase superfamily protein	ENR1	ENR2	NA	1	chloroplast
153	ATCG00830	0.64297351	NA	0.21471693	5	RIBOSOMAL PROTEIN L2, RPL2.1	ENR1	NA	ENR3	1	chloroplast
154	AT5G13030	0.35951843	0.41963307	NA	13	SELENOPROTEIN O, SELO	ENR1	ENR2	NA	1	chloroplast
155	AT4G20360	0.71087836	NA	0.52419286	5	SUPPRESSOR OF VARIEGATION11, SVR11, AtRabE1b	ENR1	NA	ENR3	1	chloroplast
156	AT5G54770	NA	0.53585932	0.76085253	2	THI1, THI4, THIAMINE4, THIAZOLE REQUIRING, TZ	NA	ENR2	ENR3	1	chloroplast
157	AT5G10540	NA	0.50087003	0.60582283	4	THIMET METALLOENDOPEPTIDASE 2, TOP2	NA	ENR2	ENR3	1	chloroplast
158	AT5G10160	0.38267824	NA	0.27713874	2	Thioesterase superfamily protein	ENR1	NA	ENR3	1	chloroplast
159	AT5G55220	NA	0.47926738	0.72144412	8	trigger factor type chaperone family protein	NA	ENR2	ENR3	1	chloroplast
160	AT3G17020	0.61165854	0.13968046	0.37840019	3	Adenine nucleotide alpha hydrolases-like superfamily protein	ENR1	ENR2	ENR3	0	NA
161	AT1G22840	0.57718483	0.47350621	0.03390256	2	CYTC-1 ATCYTC-ACYTOCHROME C-1	ENR1	ENR2	ENR3	0	NA
162	AT1G29660	0.48173746	0.49507426	0.53974812	9	GDSL-like Lipase/Acylhydrolase superfamily protein	ENR1	ENR2	ENR3	0	NA
163	AT1G10840	0.62224654	0.27404942	0.03257317	5	TIF3H1translation initiation factor 3 subunit H1	ENR1	ENR2	ENR3	0	NA
164	AT1G28290	0.79416552	NA	0.60686151	7	AGP31arabinogalactan protein 31	ENR1	NA	ENR3	1	NA
165	AT2G18960	NA	0.21444316	0.58032791	8	AHA1 PMA OST2 HA1H(+)-ATPase 1	NA	ENR2	ENR3	1	NA
166	AT3G10520	NA	0.57102205	0.26506547	1	AHB2 GLB2 ARATH GLB2 NSHB2 ATGLB2 HB2haemoglobin 2	NA	ENR2	ENR3	1	NA
167	AT1G11910	0.70679248	NA	0.49960884	13	APA1 ATAPA1aspartic proteinase A1	ENR1	NA	ENR3	1	NA

168	AT1G66680	NA	0.79522985	0.14408008	3	AR401S-adenosyl-L-methionine-dependent methyltransferases superfamily protein	NA	ENR2	ENR3	1	NA
169	AT3G12490	NA	0.1268869	0.53982134	2	ATCYSB ATCYS6 CYSBcystatin B	NA	ENR2	ENR3	1	NA
170	AT2G44100	0.61835553	0.75298544	NA	8	ATGDI1 AT-GDI1 GDI1guanosine nucleotide diphosphate dissociation inhibitor 1	ENR1	ENR2	NA	1	NA
171	AT3G13750	NA	0.68637929	0.54070481	20	BGAL1beta galactosidase 1	NA	ENR2	ENR3	1	NA
172	AT1G18210	NA	0.01606667	0.53461842	3	Calcium-binding EF-hand family protein	NA	ENR2	ENR3	1	NA
173	AT2G44310	NA	0.06753638	0.46623695	1	Calcium-binding EF-hand family protein	NA	ENR2	ENR3	1	NA
174	AT1G78830	0.38149789	0.01479322	NA	12	Curculin-like (mannose-binding) lectin family protein	ENR1	ENR2	NA	1	NA
175	AT1G78820	0.55336555	NA	0.42534367	12	D-mannose binding lectin protein with Apple-like carbohydrate-binding domain	ENR1	NA	ENR3	1	NA
176	AT3G46940	NA	0.05474797	0.2088733	1	DUT1DUTP-PYROPHOSPHATASE-LIKE 1	NA	ENR2	ENR3	1	NA
177	AT3G11400	0.49596882	0.01646947	NA	3	EIF3G1 ATEIF3G1eukaryotic translation initiation factor 3G1	ENR1	ENR2	NA	1	NA
178	AT3G19760	NA	0.10760565	0.54917652	6	EIF4A-IIIeukaryotic initiation factor 4A-III	NA	ENR2	ENR3	1	NA
179	AT2G25060	NA	0.79763721	0.25907274	4	ENODL14 AtENODL14early nodulin-like protein 14	NA	ENR2	ENR3	1	NA
180	AT1G26630	NA	0.79613515	0.5589691	4	FBR12 ATELF5A-2 ELF5A-2Eukaryotic translation initiation factor 5A-1 (eIF-5A 1) protein	NA	ENR2	ENR3	1	NA
181	AT1G65960	NA	0.26134281	0.34918468	4	GAD2glutamate decarboxylase 2	NA	ENR2	ENR3	1	NA
182	AT3G06035	NA	0.21091605	0.68942304	6	Glycoprotein membrane precursor GPI-anchored	NA	ENR2	ENR3	1	NA
183	AT1G21880	NA	0.65564793	0.10676353	15	LYM1lysm domain GPI-anchored protein 1 precursor	NA	ENR2	ENR3	1	NA
184	AT1G15340	NA	0.13761185	0.34314373	1	MBD10methyl-CPG-binding domain 10	NA	ENR2	ENR3	1	NA
185	AT2G23820	0.60638554	NA	0.69736732	8	Metal-dependent phosphohydrolase	ENR1	NA	ENR3	1	NA
186	AT2G19480	NA	0.59638255	0.37095377	3	NAP1;2nucleosome assembly protein 1;2	NA	ENR2	ENR3	1	NA
187	AT1G52380	NA	0.26225987	0.18923461	4	NUP50 (Nucleoporin 50 kDa) protein	NA	ENR2	ENR3	1	NA

188	AT2G01630	0.21751862	NA	0.10655587	7	O-Glycosyl hydrolases family 17	ENR1	NA	ENR3	1	NA
189	AT1G49760	0.54715909	NA	0.28833017	4	PAB8 PABP8poly(A) binding protein 8	ENR1	NA	ENR3	1	NA
190	AT1G65010	NA	0.13984665	0.26821216	9	Plant protein of unknown function (DUF827)	NA	ENR2	ENR3	1	NA
191	AT3G02200	0.464896	NA	0.40122349	6	Proteasome component (PCI) domain protein	ENR1	NA	ENR3	1	NA
192	AT1G47128	NA	0.61642015	0.22177504	21	RD21 RD21AGranulin repeat cysteine protease family protein	NA	ENR2	ENR3	1	NA
193	AT2G21620	NA	0.39689345	0.44753518	4	RD2Adenine nucleotide alpha hydrolases-like superfamily protein	NA	ENR2	ENR3	1	NA
194	AT3G61260	NA	0.7966162	0.55472732	2	Remorin family protein	NA	ENR2	ENR3	1	NA
195	AT1G15930	NA	0.46885454	0.58347828	6	Ribosomal protein L7Ae/L30e/S12e/Gadd45 family protein	NA	ENR2	ENR3	1	NA
196	AT1G80230	NA	0.21104433	0.28948043	5	Rubredoxin-like superfamily protein	NA	ENR2	ENR3	1	NA
197	AT1G56330	0.52486696	NA	0.5287997	1	SAR1 ATSAR1 ATSARA1B ATSAR1B SAR1Bsecretion-associated RAS 1B	ENR1	NA	ENR3	1	NA
198	AT1G07140	NA	0.2992364	0.28891241	4	SIRANBPPleckstrin homology (PH) domain superfamily protein	NA	ENR2	ENR3	1	NA
199	AT3G02180	NA	0.37529082	0.28597261	1	SP1L3SPIRAL1-like3	NA	ENR2	ENR3	1	NA
200	AT1G70310	0.41882398	NA	0.63922814	9	SPDS2spermidine synthase 2	ENR1	NA	ENR3	1	NA
201	AT1G01320	0.72874388	NA	0.6890703	17	Tetratricopeptide repeat (TPR)-like superfamily protein	ENR1	NA	ENR3	1	NA
202	AT1G04530	NA	0.15594526	0.30592737	4	TPR4Tetratricopeptide repeat (TPR)-like superfamily protein	NA	ENR2	ENR3	1	NA
203	AT1G09640	NA	0.45969822	0.16693379	4	Translation elongation factor EF1B gamma chain	NA	ENR2	ENR3	1	NA
204	AT1G57720	NA	0.31234453	0.47180031	4	Translation elongation factor EF1B gamma chain	NA	ENR2	ENR3	1	NA
205	AT3G52560	NA	0.56003949	0.62152154	3	UEV1D-4ubiquitin E2 variant 1D-4	NA	ENR2	ENR3	1	NA
206	AT5G64350	0.72111602	NA	0.61891383	2	FK506-BINDING PROTEIN 12, ATFKBP12, FK506-BINDING PROTEIN 12, FKBP12, FKP12	ENR1	NA	ENR3	1	NA
207	AT5G20010	NA	0.42332725	0.50467359	6	RAS-RELATED NUCLEAR PROTEIN, RAS-RELATED NUCLEAR PROTEIN-1	NA	ENR2	ENR3	1	NA

208	AT5G20230	0.33370853	NA	0.41931318	3	SAG14, SENESCENCE ASSOCIATED GENE 14	ENR1	NA	ENR3	1	NA
209	AT5G54160	NA	0.67594223	0.53471573	9	ATCOMT, ATOMT1, CAFFEATE O-METHYLTRANSFERASE 1, OMT3	NA	ENR2	ENR3	1	NA
210	AT4G22670	NA	0.59783522	0.71018176	1	ATHIP1, HIP1, HSP70-INTERACTING PROTEIN 1	NA	ENR2	ENR3	1	NA
211	AT5G57290	NA	0.0477104	0.68069674	1	ATP3B, P3B, RIBOSOMAL P3 PROTEIN B	NA	ENR2	ENR3	1	NA
212	AT5G25610	0.74735058	NA	0.58497207	7	ATRD22, RD22, RESPONSIVE TO DESICCATION 22	ENR1	NA	ENR3	1	NA
213	AT5G51970	0.63064175	NA	0.67826849	14	ATSDH, SORBITOL DEHYDROGENASE	ENR1	NA	ENR3	1	NA
214	AT5G11420	NA	0.46420333	0.34455285	5	Encodes a DUF642 cell wall p	NA	ENR2	ENR3	1	NA
215	AT4G22485	NA	0.4563176	0.42173064	12	Encodes a Protease inhibitor/seed storage/LTP family protein	NA	ENR2	ENR3	1	NA
216	AT5G26667	NA	0.38476821	0.124549	3	encodes a uridine 5'-monophosphate (UMP)/cytidine 5'-monophosphate (CMP) kinase. The mRNA is cell-to-cell mobile	NA	ENR2	ENR3	1	NA
217	AT5G43940	NA	0.07584205	0.29373065	15	HOT5, SENSITIVE TO HOT TEMPERATURES 5	NA	ENR2	ENR3	1	NA
218	AT5G06320	0.35715789	NA	0.22401292	9	NDR1/HIN1-LIKE 3, NHL3	ENR1	NA	ENR3	1	NA
219	AT5G09620	NA	0.19885096	0.74950418	2	Octicosapeptide/Phox/Bem1p family protein	NA	ENR2	ENR3	1	NA
220	AT5G58090	0.70032926	NA	0.40459081	8	O-Glycosyl hydrolases family 17 protein	ENR1	NA	ENR3	1	NA
221	AT4G35100	0.71540642	NA	0.06068875	4	PIP3, PLASMA MEMBRANE INTRINSIC PROTEIN 3	ENR1	NA	ENR3	1	NA
222	AT5G39570	NA	0.68570824	0.34931443	1	PLD REGULATED PROTEIN1, PLDRP1	NA	ENR2	ENR3	1	NA
223	AT3G26450	0.55507911	0.50130124	NA	2	Polyketide cyclase/dehydrase and lipid transport superfamily protein	ENR1	ENR2	NA	1	NA
224	AT4G27500	0.56769976	0.79175857	NA	2	PPI1, PROTON PUMP INTERACTOR 1	ENR1	ENR2	NA	1	NA
225	AT4G15410	NA	0.6129262	0.34802032	1	PUX5, SERINE/THREONINE PROTEIN PHOSPHATASE 2A 55 KDA REGULATORY SUBUNIT B	NA	ENR2	ENR3	1	NA
226	AT5G27470	NA	0.13727651	0.31477765	8	seryl-tRNA synthetase / serine-tRNA ligase	NA	ENR2	ENR3	1	NA
227	AT4G28100	0.4707148	0.18811958	NA	16	transmembrane protein	ENR1	ENR2	NA	1	NA

228	AT5G62690	NA	0.69513611	0.15236821	12	TUB2, TUBULIN BETA CHAIN 2	NA	ENR2	ENR3	1	NA
229	AT5G57655	0.52772861	0.64187251	NA	5	xylose isomerase family pr	ENR1	ENR2	NA	1	NA
230	AT5G47930	NA	0.24522811	0.34033498	6	Zinc-binding ribosomal protein factor	NA	ENR2	ENR3	1	NA

Bibliography

Adam Z, Frottin F, Espagne C, Meinnel T, Giglione C (2011) Interplay Between N-Terminal Methionine Excision and FtsH Protease Is Essential for Normal Chloroplast Development and Function in Arabidopsis. The Plant Cell **23:** 3745-3760

Aoyama K, Nakaki T (2012) Inhibition of GTRAP3-18 may increase neuroprotective glutathione (GSH) synthesis. Int J Mol Sci **13:** 12017-12035

Apel K, Hirt H (2004) Reactive oxygen species: metabolism, oxidative stress, and signal transduction. Annu Rev Plant Biol **55:** 373-399

Arabidopsis Genome I (2000) Analysis of the genome sequence of the flowering plant Arabidopsis thaliana. Nature **408:** 796-815

Arsova B, Hoja U, Wimmelbacher M, Greiner E, Ustun S, Melzer M, Petersen K, Lein W, Bornke F (2010) Plastidial thioredoxin z interacts with two fructokinase-like proteins in a thiol-dependent manner: evidence for an essential role in chloroplast development in Arabidopsis and Nicotiana benthamiana. Plant Cell **22:** 1498-1515

Ascencio-Ibanez JT, Sozzani R, Lee TJ, Chu TM, Wolfinger RD, Cella R, Hanley-Bowdoin L (2008) Global analysis of Arabidopsis gene expression uncovers a complex array of changes impacting pathogen response and cell cycle during geminivirus infection. Plant Physiol **148:** 436-454

Baba T, Ara T, Hasegawa M, Takai Y, Okumura Y, Baba M, Datsenko KA, Tomita M, Wanner BL, Mori H (2006) Construction of Escherichia coli K-12 in-frame, single-gene knockout mutants: the Keio collection. Mol Syst Biol **2:** 2006 0008

Bailey-Serres J, Juntawong P (2012) Dynamic Light Regulation of Translation Status in Arabidopsis thaliana. Frontiers in Plant Science **3**

Balmer Y, Stritt-Etter AL, Hirasawa M, Jacquot JP, Keryer E, Knaff DB, Schurmann P (2001) Oxidation-reduction and activation properties of chloroplast fructose 1,6-bisphosphatase with mutated regulatory site. Biochemistry **40:** 15444-15450

Beligni MV, Mayfield SP (2008) Arabidopsis thaliana mutants reveal a role for CSP41a and CSP41b, two ribosome-associated endonucleases, in chloroplast ribosomal RNA metabolism. Plant Mol Biol **67:** 389-401

Benitez-Alfonso Y, Cilia M, Roman AS, Thomas C, Maule A, Hearn S, Jackson D (2009) Control of Arabidopsis meristem development by thioredoxin-dependent regulation of intercellular transport. Proceedings of the National Academy of Sciences **106:** 3615-3620

Bennett J (1981) Biosynthesis of the light-harvesting chlorophyll a/b protein. Polypeptide turnover in darkness. Eur J Biochem **118:** 61-70

Berckmans B, Lammens T, Van Den Daele H, Magyar Z, Bogre L, De Veylder L (2011) Light-dependent regulation of DEL1 is determined by the antagonistic action of E2Fb and E2Fc. Plant Physiol **157:** 1440-1451

Bohrer AS, Massot V, Innocenti G, Reichheld JP, Issakidis-Bourguet E, Vanacker H (2012) New insights into the reduction systems of plastidial thioredoxins point out the unique properties of thioredoxin z from Arabidopsis. Journal of Experimental Botany **63:** 6315-6323

Bollenbach TJ, Sharwood RE, Gutierrez R, Lerbs-Mache S, Stern DB (2009) The RNA-binding proteins CSP41a and CSP41b may regulate transcription and translation of chloroplast-encoded RNAs in Arabidopsis. Plant Mol Biol **69:** 541-552

Bollenbach TJ, Tatman DA, Stern DB (2003) CSP41a, a multifunctional RNA-binding protein, initiates mRNA turnover in tobacco chloroplasts. Plant J.**:** 842:852

Bolwell G, Bindschedler L, Blee K, Butt V, Davies D, Gardner S, Gerrish C, Minibayeva F (2002) The apoplastic oxidative burst in response to biotic stress in plants: a three-component system. J Exp Bot.

Bowler C, Fluhr R (2000) The role of calcium and activated oxygens as signals for controlling cross-tolerance. Trends Plant Sci.

Brandes N, Schmitt S, Jakob U (2009) Thiol-based redox switches in eukaryotic proteins. Antioxid Redox Signal **11:** 997-1014

Buchanan BB, Balmer Y (2005) Redox regulation: a broadening horizon. Annu Rev Plant Biol **56:** 187-220

Burgoyne JR, Eaton P (2010) Oxidant sensing by protein kinases a and g enables integration of cell redox state with phosphoregulation. Sensors (Basel) **10:** 2731-2751

Calviello L, Sydow D, Harnett D, Ohler U (2019) Ribo-seQC: comprehensive analysis of cytoplasmic and organellar ribosome profiling data. bioRxiv **601468**

Cejudo FJ, Meyer AJ, Reichheld JP, Rouhier N, Traverso JA (2014) Thiol-based redox homeostasis and signaling. Front Plant Sci **5:** 266

Červený J, Sinetova MA, Valledor L, Sherman LA, Nedbal L. (2013) Ultradian metabolic rhythm in the diazotrophic cyanobacterium Cyanothece sp. ATCC 51142. Proc Natl Acad Sci U S A. 2013 Aug 6;110(32):13210-5. doi: 10.1073/pnas.1301171110. Epub 2013 Jul 22. PMID: 23878254; PMCID: PMC3740830.

Chan KX, Mabbitt PD, Phua SY, Mueller JW, Nisar N, Gigolashvili T, Stroeher E, Grassl J, Arlt W, Estavillo GM, Jackson CJ, Pogson BJ (2016) Sensing and signaling of oxidative stress in chloroplasts by inactivation of the SAL1 phosphoadenosine phosphatase. Proc Natl Acad Sci U S A 113: E4567-4576

Chang JS, Chen LJ, Yeh YH, Hsiao CD, Li HM (2017) Chloroplast Preproteins Bind to the Dimer Interface of the Toc159 Receptor during Import. Plant Physiol **173:** 2148-2162

Chen M, Choi Y, Voytas DF, Rodermel S (2000) Mutations in the Arabidopsis VAR2 locus cause leaf variegation due to the loss of a chloroplast FtsH protease. The Plant Journal **22:** 303-313

Chorev DS, Ben-Nissan G, Sharon M (2015) Exposing the subunit diversity and modularity of protein complexes by structural mass spectrometry approaches. Proteomics **15:** 2777-2791

Chotewutmontri P, Barkan A (2018) Multilevel effects of light on ribosome dynamics in chloroplasts program genome-wide and psbA-specific changes in translation. PLoS Genet **14:** e1007555

Chung HS, Wang SB, Venkatraman V, Murray CI, Van Eyk JE (2013) Cysteine oxidative posttranslational modifications: emerging regulation in the cardiovascular system. Circ Res **112:** 382-392

Collin V, Issakidis-Bourguet E, Marchand C, Hirasawa M, Lancelin JM, Knaff DB, Miginiac-Maslow M (2003) The Arabidopsis plastidial thioredoxins: new functions and new insights into specificity. J Biol Chem **278:** 23747-23752

Collin V, Lamkemeyer P, Miginiac-Maslow M, Hirasawa M, Knaff DB, Dietz KJ, Issakidis-Bourguet E (2004) Characterization of plastidial thioredoxins from Arabidopsis belonging to the new y-type. Plant Physiol **136:** 4088-4095

Comelli RN, Gonzalez DH (2007) Conserved homeodomain cysteines confer redox sensitivity and influence the DNA binding properties of plant class III HD-Zip proteins. Arch Biochem Biophys **467:** 41-47

Considine MJ, Foyer CH (2014) Redox regulation of plant development. Antioxid Redox Signal **21:** 1305-1326

Couturier J, Chibani K, Jacquot JP, Rouhier N (2013) Cysteine-based redox regulation and signaling in plants. Front Plant Sci **4:** 105

Dai S, Schwendtmayer C, Johansson K, Ramaswamy S, Schu$rmann P, Eklund H (2000) How does light regulate chloroplast enzymes ? Structure–function studies of the ferredoxin/thioredoxin system. Quarterly Reviews of Biophysics **33**

Daloso DM, Müller K, Obata T, Florian A, Tohge T, Bottcher A, Riondet C, Bariat L, Carrari F, Nunes-Nesi A, Buchanan BB, Reichheld J-P, Araújo WL, Fernie AR (2015) Thioredoxin, a

master regulator of the tricarboxylic acid cycle in plant mitochondria. Proceedings of the National Academy of Sciences 112: E1392-E1400

Del Giudice A, Pavel NV, Galantini L, Falini G, Trost P, Fermani S, Sparla F (2015) Unravelling the shape and structural assembly of the photosynthetic GAPDH-CP12-PRK complex from Arabidopsis thaliana by small-angle X-ray scattering analysis. Acta Crystallogr D Biol Crystallogr **71:** 2372-2385

Depege N, Bellafiore S, Rochaix JD (2003) Role of chloroplast protein kinase Stt7 in LHCII phosphorylation and state transition in Chlamydomonas. Science **299:** 1572-1575

Dietz KJ (2014) Redox Regulation of Transcription Factors in Plant Stress Acclimation and Development. Antioxidants & Redox Signaling **21:** 1356-1372

Dix MM, Simon GM, Cravatt BF (2008) Global mapping of the topography and magnitude of proteolytic events in apoptosis. Cell **134:** 679-691

Dobin A, Davis CA, Schlesinger F, Drenkow J, Zaleski C, Jha S, Batut P, Chaisson M, Gingeras TR (2013) STAR: ultrafast universal RNA-seq aligner. Bioinformatics 29: 15-21

Dogra V, Duan J, Lee KP, Lv S, Liu R, Kim C (2017) FtsH2-Dependent Proteolysis of EXECUTER1 Is Essential in Mediating Singlet Oxygen-Triggered Retrograde Signaling in Arabidopsis thaliana. Front Plant Sci **8:** 1145

Duan J, Gaffrey MJ, Qian WJ (2017) Quantitative proteomic characterization of redox-dependent post-translational modifications on protein cysteines. Mol Biosyst **13:** 816-829

Dumont S, Rivoal J (2019) Consequences of Oxidative Stress on Plant Glycolytic and Respiratory Metabolism. Front Plant Sci **10:** 166

Dunn JG, Weissman JS (2016) Plastid: nucleotide-resolution analysis of next-generation sequencing and genomics data. BMC Genomics **17:** 958

Edreva A (2005) Generation and scavenging of reactive oxygen species in chloroplasts: a submolecular approach. Agriculture, Ecosystems & Environment **106:** 119-133

Edwards, G., & Walker, D. Alan. (1983). C3, C4 : mechanisms, and cellular and environmental regulation, of photosynthesis. Oxford: Blackwell Scientific.

Ferrandez J, Gonzalez M, Cejudo FJ (2012) Chloroplast redox homeostasis is essential for lateral root formation in Arabidopsis. Plant Signal Behav **7:** 1177-1179

Foreman J, Demidchik V, Bothwell JHF, Mylona P, Miedema H, Torres MA, Linstead P, Costa S, Brownlee C, Jones JDG, Davies JM, Dolan L (2003) Reactive oxygen species produced by NADPH oxidase regulate plant cell growth. Nature 422: 442-446

Forrester MT, Foster MW, Benhar M, Stamler JS (2009) Detection of protein S-nitrosylation with the biotin-switch technique. Free Radic Biol Med **46:** 119-126

Foyer CH, Noctor G (2005) Oxidant and antioxidant signalling in plants: a re-evaluation of the concept of oxidative stress in a physiological context. Plant, Cell & Environment **28:** 1056-1071

Fu Y, Ballicora MA, Leykam JF, Preiss J (1998) Mechanism of Reductive Activation of Potato Tuber ADP-glucose Pyrophosphorylase. THE JOURNAL OF BIOLOGICAL CHEMISTRY **273:** 25045-25052

Gal A, Zer H, Ohad I (1997) Redox-controlled thylakoid protein phosphorylation. News andviews. Physiologia Plantarum**:** 869-885

Geigenberger P (2011) Regulation of starch biosynthesis in response to a fluctuating environment. Plant Physiol **155:** 1566-1577

Geigenberger P, Fernie AR (2014) Metabolic control of redox and redox control of metabolism in plants. Antioxid Redox Signal **21:** 1389-1421

Glaring MA, Skryhan K, Kotting O, Zeeman SC, Blennow A (2012) Comprehensive survey of redox sensitive starch metabolising enzymes in Arabidopsis thaliana. Plant Physiol Biochem **58:** 89-97

Go YM, Jones DP (2013) The redox proteome. J Biol Chem **288:** 26512-26520

Gorka MJ (2017) Establishing a pipeline for identification of protein-protein interactions using different native fractionation methods. Universität Potsdam, Potsdam

Gundry RL, White MY, Murray CI, Kane LA, Fu Q, Stanley BA, Van Eyk JE (2009) Preparation of proteins and peptides for mass spectrometry analysis in a bottom-up proteomics workflow. Curr Protoc Mol Biol **Chapter 10:** Unit10 25

Guo J, Gaffrey MJ, Su D, Liu T, Camp DG, 2nd, Smith RD, Qian WJ (2014) Resin-assisted enrichment of thiols as a general strategy for proteomic profiling of cysteine-based reversible modifications. Nat Protoc **9:** 64-75

Gupta A, Marzinek JK, Jefferies D, Bond PJ, Harryson P, Wohland T (2019) The disordered plant dehydrin Lti30 protects the membrane during water-related stress by cross-linking lipids. J Biol Chem **294:** 6468-6482

Gupta KJ, Igamberdiev AU (2016) Reactive Nitrogen Species in Mitochondria and Their Implications in Plant Energy Status and Hypoxic Stress Tolerance. Frontiers in Plant Science **7**

Gutle DD, Roret T, Hecker A, Reski R, Jacquot JP (2017) Dithiol disulphide exchange in redox regulation of chloroplast enzymes in response to evolutionary and structural constraints. Plant Sci **255:** 1-11

Hendriks JH, Kolbe A, Gibon Y, Stitt M, Geigenberger P (2003) ADP-glucose pyrophosphorylase is activated by posttranslational redox-modification in response to light and to sugars in leaves of Arabidopsis and other plant species. Plant Physiol **133:** 838-849

Hill BG, Reily C, Oh JY, Johnson MS, Landar A (2009) Methods for the determination and quantification of the reactive thiol proteome. Free Radic Biol Med **47:** 675-683

Hisabori T, Sunamura E, Kim Y, Konno H (2013) The chloroplast ATP synthase features the characteristic redox regulation machinery. Antioxid Redox Signal **19:** 1846-1854

Huang J, Niazi AK, Young D, Rosado LA, Vertommen D, Bodra N, Abdelgawwad MR, Vignols F, Wei B, Wahni K, Bashandy T, Bariat L, Van Breusegem F, Messens J, Reichheld J-P (2017) Self-protection of cytosolic malate dehydrogenase against oxidative stress in Arabidopsis. Journal of Experimental Botany 69: 3491-3505

Huttlin EL, Jedrychowski MP, Elias JE, Goswami T, Rad R, Beausoleil SA, Villen J, Haas W, Sowa ME, Gygi SP (2010) A tissue-specific atlas of mouse protein phosphorylation and expression. Cell 143: 1174-1189

Jacquot JP (2018) Dark deactivation of chloroplast enzymes finally comes to light. Proc Natl Acad Sci U S A **115:** 9334-9335

Jaffrey SR, Snyder SH (2001) The biotin switch method for the detection of S-nitrosylated proteins. Sci STKE **2001:** pl1

Janku M, Luhova L, Petrivalsky M (2019) On the Origin and Fate of Reactive Oxygen Species in Plant Cell Compartments. Antioxidants (Basel) **8**

Jasid S, Simontacchi M, Bartoli CG, Puntarulo S (2006) Chloroplasts as a Nitric Oxide Cellular Source. Effect of Reactive Nitrogen Species on Chloroplastic Lipids and Proteins. Plant Physiology **142:** 1246-1255

Joo JH, Bae YS, Lee JS (2001) Role of Auxin-Induced Reactive Oxygen Species in Root Gravitropism. Plant Physiology **126:** 1055-1060

Jung H-S, Crisp PA, Estavillo GM, Cole B, Hong F, Mockler TC, Pogson BJ, Chory J (2013) Subset of heat-shock transcription factors required for the early response of Arabidopsis to excess light. Proceedings of the National Academy of Sciences **110:** 14474-14479

Jung YJ, Chi YH, Chae HB, Shin MR, Lee ES, Cha JY, Paeng SK, Lee Y, Park JH, Kim WY, Kang CH, Lee KO, Lee KW, Yun DJ, Lee SY (2013) Analysis of Arabidopsis thioredoxin-

h isotypes identifies discrete domains that confer specific structural and functional properties. Biochem J **456:** 13-24

Kaiser E, Morales A, Harbinson J (2018) Fluctuating Light Takes Crop Photosynthesis on a Rollercoaster Ride. Plant Physiology **176:** 977-989

Karpinski S, Reynolds H, Karpinksa B, Wingsle G, Creissen G, Mallineaux P (1999) Systemic Signaling and Acclimation in Response to Excess Excitation Energy in Arabidopsis. Science **284:** 654-657

Kato Y, Hyodo K, Sakamoto W (2018) The Photosystem II Repair Cycle Requires FtsH Turnover through the EngA GTPase. Plant Physiol **178:** 596-611

Kikuchi S, Asakura Y, Imai M, Nakahira Y, Kotani Y, Hashiguchi Y, Nakai Y, Takafuji K, Bedard J, Hirabayashi-Ishioka Y, Mori H, Shiina T, Nakai M (2018) A Ycf2-FtsHi Heteromeric AAA-ATPase Complex Is Required for Chloroplast Protein Import. Plant Cell 30: 2677-2703

Kohzuma K, Froehlich JE, Davis GA, Temple JA, Minhas D, Dhingra A, Cruz JA, Kramer DM (2017) The Role of Light-Dark Regulation of the Chloroplast ATP Synthase. Front Plant Sci **8:** 1248

Konig J, Muthuramalingam M, Dietz KJ (2012) Mechanisms and dynamics in the thiol/disulfide redox regulatory network: transmitters, sensors and targets. Curr Opin Plant Biol **15:** 261-268

Kopriva S, Mugford S, Baraniecka P, Lee B-R, Matthewman C, Koprivova A (2012) Control of sulfur partitioning between primary and secondary metabolism in Arabidopsis. Frontiers in Plant Science **3**

Krieger-Liszkay A, Feilke K (2015) The Dual Role of the Plastid Terminal Oxidase PTOX: Between a Protective and a Pro-oxidant Function. Front Plant Sci **6:** 1147

Krishnamurthy A, Rathinasabapathi B (2014) Oxidative stress tolerance in plants. Plant Signaling & Behavior **8:** e25761

Lee EM, Lee SS, Tripathi BN, Jung HS, Cao GP, Lee Y, Singh S, Hong SH, Lee KW, Lee SY, Cho JY, Chung BY (2015) Site-directed mutagenesis substituting cysteine for serine in 2-Cys peroxiredoxin (2-Cys Prx A) of Arabidopsis thaliana effectively improves its peroxidase and chaperone functions. Ann Bot **116:** 713-725

Leichert LI, Gehrke F, Gudiseva HV, Blackwell T, Ilbert M, Walker AK, Strahler JR, Andrews PC, Jakob U (2008) Quantifying changes in the thiol redox proteome upon oxidative stress in vivo. Proc Natl Acad Sci U S A **105:** 8197-8202

Li X, Cai C, Wang Z, Fan B, Zhu C, Chen Z (2018) Plastid Translation Elongation Factor Tu Is Prone to Heat-Induced Aggregation Despite Its Critical Role in Plant Heat Tolerance. Plant Physiology **176:** 3027-3045

Liang H-C, Lahert E, Pike I, Ward M (2015) Quantitation of protein post-translational modifications using isobaric tandem mass tags. Bioanalysis **7:** 383-400

Liao Y, Smyth GK, Shi W (2014) featureCounts: an efficient general purpose program for assigning sequence reads to genomic features. Bioinformatics **30:** 923-930

Lindahl M, Spetea C, Hundal T, Oppenheim AB, Adam Z, Andersson B (2000) The Thylakoid FtsH Protease Plays a Role in the Light-Induced Turnover of the Photosystem II D1 Protein. The Plant Cell **12:** 419-431

Lindermayr C, Saalbach G, Bahnweg G, Durner J (2006) Differential inhibition of Arabidopsis methionine adenosyltransferases by protein S-nitrosylation. J Biol Chem **281:** 4285-4291

Lindermayr C, Saalbach G, Durner J (2005) Proteomic identification of S-nitrosylated proteins in Arabidopsis. Plant Physiol **137:** 921-930

Liu P, Zhang H, Yu B, Xiong L, Xia Y (2015) Proteomic identification of early salicylate- and flg22-responsive redox-sensitive proteins in Arabidopsis. Sci Rep **5:** 8625

Liu S, Zheng L, Jia J, Guo J, Zheng M, Zhao J, Shao J, Liu X, An L, Yu F, Qi Y (2019) Chloroplast Translation Elongation Factor EF-Tu/SVR11 Is Involved in var2-Mediated Leaf Variegation and Leaf Development in Arabidopsis. Front Plant Sci **10:** 295

Liu Y, Lai J, Yu M, Wang F, Zhang J, Jiang J, Hu H, Wu Q, Lu G, Xu P, Yang C (2016) The Arabidopsis SUMO E3 Ligase AtMMS21 Dissociates the E2Fa/DPa Complex in Cell Cycle Regulation. Plant Cell **28:** 2225-2237

Lodish H, Berk A, Zipursky SL (2000) Hierarchical Structure of Proteins, New York

Love MI, Huber W, Anders S (2014) Moderated estimation of fold change and dispersion for RNA-seq data with DESeq2. Genome Biol **15:** 550

Marchand C, Le Marechal P, Meyer Y, Decottignies P (2006) Comparative proteomic approaches for the isolation of proteins interacting with thioredoxin. Proteomics **6:** 6528-6537

Marchand CH, Vanacker H, Collin V, Issakidis-Bourguet E, Marechal PL, Decottignies P (2010) Thioredoxin targets in Arabidopsis roots. Proteomics 10: 2418-2428

Marri L, Zaffagnini M, Collin V, Issakidis-Bourguet E, Lemaire SD, Pupillo P, Sparla F, Miginiac-Maslow M, Trost P (2009) Prompt and easy activation by specific thioredoxins of calvin cycle enzymes of Arabidopsis thaliana associated in the GAPDH/CP12/PRK supramolecular complex. Mol Plant **2:** 259-269

Martins L, Trujillo-Hernandez JA, Reichheld JP (2018) Thiol Based Redox Signaling in Plant Nucleus. Front Plant Sci **9:** 705

Meyer Y, Reichheld JP, Vignols F (2005) Thioredoxins in Arabidopsis and other plants. Photosynth Res **86:** 419-433

Meyer Y, Siala W, Bashandy T, Riondet C, Vignols F, Reichheld JP (2008) Glutaredoxins and thioredoxins in plants. Biochim Biophys Acta **1783:** 589-600

Mieyal JJ, Chock PB (2012) Posttranslational modification of cysteine in redox signaling and oxidative stress: Focus on s-glutathionylation. Antioxid Redox Signal **16:** 471-475

Miginiac-Maslow M, Johansson K, Ruelland E, Issakidis-Bourguet E, Schepens I, Goyer A, Lemaire-Chamley M, Jacquot J-P, Le Maréchal P, Decottignies P (2000) Light-activation of NADP-malate dehydrogenase: A highly controlled process for an optimized function. Physiologia Plantarum 110: 322-329

Mittler R (2017) ROS Are Good. Trends Plant Sci **22:** 11-19

Moller IM, Jensen PE, Hansson A (2007) Oxidative modifications to cellular components in plants. Annu Rev Plant Biol **58:** 459-481

Montrichard F, Alkhalfioui F, Yano H, Vensel WH, Hurkman WJ, Buchanan BB (2009) Thioredoxin targets in plants: the first 30 years. J Proteomics **72:** 452-474

Moon JC, Jang HH, Chae HB, Lee JR, Lee SY, Jung YJ, Shin MR, Lim HS, Chung WS, Yun DJ, Lee KO, Lee SY (2006) The C-type Arabidopsis thioredoxin reductase ANTR-C acts as an electron donor to 2-Cys peroxiredoxins in chloroplasts. Biochem Biophys Res Commun **348:** 478-484

Muthuramalingam M, Matros A, Scheibe R, Mock HP, Dietz KJ (2013) The hydrogen peroxide-sensitive proteome of the chloroplast in vitro and in vivo. Front Plant Sci **4:** 54

Neil SJ, Desikan R, Clarke A, Hurst RD, Hancock JT (2002) Hydrogen peroxide and nitric oxide as signalling molecules in plants. Journal of Experimental Botany **53**

Nield J, Redding K, Hippler M (2004) Remodeling of light-harvesting protein complexes in chlamydomonas in response to environmental changes. Eukaryot Cell **3:** 1370-1380

Nikkanen L, Rintamaki E (2019) Chloroplast thioredoxin systems dynamically regulate photosynthesis in plants. Biochem J **476:** 1159-1172

Nikkanen L, Toivola J, Rintamäki E (2016) Crosstalk between chloroplast thioredoxin systems in regulation of photosynthesis. Plant, Cell & Environment **39:** 1691-1705

Nishiyama J, Kuninori T (1992) Assay of thiols and disulfides based on the reversibility of N-ethylmaleimide alkylation of thiols combined with electrolysis. Anal Biochem **200:** 230-234

Noctor G, Foyer CH (1998) ASCORBATE AND GLUTATHIONE: Keeping Active Oxygen Under Control. Annu Rev Plant Physiol Plant Mol Biol **49:** 249-279

Ojeda V, Perez-Ruiz JM, Cejudo FJ (2018) 2-Cys Peroxiredoxins Participate in the Oxidation of Chloroplast Enzymes in the Dark. Mol Plant **11:** 1377-1388

Okegawa Y, Motohashi K (2015) Chloroplastic thioredoxin m functions as a major regulator of Calvin cycle enzymes during photosynthesis in vivo. Plant J **84:** 900-913

Olsen JV, Mann M (2013) Status of large-scale analysis of post-translational modifications by mass spectrometry. Mol Cell Proteomics **12:** 3444-3452

Olsen JV, Vermeulen M, Santamaria A, Kumar C, Miller ML, Jensen LJ, Gnad F, Cox J, Jensen TS, Nigg EA, Brunak S, Mann M (2010) Quantitative phosphoproteomics reveals widespread full phosphorylation site occupancy during mitosis. Sci Signal **3:** ra3

Onda Y (2013) Oxidative protein-folding systems in plant cells. Int J Cell Biol **2013:** 585431

Pesaresi P, Varotto C, Meurer J, Jahns P, Salamini F, Leister D (2001) Knock-out of the plastid ribosomal protein L11 in Arabidopsis: effects on mRNA translation and photosynthesis. Plant J **27:** 179-189

Potocký M, Jones MA, Bezvoda R, Smirnoff N, Žárský V (2007) Reactive oxygen species produced by NADPH oxidase are involved in pollen tube growth. New Phytologist **174:** 742-751

Pulido P, Zagari N, Manavski N, Gawronski P, Matthes A, Scharff LB, Meurer J, Leister D (2018) CHLOROPLAST RIBOSOME ASSOCIATED Supports Translation under Stress and Interacts with the Ribosomal 30S Subunit. Plant Physiol **177:** 1539-1554

Qi Y, Armbruster U, Schmitz-Linneweber C, Delannoy E, de Longevialle AF, Ruhle T, Small I, Jahns P, Leister D (2012) Arabidopsis CSP41 proteins form multimeric complexes that bind and stabilize distinct plastid transcripts. J Exp Bot **63:** 1251-1270

Reactive Oxygen And Nitrogen Species Signaling and Communication in Plants (2015) Vol 23. Springer, Bonn, Germany

Rinalducci S, Murgiano L, Zolla L (2008) Redox proteomics: basic principles and future perspectives for the detection of protein oxidation in plants. J Exp Bot **59:** 3781-3801

Romero-Puertas MC, Campostrini N, Matte A, Righetti PG, Perazzolli M, Zolla L, Roepstorff P, Delledonne M (2008) Proteomic analysis of S-nitrosylated proteins in Arabidopsis thaliana undergoing hypersensitive response. Proteomics **8:** 1459-1469

Rosenwasser S, Graff van Creveld S, Schatz D, Malitsky S, Tzfadia O, Aharoni A, Levin Y, Gabashvili A, Feldmesser E, Vardi A (2014) Mapping the diatom redox-sensitive proteome provides insight into response to nitrogen stress in the marine environment. Proc Natl Acad Sci U S A **111:** 2740-2745

Rouhier N, Villarejo A, Srivastava M, Gelhaye E, Keech O, Droux M, Finkemeier I, Samuelsson G, Dietz KJ, Jacquot JP, Wingsle G (2005) Identification of plant glutaredoxin targets. Antioxid Redox Signal 7: 919-929

Sakamoto W (2006) Protein Degradation Machineries in Plastids. Annual Review of Plant Biology **57:** 599-621

Sakamoto W, Zaltsman A, Adam Z, Takahashi Y (2003) Coordinated Regulation and Complex Formation of YELLOW VARIEGATED1 and YELLOW VARIEGATED2, Chloroplastic FtsH Metalloproteases Involved in the Repair Cycle of Photosystem II in Arabidopsis Thylakoid Membranes. The Plant Cell **15:** 2843-2855

Schmidtmann E, Konig AC, Orwat A, Leister D, Hartl M, Finkemeier I (2014) Redox regulation of Arabidopsis mitochondrial citrate synthase. Mol Plant **7:** 156-169

Schurmann P, Buchanan BB (2008) The ferredoxin/thioredoxin system of oxygenic photosynthesis. Antioxid Redox Signal **10:** 1235-1274

Schurmann P, Jacquot JP (2000) Plant Thioredoxin Systems Revisited. Annu Rev Plant Physiol Plant Mol Biol **51:** 371-400

Selinski J, Scheibe R (2019) Malate valves: old shuttles with new perspectives. Plant Biol (Stuttg) **21 Suppl 1:** 21-30

Serrato AJ, Romero-Puertas MC, Lazaro-Payo A, Sahrawy M (2018) Regulation by S-nitrosylation of the Calvin-Benson cycle fructose-1,6-bisphosphatase in Pisum sativum. Redox Biol **14:** 409-416

Shaikhali J, Wingsle G (2017) Redox-regulated transcription in plants: Emerging concepts. AIMS Molecular Science **4:** 301-338

Shakir S, Vinh J, Chiappetta G (2017) Quantitative analysis of the cysteine redoxome by iodoacetyl tandem mass tags. Anal Bioanal Chem **409:** 3821-3830

Shoji S, Dambacher CM, Shajani Z, Williamson JR, Schultz PG (2011) Systematic chromosomal deletion of bacterial ribosomal protein genes. J Mol Biol **413:** 751-761

Scialdone A, Mugford ST, Feike D, Skeffington A, Borrill P, Graf A, Smith AM, Howard M. Arabidopsis plants perform arithmetic division to prevent starvation at night. eLife. 2013;2:e00669.

Smirnoff N, Arnaud D (2019) Hydrogen peroxide metabolism and functions in plants. New Phytologist **221:** 1197-1214

Smith T, Heger A, Sudbery I (2017) UMI-tools: modeling sequencing errors in Unique Molecular Identifiers to improve quantification accuracy. Genome Research **27:** 491-499

Song CJ, Steinebrunner I, Wang X, Stout SC, Roux SJ (2006) Extracellular ATP Induces the Accumulation of Superoxide via NADPH Oxidases in Arabidopsis. Plant Physiology **140:** 1222-1232

Sowokinos JR (1981) Pyrophosphorylases in Solanum tuberosum. Plant Physiol**:** 924-929

Spoel SH (2018) Orchestrating the proteome with post-translational modifications. J Exp Bot **69:** 4499-4503

Stitt M, Grosse H (1988) Interactions between Sucrose Synthesis and CO2 Fixation IV. Temperature-dependent adjustment of the relation between sucrose synthesis and CO2 fixation. Journal of Plant Physiology **133:** 392-400

Sugiura K, Yokochi Y, Fu N, Fukaya Y, Yoshida K, Mihara S, Hisabori T (2019) The thioredoxin (Trx) redox state sensor protein can visualize Trx activities in the light/dark response in chloroplasts. J Biol Chem **294:** 12091-12098

Takahashi D, Gorka M, Erban A, Graf A, Kopka J, Zuther E, Hincha DK (2019) Both cold and sub-zero acclimation induce cell wall modification and changes in the extracellular proteome in Arabidopsis thaliana. Sci Rep **9:** 2289

Thormahlen I, Ruber J, von Roepenack-Lahaye E, Ehrlich SM, Massot V, Hummer C, Tezycka J, Issakidis-Bourguet E, Geigenberger P (2013) Inactivation of thioredoxin f1 leads to decreased light activation of ADP-glucose pyrophosphorylase and altered diurnal starch turnover in leaves of Arabidopsis plants. Plant Cell Environ **36:** 16-29

Treves H, Raanan H, Finkel OM, Berkowicz SM, Keren N, Shotland Y, Kaplan A (2013) A newly isolated Chlorella sp. from desert sand crusts exhibits a unique resistance to excess light intensity. FEMS Microbiology Ecology **86:** 373-380

Treves H, Raanan H, Kedem I, Murik O, Keren N, Zer H, Berkowicz SM, Giordano M, Norici A, Shotland Y, Ohad I, Kaplan A (2016) The mechanisms whereby the green alga Chlorella ohadii, isolated from desert soil crust, exhibits unparalleled photodamage resistance. New Phytologist **210:** 1229-1243

Trewavas AJ, Malho R (1997) Signal Perception and Transduction: The Origin of the Phenotype. Plant Cell **9:** 1181-1195

Trost P, Fermani S, Marri L, Zaffagnini M, Falini G, Scagliarini S, Pupillo P, Sparla F (2006) Thioredoxin-dependent regulation of photosynthetic glyceraldehyde-3-phosphate dehydrogenase: autonomous vs. CP12-dependent mechanisms. Photosynth Res **89:** 263-275

Turkan I (2018) ROS and RNS: key signalling molecules in plants. J Exp Bot **69:** 3313-3315

Unwin RD (2010) Quantification of Proteins by iTRAQ. *In* PR Cutillas, JF Timms, eds, LC-MS/MS in Proteomics: Methods and Applications. Humana Press, Totowa, NJ, pp 205-215

Vallelian-Bindschedler L, Schweizer P, Mosinger E, Metraux J-P (1998) Heat-induced resistance in barley to powdery mildew (Blumeria graminis f.sp. hordei) is associated with a burst of active oxygen species. Physiological and Molecular Plant Pathology

van der Linde K, Gutsche N, Leffers HM, Lindermayr C, Muller B, Holtgrefe S, Scheibe R (2011) Regulation of plant cytosolic aldolase functions by redox-modifications. Plant Physiol Biochem **49:** 946-957

Vaseghi MJ, Chibani K, Telman W, Liebthal MF, Gerken M, Schnitzer H, Mueller SM, Dietz KJ (2018) The chloroplast 2-cysteine peroxiredoxin functions as thioredoxin oxidase in redox regulation of chloroplast metabolism. Elife **7**

Wang J, Yu Q, Xiong H, Wang J, Chen S, Yang Z, Dai S (2016) Proteomic Insight into the Response of Arabidopsis Chloroplasts to Darkness. PLoS One **11:** e0154235

Wolosiuk RA, Buchanan BB (1977) Thioredoxin and Glutathione Regulate Photosynthesis in Chloroplasts. Nature **266:** 565-567

Yang H-Y, Lee T-H (2015) Antioxidant enzymes as redox-based biomarkers: a brief review. BMB Reports **48:** 200-208

Ying J, Clavreul N, Sethuraman M, Adachi T, Cohen RA (2007) Thiol oxidation in signaling and response to stress: detection and quantification of physiological and pathophysiological thiol modifications. Free Radic Biol Med **43:** 1099-1108

Yoshida K, Hara A, Sugiura K, Fukaya Y, Hisabori T (2018) Thioredoxin-like2/2-Cys peroxiredoxin redox cascade supports oxidative thiol modulation in chloroplasts. Proceedings of the National Academy of Sciences **115:** E8296-E8304

Yoshida K, Hisabori T (2014) Mitochondrial isocitrate dehydrogenase is inactivated upon oxidation and reactivated by thioredoxin-dependent reduction in Arabidopsis. Frontiers in Environmental Science **2**

Yoshida K, Noguchi K (2011) Interaction Between Chloroplasts and Mitochondria: Activity, Function, and Regulation of the Mitochondrial Respiratory System during Photosynthesis. 383-409

Yoshida K, Noguchi K, Motohashi K, Hisabori T (2013) Systematic exploration of thioredoxin target proteins in plant mitochondria. Plant Cell Physiol **54:** 875-892

Yoshida K, Uchikoshi E, Hara S, Hisabori T (2019) Thioredoxin-like2/2-Cys peroxiredoxin redox cascade acts as oxidative activator of glucose-6-phosphate dehydrogenase in chloroplasts. Biochemical Journal **476:** 1781-1790

Yu C-W, Murphy TM, Lin C-H (2003) Hydrogen peroxide-induced chilling tolerance in mung beans mediated through ABA-independent glutathione accumulation. Functional Plant Biology **30:** 955

Zaltsman A, Ori N, Adam Z (2005) Two Types of FtsH Protease Subunits Are Required for Chloroplast Biogenesis and Photosystem II Repair in Arabidopsis. The Plant Cell **17:** 2782-2790

Zannini F, Couturier J, Keech O, Rouhier N (2017) In Vitro Alkylation Methods for Assessing the Protein Redox State. Methods Mol Biol **1653:** 51-64

Zhang N, Portis AR, Jr. (1999) Mechanism of light regulation of Rubisco: a specific role for the larger Rubisco activase isoform involving reductive activation by thioredoxin-f. Proc Natl Acad Sci U S A **96:** 9438-9443

List of co-authored publications:

Burschel S, Kreuzer Decovic D, Nuber F, Stiller M, Hofmann M, Zupok A, Siemiatkowska B, Gorka M, Leimkuhler S, Friedrich T (2019) Iron-sulfur cluster carrier proteins involved in the assembly of Escherichia coli NADH:ubiquinone oxidoreductase (complex I). Mol Microbiol **111:** 31-45

Gorka M, Swart C, Siemiatkowska B, Martínez-Jaime S, Skirycz A, Streb S, Graf A (2019) Protein Complex Identification and quantitative complexome by CN-PAGE. Scientific Reports **9:** 11523

Riedel S, Siemiatkowska B, Watanabe M, Muller CS, Schunemann V, Hoefgen R, Leimkuhler S (2019) The ABCB7-Like Transporter PexA in Rhodobacter capsulatus Is Involved in the Translocation of Reactive Sulfur Species. Front Microbiol **10:** 406

Zhang Y., Natale R., Pereira Domingues Junior A., Toleco M.R, Siemiatkowska B., Fàbregas N., Fernie AR (2019) Rapid identification of enzyme-enzyme interactions in plants. Current Protocols in Plant Biology

Zupok A, Gorka M, Siemiatkowska B, Skirycz A, Leimkuhler S (2019) Iron-Dependent Regulation of Molybdenum Cofactor Biosynthesis Genes in Escherichia coli. J Bacteriol **201**

Correa Galvis, V., Strand, D. D., Messer, M., Thiele, W., Bethmann, S., Hübner, D., Uflewski, M., Kaiser, E., Siemiatkowska, B., Morris, B. A., Tóth, S. Z., Watanabe, M., Brückner, F., Höfgen, R., Jahns, P., Schöttler, M. A., & Armbruster, U. (2020). H^+ Transport by K^+ EXCHANGE ANTIPORTER3 Promotes Photosynthesis and Growth in Chloroplast ATP Synthase Mutants. *Plant physiology*, *182*(4), 2126–2142. https://doi.org/10.1104/pp.19.01561

Treves H, Siemiatkowska B, Luzarowska U, Murik O, Fernandez-Pozo N, Moraes TA,

Erban A, Armbruster U, Brotman Y, Kopka J, Rensing SA, Szymanski J, Stitt M. Multi-omics reveals mechanisms of total resistance to extreme illumination of a desert alga. Nat Plants. 2020 Aug;6(8):1031-1043. doi: 10.1038/s41477-020-0729-9. Epub 2020 Jul 27. PMID: 32719473.